



Università
Ca' Foscari
Venezia

Master's Degree programme

in

Biotechnology for the Environment and Sustainable Development

Final Thesis

**Optimization of hydrogen production through
immobilization of *Rhodopseudomonas palustris* in
polymeric matrices.**

Supervisor

Prof.ssa Cristina Cavinato

Assistant supervisor

Dott.ssa Eva Carraro

Graduand

Letizia Tacconi

Matriculation Number 900978

Academic Year

2024/2025

Index

1.	Introduction.....	1
1.1.	Purple phototrophic bacteria	2
1.1.1.	Growth of purple non-sulfur bacteria	3
1.1.2.	<i>Rhodopseudomonas palustris</i>	4
1.1.3.	Industrial and biotechnological applications.....	5
1.1.4.	Traditional cultivation systems.....	7
1.1.5.	Photobioreactors for hydrogen production.....	9
1.2.	Hydrogen as an energy carrier.....	10
1.3.	Bio-hydrogen production	11
1.3.1.	Photofermentation	14
1.4.	Cell immobilization	16
1.4.1.	Effects of immobilization: advantages and disadvantages	16
1.4.2.	Main immobilization techniques.....	17
1.4.3.	Alginate	19
2.	Thesis objectives	21
3.	Materials and methods	22
3.1.	Microorganism and inoculum preparation.....	22
3.1.1.	Colony selection on solid agar.....	22
3.2.	Synthetic media composition.....	23
3.3.	Fermented effluent.....	25
3.4.	Light source	26
3.5.	Batch tests in suspension for biomass production.....	27
3.6.	Growth monitoring.....	28
3.6.1.	Optical density.....	29
3.6.2.	Dry weight	29
3.6.3.	Growth rate and biomass productivity.....	30
3.7.	Batch tests for H ₂ production.....	31
3.7.1.	H ₂ production monitoring	32

3.8.	Medium Analysis.....	33
3.8.1.	VFA analysis	34
3.8.2.	Ammonium concentration.....	34
3.9.	Immobilization on alginate matrix.....	35
3.9.1.	Immobilization procedure	35
3.9.2.	Growth monitoring of immobilized biomass	37
3.9.3.	H ₂ production with immobilized <i>R. palustris</i>	37
3.10.	Biomass characterization	38
3.10.1.	Lipid analysis.....	38
3.10.2.	Protein analysis.....	38
3.10.3.	Carbohydrate analysis.....	39
4.	Results and discussion	40
4.2.	Batch tests with suspended biomass for growth.....	41
4.2.1.	Effects of media composition on growth kinetics	42
4.2.2.	Effect of carbon source on growth kinetics	43
4.2.3.	Ammonium consumption in batch test.....	50
4.3.	Hydrogen production by <i>Rhodopseudomonas palustris</i>	53
4.3.1.	Cumulative hydrogen production	53
4.3.2.	Relationship between substrate consumption and hydrogen evolution.....	62
4.3.3.	Hydrogen yields and substrate conversion efficiency	69
4.4.	Immobilization of <i>R. palustris</i> on alginate matrix.....	74
4.4.1.	Effect of alginate concentration on biomass growth.....	74
4.4.2.	Hydrogen production tests with immobilized biomass.....	78
4.5.	Biomass characterization	81
4.5.1.	Biomass composition under different cultivation conditions	81
4.5.2.	Biomass characterization of immobilized biomass.....	84
5.	Conclusions	87
6.	References	89

ABSTRACT

The growing need for sustainable energy sources encouraged the development of innovative biotechnological processes for hydrogen production, a clean and highly efficient energy carrier. In this context, the present thesis investigates the growth behavior and photofermentative hydrogen production potential of *Rhodopseudomonas palustris*, a purple non-sulfur bacterium (PNSB), cultivated on both defined carbon substrates and volatile fatty acids (VFA)-rich fermented effluent.

This research activity is part of the Italian Space Agency's (ASI) project “*BioMOON – Low Gravity Biorefinery Platform*,” which aims to develop advanced biotechnological systems for resource production and recovery in low-gravity environments. Within this framework, the fermentation effluent was obtained from semi-solid anaerobic fermentation of a mixed organic feedstock composed of excess activated sludge and organic residues, such as vegetable waste, lignocellulosic material, and cellulose-based substrates, designed to simulate waste streams potentially generated in bioregenerative life support systems for space habitats.

Batch experiments focused on three defined carbon sources; malic acid, lactic acid, and acetic acid to assess the growth performance of *R. palustris* and its hydrogen-producing ability. Then, *R. palustris* was tested on the fermented effluent to test its ability to valorize complex substrates under conditions relevant to circular and space-oriented bioprocesses.

Hydrogen production was strongly substrate-dependent; results shows that acetate supported the highest H₂ accumulation (5.38 mmol H₂ L⁻¹), whereas malate and lactate showed only short hydrogen-producing phases and very low conversion efficiencies (<1%).

The VFA-rich fermented effluent also showed photofermentative H₂ production (1.42 mmol H₂ L⁻¹) but with a delayed onset, highlighting the impact of matrix complexity on hydrogen production kinetics.

Biomass immobilization in calcium–alginate matrices was also evaluated, in order to compare growth behavior and hydrogen production in free and immobilized-cell systems and to improve process stability. First, the aim was to find suitable conditions to allow biomass retention and growth. Immobilization in alginate (4% v/v) shows compatible with *R. palustris* survival and growth, but hydrogen evolution was not detected under the tested condition, suggesting that this approach requires further optimization that will be addressed in future works.

1. Introduction

The current global energy model is still strongly linked to the use of fossil fuels, which are the main sources for the production of energy, but also raw materials, and chemicals. Their extensive use has caused significant environmental impacts, including greenhouse gas (GHG) emissions, air pollution, and the progressive depletion of nonrenewable resources, thus contributing greatly to ecosystem degradation (Ghimire *et al.*, 2015).

For this reason, the transition to a more sustainable and environmentally friendly circular economy is one of the most urgent priorities worldwide (Budiman and Wu, 2018; Sagir and Alipour, 2021). In this context, biohydrogen production (BHP) is gaining lot of attention as a promising strategy for developing sustainable energy carriers (Chen *et al.*, 2011; Akram *et al.*, 2024).

Despite its potential, this approach still need to face important technological and biological limitations and, for this reason, further research and development are needed before it can be applied at larger scale (Hallenbeck, Abo-Hashesh and Ghosh, 2012).

In biological systems, hydrogen can be produced through different biotechnological pathways, including biophotolysis by cyanobacteria and microalgae, dark fermentation (DF) by anaerobic bacteria, and photofermentation by photosynthetic microorganisms (Jeong *et al.*, 2008).

Among photosynthetic microorganisms, photosynthetic purple bacteria (PPB) represent an interesting option (Adessi and De Philippis, 2014). PPB can exploit light as an energy source and short-chain carboxylic acids as electron donors (Li *et al.*, 2022).

These bacteria can work under anaerobic conditions, using light as an energy source and organic compounds as electron donors. Hydrogen production is typically favored under nitrogen-limited conditions, to promote nitrogenase activity (Brown, Wilkins and Saha, 2022; Amini *et al.*, 2025). Effluents rich in VFA from anaerobic fermentation represent interesting feedstock for biohydrogen production, supporting both waste valorization and at the same time contributing to renewable energy generation (Ghosh *et al.*, 2017).

This study focuses on the use of *Rhodospseudomonas palustris*, which can produce hydrogen by photofermentation under anaerobic conditions using different organic substrates (Brown, Wilkins and Saha, 2022).

In literature different cells immobilization techniques have been proposed in order to improve process stability and management (Zhang *et al.*, 2017). Immobilization can increase biomass stability and facilitate biomass reuse and it has also been associated with improved hydrogen production (Guevara-López and Buitrón, 2015; Sagir and Alipour, 2021).

The main objective of this work is to evaluate hydrogen production by *R. palustris* through photofermentation testing different carbon sources and determine growth kinetic parameters and hydrogen yields also using VFA-rich substrates, to support a waste valorization strategy.

Finally, to compare the performance of suspended-cell systems and immobilized-cell systems.

1.1. Purple phototrophic bacteria

Purple phototrophic bacteria are Gram-negative prokaryotes. Their name is due to the typical red-purple color given by photosynthetic pigments such as bacteriochlorophylls and carotenoids which are produced under phototrophic conditions (Morrison and Bose, 2025).

PPBs are well known for their metabolic versatility, a feature that allows them to adapt to many different environments and growth conditions (Dhar, Venkateswarlu and Megharaj, 2023; Morrison and Bose, 2025b).

PPBs can grow in both anaerobic and aerobic conditions and when light is available, can convert it into chemical energy through a process known as anoxygenic photosynthesis without producing oxygen (Madigan and Jung, 2009; Adessi and De Philippis, 2013).

Some PPBs can tolerate extreme conditions, including high salinity and the presence of heavy metals and toxic contaminants such as H₂S (Dhar, Venkateswarlu and Megharaj, 2023).

Purple phototrophic bacteria are mainly divided into two groups: purple sulfur bacteria (PSB), and purple non-sulfur bacteria (PNSB) (George, Vincent and Mackey, 2020; Morrison and Bose, 2025a).

PSBs are photoautotrophic, they can fix CO₂ as their sole carbon source and have a limited ability to grow under photoheterotrophic conditions and in absence of light (Larimer *et al.*, 2004; Brown, Wilkins and Saha, 2022).

PNSB are widely distributed in aquatic and terrestrial habitats, preferring sunlight exposed, waterlogged, oxygen-deficient environments. In nature purple non-sulfur bacteria are often found to coexist with other phototrophic bacteria (Dhar, Venkateswarlu and Megharaj, 2023).

PNSB constitutes a highly diverse group in terms of morphology, internal membrane structure, carotenoid composition, and utilization of carbon sources. Based on their ecological distribution they can also show differences in lipid composition and other cell envelopes, a feature that allows them to adapt to different environments (Madigan and Jung, 2009; Adessi and De Philippis, 2014).

Many purple non-sulfur bacteria shows the ability to used different metabolic modes, depending on light availability, oxygen concentration, and nutrients; this flexibility allows them to adapt well in complex and variable environments such as waste streams, where carbon sources and light conditions can change over time (Morrison and Bose, 2025b).

They can adopt different metabolic strategies including:

- Photoautotrophy, the ability to synthesize organic matter from light energy using carbon dioxide as a carbon source.
- Photoheterotrophy, the acquisition of energy from light and assimilation of carbon from organic compounds.
- Chemoheterotrophy, deriving both carbon and energy from organic substrates.

- Chemoautotrophy, deriving energy from inorganic compounds and using carbon dioxide as a carbon source. (Li *et al.*, 2022; Dhar, Venkateswarlu and Megharaj, 2023)

At the taxonomic level, PNSB are predominantly classified within the class Alphaproteobacteria, (*Rhodospirillum*, *Rhodopseudomonas* (α -2) and *Rhodobacter* (α -3)) and Betaproteobacteria (*Rhodocyclus sp.*, *Rhodoferax sp.* and *Rubrivivax sp.* Belongs) (Tiang *et al.*, 2020).

Many different species of PNSB have been identified but scientific research has been primarily focused on few well-characterised model organisms, such as *Rhodopseudomonas palustris*, *Rhodospirillum rubrum*, *Rhodopseudomonas capsulatus* e *Rhodobacter sphaeroides* (Tiang *et al.*, 2020; Morrison and Bose, 2025a).

1.1.1. Growth of purple non-sulfur bacteria

In batch culture, purple non-sulfur bacteria exhibit a sigmoidal growth curve, typical of bacterial growth, with variations depending on the bacterial species, the culture medium, and operational conditions.

A batch growth curve can be described through 5 distinct phases:

1. Lag phase (latent phase) – this is the period following inoculation during which the cells adapt to the new environment, and activate the metabolic pathways needed for cell proliferation. Its duration depends on the physiological conditions of the inoculum and on the culture medium. Stressing conditions are typically associated to longer lag phases.
2. Exponential phase – in this phase there is active cell division and a constant growth rate. biomass accumulation increases exponentially, due to optimal environmental conditions (light, nutrients, temperature).
3. Deceleration phase - Characterized by a decline in the growth rate, linked to nutrients depletion and an accumulation of metabolic byproducts.
4. Stationary phase – Cells proliferation stops, and the total number of viable cells remains relatively constant because cell division is balanced by cell death. During this phase, cells can activate survival mechanisms and accumulating energy reserves.
5. Decline phase (death phase) - Characterized by nutrients depletion and potential accumulation of inhibitory compounds. As a result, cellular death and lysis occur.

The five phases just described are represented graphically, as illustrated in Figure 1 below:

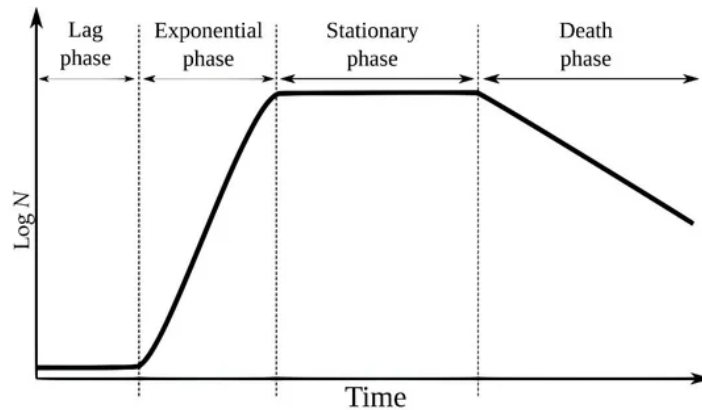


Figure 1 A typical microbial growth curve in a closed system, where N represents the number of bacterial cells (Štumpf *et al.*, 2020)

Understanding PNSB growth dynamics is important for hydrogen production studies since growth phases strongly influence nutrient consumption and metabolic activity (Chen, Wu and Lee, 2012).

1.1.2. *Rhodopseudomonas palustris*

Rhodopseudomonas palustris is a Gram-negative α -proteobacterium belonging to the purple non-sulfur bacteria group. It is widely distributed in nature, especially in illuminated, anaerobic aquatic environments, including lakes, marshy soils and sea (Li *et al.*, 2022).

R. palustris can use all four major metabolic modes (Brown, Wilkins and Saha, 2022). Its genome consists of a single circular chromosome of approximately 5.46 Mb in which many genes are involved in energy metabolism (Larimer *et al.*, 2004).

When light is available, it can grow as a photoautotroph or as a photoheterotroph, while in the dark it can adopt either chemoheterotrophic or chemoautotrophic metabolism, obtaining carbon and energy from organic compounds or deriving energy from inorganic compounds and carbon from CO_2 , respectively (Brown, Wilkins and Saha, 2022; Li *et al.*, 2022; Dhar, Venkateswarlu and Megharaj, 2023).

In presence of oxygen, *R. palustris* can oxidize carbon compounds to obtain energy and carbon through aerobic respiration. On the other hand, in anaerobic or oxygen-depleted conditions (2-6% O_2), *R. palustris* synthesize photosynthetic pigments and develop the photosynthetic apparatus, which gives to the culture the typical red-purple color (Brown, Wilkins and Saha, 2022). *R. palustris* can assimilate short-chain organic acids, including VFAs (Ross and Pott, 2021) alcohols (Liu, Ghosh and Hallenbeck, 2015), inorganic compounds (Luxem, Nguyen and Zhang, 2022), and aromatic molecules (Pakpour *et al.*, 2014) (Li *et al.*, 2022).

Due to its remarkable metabolic flexibility, *R. palustris* has been widely studied as a model organism for understanding how metabolism responds to environmental changes, and to explore

different biotechnological applications (Larimer *et al.*, 2004; Brown, Wilkins and Saha, 2022; Li *et al.*, 2022; Dhar, Venkateswarlu and Megharaj, 2023).

Common applications include wastewater treatment and bioremediation (Tao *et al.*, 2008), biodegradation of aromatic and xenobiotic compounds, synthesis of bioplastics such as polyhydroxybutyrate (PHB), natural pigments, biostimulant used in agriculture, and can be used in bioelectrochemical systems to generate bioelectricity (Chen, Wu and Lee, 2012; Li *et al.*, 2022). Among other bacteria, *Rhodospseudomonas palustris* is recognized as a model organism to study biological H₂ production through photofermentation in anaerobic conditions, often integrated with dark fermentation processes, using organic substrates and VFAs as electron donors (Ghimire *et al.*, 2016; Brown, Wilkins and Saha, 2022).

1.1.3. Industrial and biotechnological applications

In the last decades, research on PNSBs have attracted growing interest largely because these bacteria can adapt to different and challenging environments and can use many substrates including waste-derived streams (Dhar, Venkateswarlu and Megharaj, 2023).

For this reason, several biotechnological applications have been proposed, often in a circular economy perspective (Morrison and Bose, 2025a).

An overview of the main applications of PNSBs is shown in Figure 2.

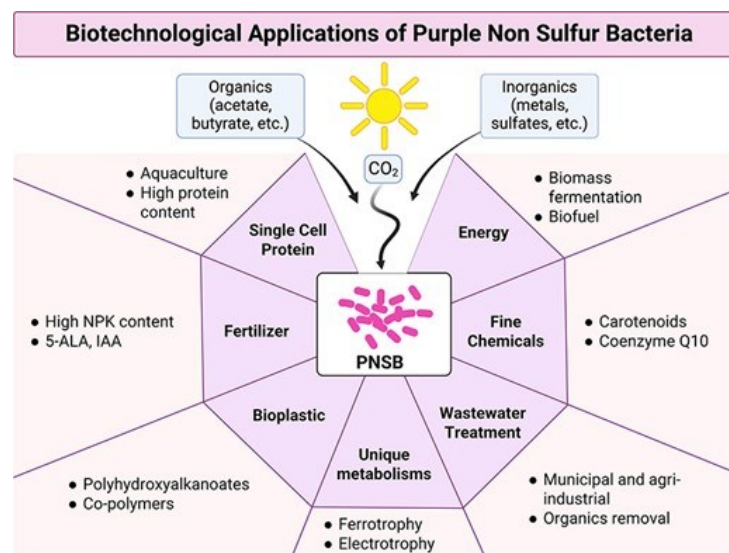


Figure 2 Main biotechnological applications of purple non-sulfur bacteria.
(Morrison and Bose, 2025b)

PNSB have been widely investigated for their potential use in sustainable biohydrogen production. Under anaerobic light conditions they can use a broad range of organic substrates as electron donors, including simple organic acids and VFAs derived from wastewater fermentation

processes (Larimer *et al.*, 2004; Moia *et al.*, 2024); this possibility to use low cost, waste derived carbon sources made them really interesting candidates for scientific researches in integration of biological hydrogen generation process into circular bioeconomy and wastewater valorization strategies.

In addition to bio-hydrogen production processes, that will be further discussed in the following sections, PNSB gained a lot of interest for their potential applications in wastewater treatment and resource recovery. Several studies in literature assess their ability to remove contaminants such as ammonia, phosphorus, sulphides and even toxic heavy metals or metalloids. Some strains also demonstrate capable to transform or degrade recalcitrant organic pollutants (Dhar, Venkateswarlu and Megharaj, 2023; Sun, Sun and Li, 2023).

In addition, PNSB can generate nutrient-rich biomass which can be valorised as single-cell protein or biobased products for agricultural use, such as fertiliser and animal feed (Kantachote *et al.*, 2016; González Cámara *et al.*, 2025; Morrison and Bose, 2025b).

A large area of research is also focusing on the ability of PNSB to accumulate intracellular storage polymers which can be valorised for the production of biopolymers, bioplastics, and biofuels (Li *et al.*, 2022; Morrison and Bose, 2025a).

Many other applications have been investigated; for example in relation to Bioregenerative Life Support Systems (BLSSs) to support long-term missions on the Moon or Mars. PNSB could be used for the valorization of organic waste, the production of edible biomass, and the generation of biohydrogen as an energy carrier.

For example, European Space Agency examined the MELiSSA concept, in which purple non-sulfur bacteria have been considered for the conversion of volatile fatty acids into biomass under anaerobic light conditions (Hendrickx *et al.*, 2006; Chiarini *et al.*, 2025).

Focusing on *R. palustris* only, it has been studied for many different of biotechnological applications, as illustrated in Figure 3, (Brown, Wilkins and Saha, 2022).

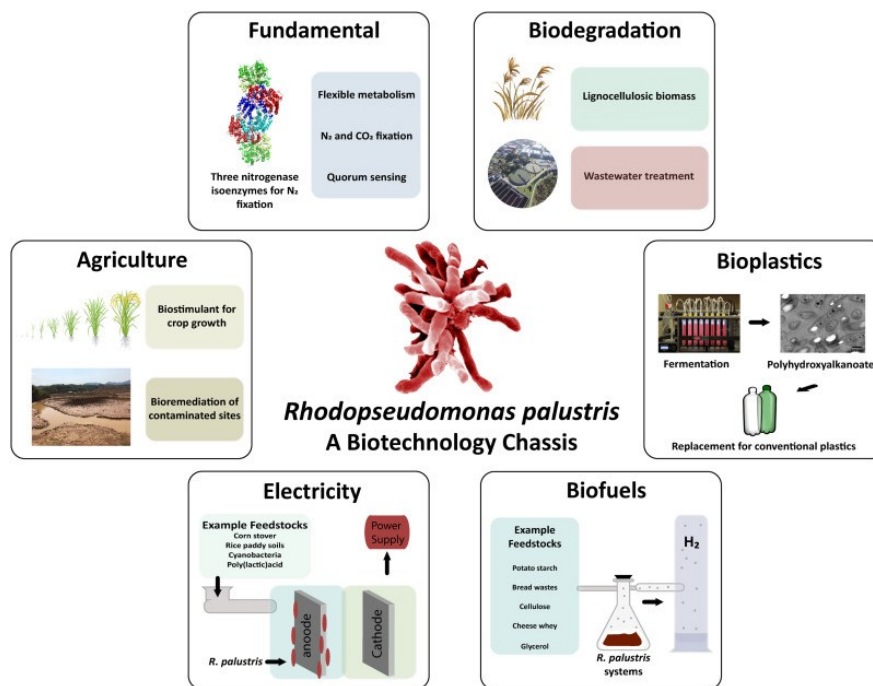


Figure 3 Main applications of *R. palustris* in biotechnological processes
(Brown, Wilkins and Saha, 2022)

R. palustris has traditionally been employed in wastewater treatment and bioremediation particularly the biodegradation of aromatic compounds and other pollutants (Brown, Wilkins and Saha, 2022; Dhar, Venkateswarlu and Megharaj, 2023).

Many studies focused on the production of valuable chemicals and valuable products such as polyhydroxyalkanoates, with a particular propensity for polyhydroxybutyrate, (Chen, Wu and Lee, 2012; Ghimire *et al.*, 2016) , biofertilizers (Kantachote *et al.*, 2016), and natural pigments such as carotenoids, which can be used as natural colorants or further converted into high-value products(Lopez-Romero *et al.*, 2020).

This thesis focuses on hydrogen production by *Rhodospseudomonas palustris*, is a research area that has gained increasing attention in these last decades. (Luxem, Nguyen and Zhang, 2022).

1.1.4. Traditional cultivation systems

Cultivation of photosynthetic bacteria is typically carried out in photobioreactors (PBRs), which are culture systems designed to support the growth of photosynthetic microorganisms, such as microalgae, cyanobacteria, and purple non-sulfur bacteria, by providing optimized and controlled illumination and environmental conditions (Chen *et al.*, 2011).

Depending on the mode of operation, photobioreactors used for biomass and hydrogen production can be broadly classified into batch, fed-batch, and continuous systems.

In general, cultivation systems can be divided into open and closed configurations.

Open systems, such as ponds or reservoirs, are primarily used for biomass production. These systems cannot provide the anaerobic conditions necessary for hydrogen production and possess a very limited degree of control over key parameters such as temperature, pH, and nutrient concentration.

In contrast, closed systems offer better control of operating conditions, and lower the risk of contamination, making them more suitable for applications, such as photofermentation. The classification of such systems is typically based on their geometric configuration, which can be tubular, flat-panel, or fermenter-type reactors, among other variants designed to optimize microbial growth and the desired metabolic production (Touloupakis, Faraloni and Carlozzi, 2022).

Batch cultivation represents the simplest and most widely used operational mode in laboratory. Microbial growth continues until one of the essential nutrients is depleted or the environmental conditions become inhibitory. This method is employed in the context of small-scale studies or for the production of initial biomass.

A fed-batch cultivation is a hybrid operating mode. The fed-batch system involves a controlled supply of one or more substrates during the process, and the product is typically collected only at the end. This approach helps avoid inhibition caused by excessive substrate concentrations, and it can prolong metabolic activity. For photofermentative processes, fed-batch operation has been widely investigated, as it offers improved control over hydrogen production rates and biomass accumulation compared to simple batch cultivation, while maintaining the advantages of a closed system (Padovani, Vaičiulyte and Carlozzi, 2015) .

Continuous cultivation involves a constant influx of fresh culture medium into the bioreactor, while an equivalent volume of culture is simultaneously removed. This configuration allows the establishment of steady-state conditions, characterized by constant biomass concentration and substrate levels, and enables sustained production over extended periods. Continuous systems are generally more complex to manage and can be more sensitive to instability or contamination. The influence of batch, fed-batch and semi-continuous cultivation strategies on photofermentative hydrogen production by *R. palustris* has been extensively investigated in controlled photobioreactor systems (Padovani et al., 2016).

1.1.5. Photobioreactors for hydrogen production

Photobioreactors are essential for cultivating photosynthetic microorganisms such as PNSB and allow photobiological hydrogen production.

Main constraints of photofermentative hydrogen production are the low light conversion efficiency, the relatively low hydrogen production rates (HPR), and the strong dependence on light availability (Adessi and De Philippis, 2014).

The design of photobioreactors for hydrogen production is fundamentally important. A key requirement for hydrogen production with PNSB is maintaining strictly anaerobic conditions, for this reason photobioreactors must be closed systems, reducing potential oxygen intrusion, and should be designed to ensure a better control of operating parameters such as pH, temperature and irradiance and allow the collection of the produced gas.

In several lab-scale studies, anaerobiosis is obtained by flushing an inert gas such as argon in the headspace of the photobioreactor, other setups avoid the headspace filling the reactor completely thus increasing the working volume and avoiding gas flushing (Uyar *et al.*, 2007).

For an efficient photofermentative process, photobioreactors must be transparent and have a high surface-area-to-volume ratio, both are critical to maximize light capture, and provide an efficient mixing to ensure uniform illumination within the reactor and to help to limit the self-shading effect at higher cell densities (Adessi and De Philippis, 2014).

Tubular and flat-panel reactors are widely adopted in laboratory and pilot-scale studies, because they can provide a short light path and a good light distribution (Adessi and De Philippis, 2014; Moia *et al.*, 2024).

Light is the key parameter (Chen *et al.*, 2011). Light intensity, spectral quality, distribution, and source have a strong influence on photosynthetic activity and hydrogen production. PNSB mainly absorb in the near-infrared region (typical peaks around 800–880 nm, linked to bacteriochlorophyll complexes), while carotenoids mainly absorb in the visible range between 450–550 nm. Artificial light sources commonly used include tungsten, halogen, and incandescent lamps, which provide broad spectra but are energy-intensive (Bosman, Pott and Bradshaw, 2023).

Light Emitting Diodes (LEDs) are increasingly used in photofermentative photobioreactors systems because it allows better control of light conditions compared to conventional lamps. LEDs emit in narrow wavelength bands and the spectrum can be selected to better match the absorption of PNSB pigments.

Besides spectrum, hydrogen production is strongly affected by light intensity.

In scaled-up system a cost-effective and sustainable solution could be the utilization of natural solar radiation, which covers the entire visible and near-infrared spectrum, however it is a variable

and discontinuous light source subjected to diurnal cycles and weather-related fluctuations (Adessi and De Philippis, 2014).

Temperature and pH also play an important role. These parameters influence bacterial physiology and enzyme activity, so keeping them in a suitable range supports stable growth and more reproducible hydrogen production. Most photosynthetic bacteria show optimal growth and metabolic activity at temperatures between 30 and 40 °C, and pH close to neutrality (Chen *et al.*, 2011).

1.2. Hydrogen as an energy carrier

Global energy demand is constantly increasing as a consequence of the expanding human activity and industrialization. At present, energy demand is still largely dominated by the use of fossil fuels; among these, oil (32%), coal (27%), and natural gas (22%) represent the most significant component of the primary energy supply, while biomass and waste (10%), nuclear energy (5%), hydroelectric power (2%), and other sources (2%) account for a relatively small amount (Sagir and Alipour, 2021).

The intensive use of fossil resources has important impacts on the environment and society; such as resource depletion and amplify concerns about energy security, geopolitical instability, and price fluctuations.

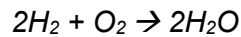
In addition, massive emissions of greenhouse gases, including carbon dioxide (CO₂) and carbon monoxide (CO) and other pollutants contribute to climate change and environmental degradation, with adverse effects on ecosystems and human health (Tiang *et al.*, 2020; Sagir and Alipour, 2021).

In response to these challenges, the development of alternative and more sustainable energy pathways has become a global priority.

In this context, hydrogen is often proposed as a sustainable energy carrier, and has gained significant attention from the scientific community and industry because it allows low-carbon energy conversion and storage when produced from renewable resources (Sagir and Alipour, 2021).

Hydrogen is the lightest and most abundant element in the universe, and under ambient conditions (25 °C, 1 atm), two hydrogen atoms form molecular hydrogen (H₂), which is a colorless and odorless gas. It has a lower heating value of 241.83 kJ/mol and exhibits a very high specific energy among known fuels (122 kJ/g) making it attractive for energy applications (Tiang *et al.*, 2020).

When hydrogen reacts with oxygen it forms water, as shown in *Formula 1*



Formula 1 (Tiang et al., 2020)

As a result, hydrogen use does not produce CO₂ during combustion. Respect to wind and solar systems, the conversion of hydrogen into electricity is independent by climate or weather conditions. This flexibility enables energy storage and the decoupling of energy generation from demand (Sagir and Alipour, 2021).

At present, hydrogen produced for industrial purposes is derived from fossil resources (approximately 96%), while a smaller fraction (around 4%) is produced by water electrolysis.

The main industrial processes for H₂ production include steam reforming of methane, coal gasification, refining and chemical waste gas utilization, and water electrolysis (Postels *et al.*, 2016; Hossain Bhuiyan and Siddique, 2025).

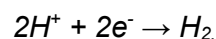
Although electrolysis does not involve direct CO₂ emissions it strongly depends on electricity, this makes its operation economically and environmentally complex (Postels *et al.*, 2016).

For these reasons, is necessary to develop alternative hydrogen production pathways with lower environmental impact and a reduced carbon footprint, while keeping the process economically competitive. Among these alternatives is Bio-hydrogen production represents an interesting option within the broader context of renewable and sustainable technologies (Tiang *et al.*, 2020).

1.3. Bio-hydrogen production

Bio-hydrogen production represents an environmentally friendly alternative to conventional H₂ production processes due to its minimal environmental impact; it can operate under mild conditions at ambient temperature and pressure, and offer the possibility to valorize renewable resources and organic-rich wastewaters. BHP processes may offer cost advantages and sustainability benefits, especially when coupled to circular bioeconomy strategies (Bianchi *et al.*, 2010; Tiang *et al.*, 2020).

The process is carbon-neutral and relies on microorganisms acting as electron sinks, reducing protons (H⁺) to molecular H₂, requiring two electron equivalents (Lee, Vermaas and Rittmann, 2010):



In addition hydrogen exhibits low solubility in water, facilitating its recovery from the liquid phase as a gas (Lee, Vermaas and Rittmann, 2010).

BHP technologies are generally classified into light-dependent processes (biophotolysis and photofermentation) and light-independent processes (dark fermentation and microbial electrolysis)(Ghimire *et al.*, 2016).

Bio-hydrogen production is based on the conversion of water and organic substrates into molecular hydrogen through organisms able to catalyze specific redox reactions by means of specific metalloenzymes; hydrogenases and nitrogenases (Luxem, Nguyen and Zhang, 2022).

Nitrogenase is a metalloenzyme that facilitates biological nitrogen fixation, reducing molecular nitrogen (N₂) to ammonium (NH₄⁺). This reaction is metabolically expensive, requiring a significant amount of ATP and a high electron supply.

Under anaerobic conditions, nitrogenase can also catalyze proton reduction to H₂, in environments where molecular nitrogen is a limiting factor (Adessi and De Philippis, 2014).

Classic or reversible hydrogenase has the capacity to catalyze both the oxidation and synthesis of molecular hydrogen via a reversible reaction.

Uptake hydrogenase, when present, functions as a catalyst, oxidize hydrogen produced by nitrogenase thereby reducing the net hydrogen yield.

Among light dependent pathways, some microalgae and cyanobacteria can produce H₂ via biophotolysis, by splitting water into H₂ and oxygen O₂ using light energy (Hallenbeck, Abo-Hashesh and Ghosh, 2012). Specific species of algae and cyanobacteria possess the capacity to utilize their photosynthetic apparatus and the enzyme hydrogenase to catalyse the following reaction:



Direct biophotolysis is strongly limited by the extreme oxygen sensitivity of hydrogenase to the oxygen produced during the reaction itself, which can rapidly inhibit enzymatic activity.

Indirect biophotolysis can overcome this issue by separating the production of oxygen from that of hydrogen in time and space. In this way enzymes are not inhibited allowing for more efficient and stable production of H₂ over time (Hallenbeck, Abo-Hashesh and Ghosh, 2012).

Dark fermentation is an anaerobic biological process in which obligate or facultative anaerobic bacteria convert complex organic substrates into progressively simpler molecules through a series of metabolic reactions, producing a biogas primarily composed of H₂ and CO₂.

It allows hydrogen to be produced from a wide variety of organic compounds and waste streams, making it one of the most practical and extensively studied methods for biological H₂ generation. Depending on the microbial community and operating conditions, fermentative reactions can occur in mesophilic (25–40°C), thermophilic (40–65°C), extreme thermophilic (65–80°C), or even hyperthermophilic (>80°C) ranges.

Unlike biophotolytic processes, dark fermentation does not produce pure molecular hydrogen and an additional downstream gas-purification step is required to obtain a hydrogen stream suitable for further use or storage (Hallenbeck, Abo-Hashesh and Ghosh, 2012).

Among the biological routes for hydrogen generation, photofermentation represents a particularly promising approach, it relies on metabolic versatility of photosynthetic bacteria to convert organic substrates into hydrogen using light as the primary energy source. This approach can be especially relevant when integrated with upstream fermentative processes, potentially improving overall substrate conversion and process sustainability (Cheng *et al.*, 2011; Ghosh *et al.*, 2017).

Table 1 synthesizes the key aspects of the biological processes for hydrogen production discussed above.

*Table 1 Biological processes for H₂ production
(Hallenbeck and Benemann, 2002; Levin, Pitt and Love, 2004; Basak and Das, 2007)*

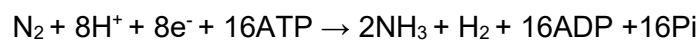
Processes	Organisms	Advantages	Disadvantages
Direct biophotolysis	Microalgae	Direct conversion of solar energy into H ₂	Self-inhibition
		High light-to-hydrogen conversion efficiency	Requirement for high light intensities
Indirect biophotolysis	Cyanobacteria	H ₂ production from water and sunlight	Requirement for high light intensities
		Presence of the nitrogenase enzyme	High ATP demand
			Presence of uptake hydrogenase
Dark-fermentation	Anaerobic bacteria	H ₂ production in the absence of light	CO ₂ and traces of CH ₄ and H ₂ S in the biogas
		Use of waste materials as substrates	Post-treatment of the effluent required
		Presence of commercially valuable by-products	Incomplete substrate utilization
Photo-fermentation	PNSB	Use of waste materials and DF effluents as substrates	Requirement for light energy to produce H ₂
		Good theoretical yields	Low light-conversion efficiency
		Complete substrate utilization	Presence of uptake hydrogenase
		Broad wavelength range	

1.3.1. Photofermentation

Photofermentation is a light-dependent biological process in which specific photosynthetic microorganisms convert organic compounds into hydrogen using light as the primary energy source.

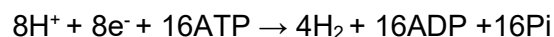
Among these organisms, purple non-sulfur bacteria (PNSBs)—such as *Rhodopseudomonas palustris*—are the most extensively studied due to their highly versatile metabolism and their ability to utilize a wide range of substrates, including malate, lactate, succinate, sugars, and volatile fatty acids typically found in dark-fermentation effluents or wastewater (Chen *et al.*, 2011). Under anaerobic and nitrogen-limited conditions, PNSB perform anoxygenic photosynthesis using light energy to generate ATP by photophosphorylation while oxidizing organic substrates as carbon and electron sources (Chen *et al.*, 2011).

Hydrogen production in PNSBs is mainly catalyzed by the enzyme nitrogenase, which is normally involved in the biological nitrogen fixation process and is strictly active under anaerobic conditions. Nitrogenase reduces molecular nitrogen (N₂) to ammonium (NH₃/NH₄⁺) through an energy-demanding reaction that requires ATP and reducing equivalents and unavoidably releases H₂ as a by-product per molecule of N₂ reduced, according to the Reaction 1 (Sagir and Alipour, 2021):



Reaction 1

Nitrogenase expression and activity are strongly repressed in the presence of excess ammonium ions (NH₄⁺). On the contrary, when nitrogen is a limiting factor, nitrogenase directly utilizes protons as electron acceptors, converting them into hydrogen according to the following Reaction 2:



Reaction 2 (Morrison and Bose, 2025a)

Nitrogenase requires high amounts of ATP, which is supplied by the photosynthetic apparatus. Electrons required for hydrogen production derive from the oxidation of organic substrates through central metabolism (mainly the tricarboxylic acid cycle) and are transferred to nitrogenase via intracellular carriers such as reduced ferredoxin and/or NADH-dependent electron transfer routes. Figure 4. Photofermentative hydrogen production process (Sagir and Alipour, 2021).

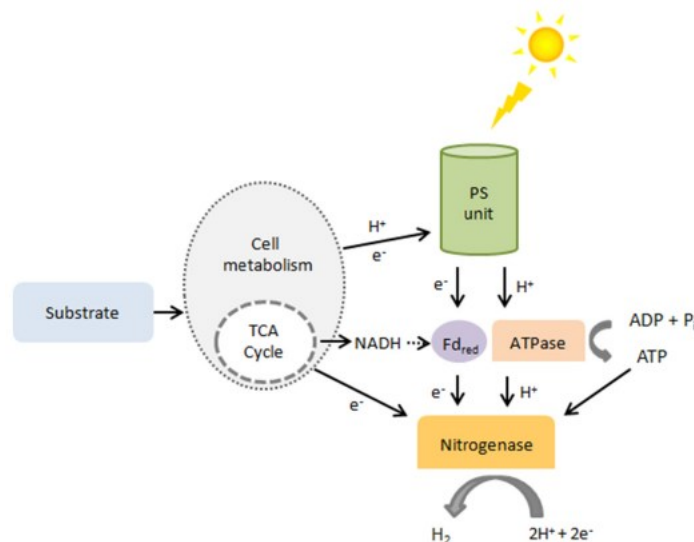
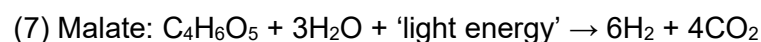
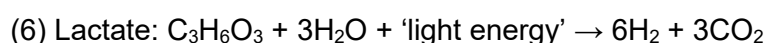
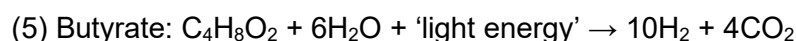
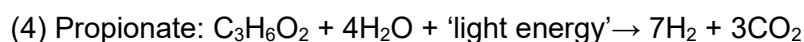
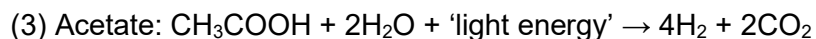


Figure 4. Photofermentative hydrogen production process(Sagir and Alipour, 2021).

In ideal nitrogen-limited and anaerobic conditions, photofermentation may approach near-stoichiometric conversion of organic acids to H_2 and CO_2 ; but actual yields are typically lower because carbon and reducing power are also needed for biomass synthesis and maintenance of metabolism, and could be redirected to intracellular storage polymer accumulation (e.g., PHB), and hydrogen re-uptake by uptake hydrogenases when present (Bianchi *et al.*, 2010; Sagir and Alipour, 2021).

Theoretical conversions for common VFAs are reported in Reactions 3 – 7:



Reactions 3 – 7(Chen *et al.*, 2011; Baeyens *et al.*, 2020)

Maximum hydrogen production in *Rhodospseudomonas palustris* is achieved when several key physiological and metabolic conditions occur.

First, highly efficient nitrogenase synthesis and activity is essential, which requires reducing power and light energy necessary to satisfy the ATP demand (Morrison and Bose, 2025a).

Finally, inoculating cultures during the exponential growth phase ensures metabolically active cells with high enzymatic activity, thereby supporting a stronger photosynthetic energy flow and enhancing overall hydrogen productivity (Androga *et al.*, 2012).

Photofermentation offers significant environmental and energetic advantages, as it can use solar energy or low-consumption artificial light sources, can operate under mild temperature and pressure conditions, and can use low-cost waste derived substrates (Sagir and Alipour, 2021). However, the process is still limited by economic and technological challenges, due to the complexity of photobioreactor design, light attenuation and distribution and in general low light conversion efficiency (Hallenbeck and Benemann, 2002; Chen *et al.*, 2011; Touloupakis, Faraloni and Carozzi, 2022) .

Photofermentative systems are also gaining interest in the aerospace sector. In the context of long-duration missions to the Moon or Mars, microbial systems are considered key components of Bioregenerative Life Support Systems, closed ecological units designed to recycle essential resources such as oxygen, water, and nutrients. Within this framework, owing to their metabolic versatility and ability to valorize organic substrates derived from waste streams, PNSB represent promising candidates for integrated bioenergy platforms supporting extraterrestrial habitats, and could contribute to resource recovery, and in situ biohydrogen (Chiarini *et al.*, 2025).

1.4. Cell immobilization

Cell immobilization is a technique in which living cells are retained within or on the surface of a solid matrix. Cells are confined into a structured microenvironment, but nutrients and gases can still diffuse so that cells can continue to carry out their metabolism but separated from the liquid media.

Immobilization has been used since the 1980s and has gradually become as a promising tool for the optimization of various biotechnological processes, including photofermentative hydrogen production (Zhang *et al.*, 2017; Ross and Pott, 2021; Sagir and Alipour, 2021).

1.4.1. Effects of immobilization: advantages and disadvantages

Cell immobilization can make the process more efficient, easier to manage and economically competitive. One of the main advantages of retaining biomass in the reactor, is that it helps to avoid cell washout and allows to operate for a longer of time without the need to harvest and re-inoculate the culture. Immobilized systems are also characterized by improved mechanical stability and to a lower risk of contamination (Sagir and Alipour, 2021; Moia *et al.*, 2024).

In addition, this technique allows to work with high cell densities than in suspended cultures and this might support higher hydrogen production rates. Working with a concentrated biomass allows to reduce reactor volume and the amount of medium required, working with a compact photobioreactor represent an advantage in terms of cost and efficiency for scaled up systems

Biomass is stably confined inside a matrix and can also be reused (Moia *et al.*, 2024). However, immobilization also has some important limitations. The matrix can be a barrier for mass transfer, limiting nutrients and metabolites transition, but also limiting light penetration which can affect photofermentative activity. For this reason, photobioreactors of immobilized systems needs to be optimized and ensure proper mixing and light distribution (Sagir and Alipour, 2021).

1.4.2. Main immobilization techniques

Immobilization can occur through natural processes or through synthetic techniques. Natural immobilization occurs spontaneously through mechanisms specific to microorganisms, a common example is as biofilm formation, where cells attach to a surface and produce extracellular polymers. This is a natural process that represents a survival strategy developed by bacteria to adapt to challenging environmental conditions, ensuring protection and structural stability (Ross and Pott, 2021; Sagir and Alipour, 2021).

With synthetic techniques specific materials and methods are used to intentionally entrap or anchor cells.

The immobilization matrix should be biocompatible with the cell, mechanically stable over time, and sufficiently porous to allow the diffusion of substances. In addition, when applied to photofermentative processes the matrix must be sufficiently transparent to allow efficient light penetration. To allow a scalable and economically competitive process the immobilization procedure should be simple and cost-effective to apply.

The most common immobilization methods are described in a review by Sagir and Alipour, (2021) and reported in Figure 5, these include adsorption, encapsulation, and gel trapping.

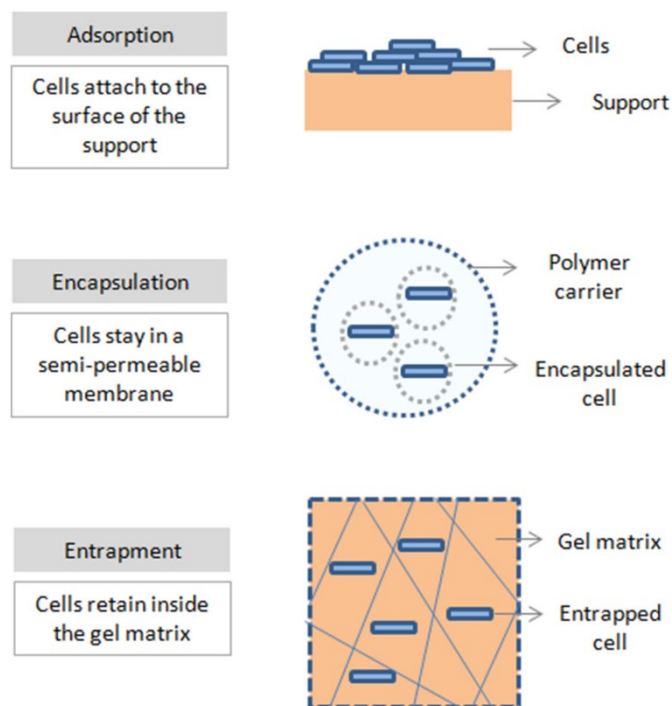


Figure 5 main methods for cells immobilization. (Sagir and Alipour, 2021)

Adsorption is a simple and reversible process based on the adhesion of cells to the surface of a physical support through weak physicochemical interactions. It is inexpensive and easy to apply, but the attachment can be unstable especially if subjected to dynamic operating conditions such as mixing.

Encapsulation confines cells within semi-permeable membranes that allow the selective passage of nutrients and metabolites while providing protection from external stresses. The most commonly used materials for encapsulation of PNSB are alginate, silica, and PVA-based systems, which are often combined to enhance optical transparency, mechanical flexibility, porosity, and stability; those properties rarely coexist in a single material so composite polymers, such as alginate reinforced with chitosan, polyurethane, or PVA, are often used to enhance mechanical strength and stability (Ross and Pott, 2021).

In gel trapping, cells are incorporated into a polymer network, that restrict their movement while enabling the exchange of nutrients and gases. This approach can protect the cells from environmental fluctuations and support promotes the formation of an anaerobic microenvironment ideal for biohydrogen production. A wide range of natural or synthetic organic and inorganic materials can be used, including carbohydrates, proteins, and polymers, but polysaccharides remain the most widely used matrices, despite their limited chemical and physical stability (Sagir and Alipour, 2021).

Among the various methods, gel trapping is one of the most promising for PNSBs such as *Rhodospseudomonas palustris*, because is relatively simple and allows to maintain high cell

density, potentially improving the productivity and stability of photofermentation process (Moia *et al.*, 2024). However, some of the materials commonly employed for gel entrapment, such as polysaccharides, exhibit low mechanical strength and stability, which can result in degradation or loss of structural integrity over time. Those properties are also strongly influenced by environmental factors such as pH, ionic strength, and the presence of chelating agents of the media (Sagir and Alipour, 2021; Moia *et al.*, 2024).

1.4.3. Alginate

Alginates are unbranched polysaccharides mainly derived from brown algae. They are composed of linear chains of (1–4)-linked α -L-guluronic acid (G) and β -D-mannuronic acid (M) residues in varying proportions. The general composition is reported in Figure 6.

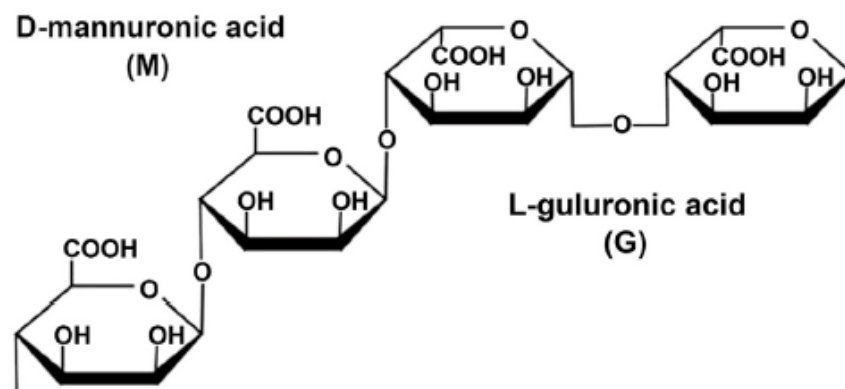


Figure 6 The main structure of alginate (Moia *et al.*, 2024)

Alginate gelation occurs through a process of ionic cross-linking, due to the exchange between the Na^+ ions of the alginate salt and divalent cations, such as Ca^{2+} .

The ability of alginate to form a gel is therefore based on ionic bonds, and its affinity for metal cations follows the ascending order: $\text{Mg}^{2+} < \text{Ca}^{2+} < \text{Sr}^{2+} < \text{Ba}^{2+}$.

Among these, the use of Ca^{2+} is the most common strategy for gelation in the presence of living cells, as it allows for a mild process that is compatible with cell vitality (Moia *et al.*, 2024).

Alginate is widely used in biotechnology because it is abundant in nature, low cost, non-toxic, and have high biocompatibility.

Among the properties that make alginate gels suitable for immobilization of photosynthetic microorganisms are:

- high transparency, which ensures adequate light penetration within the matrix;
- a relatively inert aqueous microenvironment, which preserves cell viability;
- mild encapsulation process;

- high porosity, which promotes the exchange of gases and nutrients
- the reversibility of the gelation process, which allows for the eventual recovery or reuse of immobilized cells (Draget and Taylor, 2011).

Despite these advantages, alginate-based immobilization also has some limitations. The main critical issues are about possible mass diffusion, low mechanical strength, and progressive degradation of the gel over time. Alginate gels exhibit sensitivity to chelating agents, phosphates, and anti-gelling cations, including magnesium. The mechanical and gelling properties of alginate are significantly influenced by its composition and concentration, as well as by the pH and ionic strength of the medium (Moia et al., 2024).

2. Thesis objectives

The overall goal of this thesis is to contribute to the research and development of sustainable ways for hydrogen production, focusing on photofermentation by *Rhodospseudomonas palustris*, a purple non-sulfur bacterium known for its metabolic versatility. The aim is to better understand how this microorganism behaves under different cultivation conditions and how its metabolism adapt to convert organic acids into hydrogen.

Particular attention is given to the valorization of fermentation-derived effluents, rich in volatile fatty acids, which can be used as a carbon sources. The integration of fermentation-derived effluents into photofermentative H₂ production processes is gaining particular interest in the scientific research because allows the valorization of these complex matrices, improving the overall sustainability of the processes and supporting the idea of a circular use of resources.

Compared to defined substrates, fermentation effluents represent a complex and challenging matrix, it requires to address issues related to variability in composition and the presence of possible inhibitory compounds can affect process performance.

The objectives of this thesis are to monitor the growth and metabolic activity of *R. palustris* under different operating conditions, evaluating the influence of the carbon source and nutrients availability on biomass development and performance.

Batch tests were conducted with suspended biomass using different organic substrates including malic acid, acetic acid, lactic acid, and a fermentation effluent rich in VFA. Then to compare hydrogen production among the tested conditions, to relate H₂ evolution to biomass growth and substrate consumption.

A further objective was to explore the effect of cell immobilization on alginate matrix as a potential tool to improve operational robustness and stability. Immobilized biomass and suspended system behaviour were compared in order to analysing the potential impact of immobilization on photofermentative hydrogen production.

Finally, the biomass obtained from each test was characterized in terms of lipids, carbohydrates, and proteins in order to correlate cell composition with growth, substrate consumption and photofermentative capacity.

3. Materials and methods

All experimental activities were performed at the Environmental engineering Laboratory of Ca' Foscari University of Venice. This chapter outlines the equipment, materials, and methods used during the study. Standardized procedures and consistent analytical techniques were applied in all tests to ensure uniform, reliable, and comparable results.

3.1. Microorganism and inoculum preparation

The initial inoculum was obtained from a pre-existing *Rhodopseudomonas palustris* culture, which was subsequently acclimatised and routinely maintained in suspension on synthetic RPN and RPP media with malic acid as carbon source. Cultures were incubated under sterile conditions at 30°C, with continuous lighting using a white-LED light at 4000 K at a light intensity of 80 $\mu\text{mol m}^{-2} \text{s}^{-1}$, and constant orbital shaking at 150 rpm to ensure homogeneous mixing.

3.1.1. Colony selection on solid agar

Rhodopseudomonas palustris colonies were isolated and maintained on tubes containing RPN medium supplemented with 1.5% (w/v) agar solidified in a slanted position. To ensure anaerobic conditions the headspace of each tube was purged with argon gas to displace oxygen before incubation. After incubation well-isolated colonies were selected based on morphological appearance and characteristic reddish color, typical of purple non-sulfur bacteria. Selected colonies were then transferred into liquid RPN medium to establish starter cultures, which were used as inocula for subsequent experiments.

3.2. Synthetic media composition

R. palustris was cultivated in two different synthetic media: RPN synthetic medium (Table 2), designed to promote cell growth, and RPP medium, formulated to stimulate hydrogen production under photofermentative conditions (Bianchi *et al.*, 2010).

Table 2 Composition of the synthetic RPN medium used for the growth of *Rhodospseudomonas palustris*.

RPN	Conc (g L ⁻¹)
DL-malic acid	2.0
NH ₄ Cl	0.5
K ₂ HPO ₄	0.5
KH ₂ PO ₄	0.3
MgSO ₄ ·7H ₂ O	0.4
NaCl	0.4
CaCl ₂ ·2H ₂ O	0.075
Ferric citrate(1g·L ⁻¹)	5 mL L ⁻¹
Yeast extract	0.4
Trace elements PNSB	1 mL L ⁻¹
Vitamins	1 mL L ⁻¹

Trace elements composition is shown in Table 3

Table 3 Trace elements in synthetic RPP and RPN media

1000x Trace elements PNSB	Conc (g L ⁻¹)
H ₃ BO ₃	0.30
MnCl ₂ ·4H ₂ O	0.03
ZnSO ₄ ·7H ₂ O	0.10
Na ₂ MoO ₄ ·2H ₂ O	0.30
CuCl ₂ ·2H ₂ O	0.01
NiCl ₂ ·6H ₂ O	0.02
CoCl ₂ ·6H ₂ O	0.02

The final pH of the medium was adjusted to 6.8 by adding KOH.

After sterilizing the medium in an autoclave (120°C, 1.1 bar, 20 min), a vitamin solution (1 mL, sterilized by 0.2 µm filtration) was added. Its composition is shown in Table 4

Table 4 Vitamin's solutions composition used for RPN and RPP media

1000x Vitamins	Conc (g L ⁻¹)
Biotin	0.3
Niacin	0.03
Tiamin dichloride	0.1
p-aminobenzoic acid	0.3
Pyridoxolium hydrochloride	0.01
Ca-pantothenate	0.02
Vitamin B12	0.02

The RPP medium differs from RPN because it contains a higher concentration of DL-malic acid (4 g L⁻¹) and sodium glutamate (0.4 g L⁻¹) as a readily assimilable nitrogen source, and yeast extract and NH₄Cl were omitted to avoid additional nitrogen inputs.

In hydrogen production tests, the RPP medium was supplemented with malic acid (4.0 g L⁻¹), lactic acid (3.7 g L⁻¹), or acetic acid (3.8 g L⁻¹), depending on the experimental condition. Lactic acid and malic acid were chosen since they are the most used for H₂ production, acetic acid is on the other hand the main component of fermentations effluents (Barbosa *et al.*, 2001).

To enable *Rhodopseudomonas palustris* to use acetic acid and lactic acid as its sole carbon sources, a progressive adaptation protocol was implemented. This strategy follows the approach used in a study where *R. palustris* strains are gradually adapted to metabolize challenging substrates, such as halogenated aromatic compounds (e.g., 3-chlorobenzoate) (Haq, Christensen and Fixen, 2024).

The adaptation procedure consisted of a series of sequential cultivation steps in which the concentration of the target substrate was gradually increased while reducing the amount of DL-malic acid from the standard RPP medium. This incremental exposure allowed the microbial population to gradually acclimate metabolically.

Medium used in hydrogen production test with immobilized biomass, named “modified RPP medium” differs from the standard RPP since glutamate was excluded to maintain the culture under nitrogen-limited conditions and stabilize biomass concentration, and phosphates were reduced to avoid beads degradation. Trace elements and vitamin composition were identical to those of the standard media (Table 3 - Table 4).

3.3. Fermented effluent

A real fermented effluent (Figure 7) was used to evaluate the growth and hydrogen production performance of *Rhodospseudomonas palustris* on complex waste derived substrates.

The effluent was obtained from semi-solid anaerobic fermentation of a mixed organic feedstock composed of excess activated sludge and a blend of organic residues, including vegetable waste (lettuce and beetroot), lignocellulosic material (straw), and cellulose-based waste (toilet paper). This mixture was designed to simulate organic waste streams potentially generated in bioregenerative life support systems for space habitats.

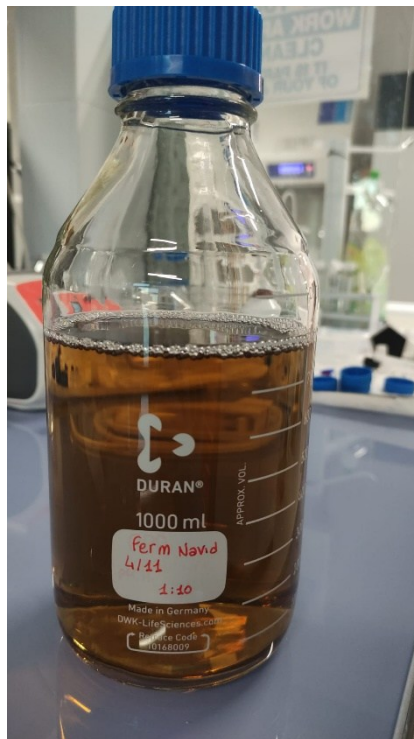


Figure 7 Fermented substrate used in batch experiments, after dilution (1:10) and prior to inoculation

Prior to its use in biological experiments, the effluent was chemically characterized in terms of total volatile fatty acids and ammonium nitrogen ($\text{NH}_4^+ - \text{N}$).

Based on this characterization, a dilution factor (FD) of 10 was selected to reduce potential matrix-related limitations (for example, high turbidity and elevated ammonium).

Table 5 Chemical characterization of the diluted fermented effluent used in batch experiments.

Before being used as a cultivation medium, the fermentation effluent was pretreated to minimize inhibitory effects and ensure suitable growth conditions for *R. palustris*:

- Centrifugation: to remove suspended and colloidal particles, which would otherwise increase turbidity and impair light penetration.

- Filtration: the supernatant was passed through a 0.2 μm syringe-filter to further clarify the medium and remove residual solids.
- Dilution: the clarified broth was diluted 1:10 with distilled water to reduce matrix complexity and potential inhibitory compounds.
- pH adjustment: the pH was adjusted to 6.8 using NaOH to match standard cultivation conditions.
- Sterilization: the treated broth was sterilized by autoclaving prior to use to prevent contamination and ensure controlled growth conditions.

Table 5 Chemical characterization of the diluted fermented effluent used in batch experiments.

VFA tot	N-NH ₄ ⁺	C/N
g L^{-1}	mg L^{-1}	mol-C/mol-N
8.23	≈105	≈48

In the diluted effluent, acetate was a major component and the most abundant single VFA (2.14 g L^{-1}), together with propionate (1.15 g L^{-1}), Relevant fractions of C₅ and C₆ VFAs were also detected, corresponding to valeric acid and caproic (hexanoic) acid and their branched isomers (i-C₅, n-C₅, i-C₆, n-C₆).

3.4. Light source

All batch experiments were carried out under continuous illumination provided by 4000 K white LEDs at a light intensity of 80 $\mu\text{mol m}^{-2} \text{s}^{-1}$, measured at reactor surface.

Light is a key operational parameter for purple non sulfur bacteria since their photoheterotrophic metabolism relies on light harvesting pigments to convert light energy into ATP and reducing power, essential for both growth and nitrogenase-driven hydrogen production (Sagir and Alipour, 2021).

The absorption spectrum of purple bacteria covers the visible region and the near-infrared region, where bacteriochlorophylls show major absorption peaks.

Also, spectral composition and light distribution inside the culture are critical factors affecting hydrogen productivity (Tiang *et al.*, 2020).

The use of LED lighting was motivated by its low thermal emission, and by the ability to provide stable and reproducible illumination conditions across the tests and the chosen light intensity represents a compromise between biological requirements and cost optimization, which is

particularly relevant in view of potential scale-up. In addition, LEDs are reported as a more energy-efficient alternative to conventional tungsten lighting, with a substantially longer lifetime and lower operating costs (Adessi and De Philippis, 2014; Tiang *et al.*, 2020).

It should be noted that these light conditions were not specifically optimized for maximum hydrogen production. In particular, Tiang *et al.* (2020) report hydrogen productivity in PNSB can vary depending on light source and wavelength. In their review they explain that LED-based systems are widely adopted with white LEDs often performing well in *R. palustris* compared to other visible wavelengths since they provides a broad emission spectrum in the visible range, but red/NIR- illumination can be more favourable for optimized H₂ production with PNSB. This is further supported by Uyar *et al.* (2007) which report that when the 750–950 nm region is removed, hydrogen production can be markedly reduced and delayed.

The selected light intensity in this study provides a sufficient photon flux to ensure robust and comparable growth across experiments to allow the evaluation of the effects of carbon source and medium composition on H₂ production.

3.5. Batch tests in suspension for biomass production

Batch were conducted in glass bottles with a working volume of 200 mL, an initial OD₆₆₀ of 0.1. Cultures were incubated at 30 °C under continuous orbital shaking (150 rpm) and constant illumination. The bottles were sealed using screw caps with silicone seals perforated to allow the insertion of a 1 mL syringe fitted with a hydrophilic cotton filter, providing a controlled pathway for gas exchange, as shown in Figure 8.

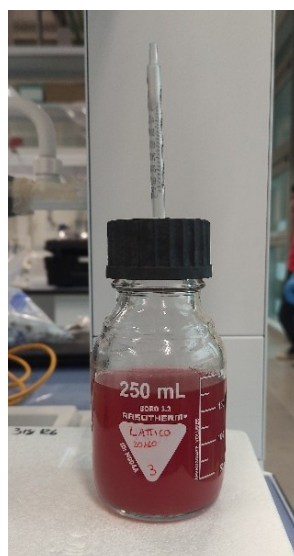


Figure 8 250 mL glass bottle used to for growth monitoring of *R. palustris* in batch

The tests using both RPN and RPP media with different carbon sources were performed in triplicate and lasted for one week each.

The experimental design included the culture conditions reported in Table 6

Table 6 Overview of growth tests in suspension performed with Rhodopseudomonas palustris

BATCH TEST IN SUSPENSION	
Growth Media	Carbon Source
RPN	Malic acid
	Acetic acid
	Lactic acid
RPP	Malic acid
	Acetic acid
	Lactic acid
Fermented substrate	Complex mix of VFA, mostly acetate

3.6. Growth monitoring

Samples were collected by temporarily opening the vessels under sterile conditions. Prior to each sampling event, agitation was temporarily increased to ensure homogeneous suspension of the biomass.

Liquid samples were collected at regular time intervals to monitor biomass growth and process evolution. In all experiments, sampling was performed every 24 h by withdrawing 2 mL of culture. During the exponential growth phase, corresponding to the first 24 - 28 h of cultivation, the sampling frequency was increased to better capture rapid variations in biomass concentration.

Collected samples were immediately analysed for optical density. Subsequently, samples were filtered through 0.2 µm membrane filters to remove residual biomass and stored at -5 °C.

Filtered samples were later used for the quantification of organic substrates by high-performance liquid chromatography (HPLC) or enzymatic kit (for D/L lactic acid) and for the determination of ammonium concentration.

At the end of each test biomass was collected for dry weight measurement to determine the OD-DW calibration curve for each tested condition.

In immobilized tests only optical density was considered.

3.6.1. Optical density

Optical density was used as an indirect measure of cell concentration. The analysis was conducted using UV–Vis spectrophotometry at a wavelength of 660 nm, corresponding to the maximum absorption characteristic of the bacterial suspension (Bosman, Pott and Bradshaw, 2023).

The instrument (Spectrophotometer ONDA UV-31 SCAN, Spectrophotometer UV/VISIBLE) quantifies the turbidity of the culture, which is proportional to the biomass concentration, by measuring the amount of light scattered or absorbed by the sample. The blank, consisting of the culture medium alone, was measured at the same wavelength and subtracted from the sample absorbance.

The optical density was calculated according to the following equation:

$$OD_{660} = Abs \times Df$$

Where OD_{660} is the optical density at 660 nm,
 Abs is the absorbance of the sample without blank,
 Df is the dilution factor.

3.6.2. Dry weight

Dry weight measurement allows the determination of the amount of biomass present in known volume of a sample.

The appropriately diluted samples were filtered on a vacuum filtration system through 0.22 μm pre-weighted (P_0) acetate cellulose sterile filters. After filtration, the filters were placed in an oven at 105°C for 24 hours and then weighed again (P_1).

The biomass concentration in each volume was calculated using the following formula:

$$\text{Dry weight (g L}^{-1}\text{)} = \frac{P_1 - P_0}{V}$$

The DW measurements were correlated with OD_{660} values obtained by spectrophotometry to generate a calibration curve for estimating biomass concentrations during the experiments.

To enable a quantitative comparison of biomass formation under the different experimental conditions, calibration curves correlating OD-DW were established for each culture medium and carbon source.

Linear regression models were used to describe the relationship between OD_{660} and DW, and the resulting equations and coefficients of determination (R^2) are reported in Table 7.

Table 7 OD_{660} -dry weight calibration curves (linear regression equations and R^2) for each medium/substrate condition.

TEST	Equation	R^2
RPN	$y = 3,6528x$	$R^2 = 0,9878$
RPP	$y = 4,6801x$	$R^2 = 0,9788$
RPN +AA	$y = 1,7635x$	$R^2 = 0,9206$
RPP+AA	$y = 4,3641x$	$R^2 = 0,9752$
RPN+AL	$y = 3.3306x$	$R^2 = 0,9714$
RPP+AL	$y = 3,3758x$	$R^2 = 0,9964$
FERMENTED	$y = 1,3412x$	$R^2 = 0,9752$

For all tested conditions, the obtained R^2 values were consistently high ($R^2 \geq 0.92$), indicating a strong linear correlation between optical density and biomass concentration. These results confirm that OD_{660} can be reliably used as a proxy for biomass quantification within the investigated range.

3.6.3. Growth rate and biomass productivity

The evaluation of *R. palustris* growth kinetics was performed to quantify the rate of biomass formation under the tested culture conditions.

The specific growth rate (μ) was determined by linearizing the exponential growth model of microorganisms using the natural logarithm transformation.

$$X = X_0 e^{\mu t}$$

The equation becomes:

$$f(\mu) = \ln\left(\frac{X_n}{X_0}\right)$$

Where:

- X_n : biomass concentration at time t (g L^{-1}),
- X_0 : initial biomass concentration (g L^{-1}).

The specific growth rate therefore represents the daily rate of biomass increase and it is measured in h^{-1} .

Biomass productivity (P_x) is a measure of the rate at which biomass is produced in a bacterial culture. It is expressed in grams per liter per day ($\text{g L}^{-1} \text{d}^{-1}$).

The formula used to calculate biomass productivity is as follows:

$$P_x = \frac{(DW_2 - DW_1)}{t_2 - t_1}$$

Where:

- DW_2 = Final dry weight (g L^{-1}) of the exponential phase;
- DW_1 = Initial dry weight (g L^{-1}) of the exponential phase;
- t_2 = Final time (d) corresponding to the end of the exponential phase;
- t_1 = Initial time (d) corresponding to the beginning of the exponential phase.

3.7. Batch tests for H_2 production

Photofermentative hydrogen production was conducted in a cylindrical glass photobioreactor, with a total volume of 550 mL, with internal diameter of 4 cm.

The experimental setup was placed on a thermostatic chamber with an heating plate that maintained a constant temperature of 30°C and mixed by continuous magnetic stirring with white-LED light (4000K) with $80 \mu\text{mol m}^{-2} \text{s}^{-1}$ intensity at placed the top of the photobioreactor. To ensure anaerobic conditions the headspace was purged with Argon gas for 15 minutes.

The initial inoculum was established at $\text{OD}_{660} = 0.1$ to facilitate the observation of microbial growth and to correlate organic acids consumption with hydrogen production and biomass formation.

For OD_{660} analysis liquid samples were withdrawn through a dedicated sampling port, minimizing disturbance of the system.

pH was constantly monitored and kept at 6.8 ± 0.2 , adding NaOH (1M) if necessary.

The gas generated during the photofermentation tests was quantified using a volumetric measurement method based on the principle of liquid displacement. The system consists of a graduated column filled with distilled water and hermetically connected to the photobioreactor. The gas produced inside the reactor rises through the connecting pipe and accumulates at the top of the column, gradually displacing the liquid. The volume of gas collected is equivalent to the volume of liquid displaced by the measuring cylinder.

Figure 9 illustrates the layout of the experimental system used for photofermentative hydrogen production:

1. Heating plate,
2. Magnetic stir bar
3. Cylindrical Photobioreactor;
4. pH probe;
5. Connection to the gas trap and gas sampling point
6. Beaker with distilled water and graduated column for gas collection;

7. White LED

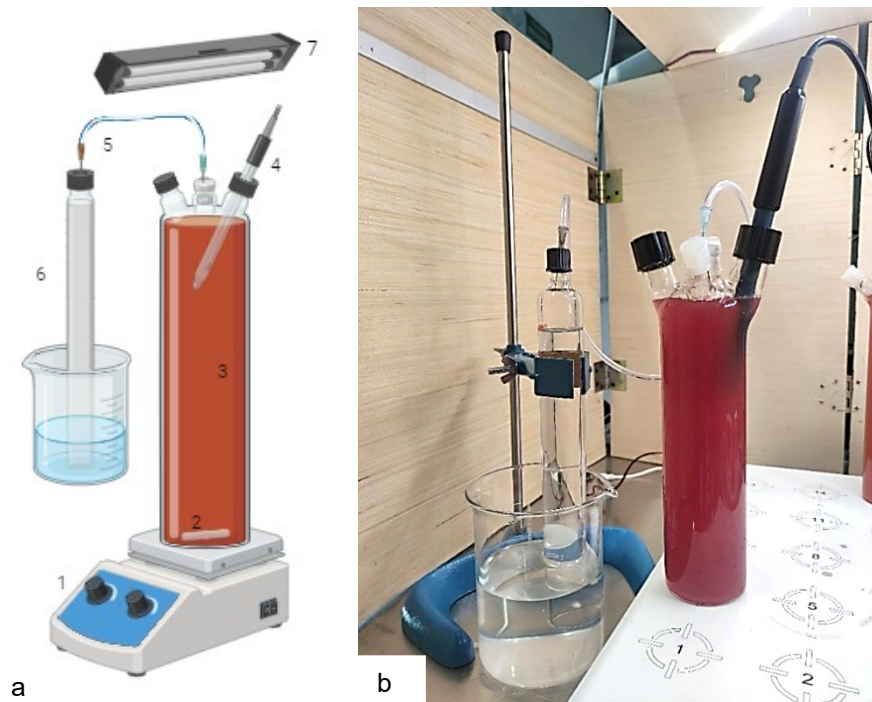


Figure 9 a. Schematic representation of experimental system.
b. Photobioreactors for H₂ production

This configuration allows for a direct and continuous estimation of the volume of hydrogen produced and also the monitoring the progress of the photofermentation process over time, providing a quantitative indication of the bacterial metabolic activity.

Qualitative and quantitative analysis of the gases produced was performed using a portable Agilent 990 Micro Gas Chromatograph (Mobile Micro GC) to determine their percentage composition and confirm the presence of hydrogen as the main component.

3.7.1. H₂ production monitoring

During batch experiments for hydrogen production, gas generation was monitored over time and the composition of the produced biogas was analysed at regular intervals.

Gas samples were collected through the reactor sampling port and analysed by micro gas chromatography (microGC) equipped with a thermal conductivity detector (TCD) for the quantification of H₂ and CO₂. Argon and helium were used as carrier gases.

The volumetric fraction of hydrogen in the gas phase was determined for each sampling time and used to calculate the corresponding hydrogen volume based on the total volume of gas produced.

The cumulative hydrogen production ($V_{H_2,cum}$) was calculated by summing the incremental hydrogen volumes measured over time (ΔV_{H_2}) throughout the experimental duration.

All gas volumes were converted into molar hydrogen production (n_{H_2}) using the ideal gas law assuming the operating as conditions $T = 30^\circ\text{C}$, and atmospheric pressure.

Hydrogen production performance was evaluated by calculating the hydrogen production rate (HPR) and the substrate-to-hydrogen conversion yield (SCE).

HPR was defined as the discrete variation of cumulative hydrogen production over time, normalized to the reactor working volume (V_R), as reported in Equation 1:

$$HPR = \frac{n_{H_2,cum}(t_2) - n_{H_2,cum}(t_1)}{V_R(t_2 - t_1)}$$

Equation 1

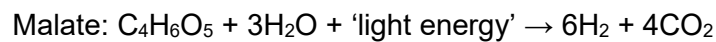
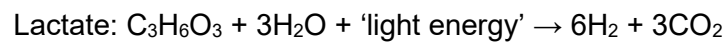
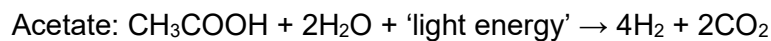
Where $n_{H_2,cum}(t)$ is the cumulative hydrogen produced (mmol) at time t , V_R is the reactor working volume (L), and t is expressed in days.

HPR_{max} was taken as the maximum value among the sampling intervals.

The substrate conversion efficiency (Equation 2) was calculated as the ratio between the experimentally produced hydrogen and the theoretical hydrogen production expected from complete conversion of the consumed substrate according to stoichiometric reactions reported in the literature (Uyar *et al.*, 2007).

$$SCE = \frac{H_2 \text{ experimental}}{H_2 \text{ theoretical}} \times 100$$

Equation 2



3.8. Medium Analysis

Particular attention was given to VFA and ammonium ions, as they play a central role in photofermentative metabolism. VFAs serve as key carbon and electron sources for *R. palustris* and monitoring their temporal profiles is important to quantify substrate depletion and relate carbon conversion patterns to biomass growth and H_2 production kinetics. Ammonium was

monitored because it is a readily assimilable nitrogen source for *R. palustris* and is known to repress nitrogenase activity, thereby negatively affecting hydrogen production.

3.8.1. VFA analysis

To monitor VFA consumption trends, a 2-ml sample of the culture was collected daily and filtered through a 0.2 µm syringe filter to remove cells and suspended particles. The concentration of acetic and malic acid in the cultivation media was measured using an HPLC (Agilent Technologies 1100 series, Santa Clara, CA, USA) column Acclaim™ Organic Acid 5 µm 4x150 mm with a mobile phase of methanesulphonic acid 2.5 mM and acetonitrile at a flow rate of 1 mL/min.

The D/L-Lactic Acid Assay Kit (Megazyme) has been used for the specific determination of lactic acid content.

Substrate removal efficiency was calculated to quantify VFA consumption over the experimental period. In particular, the removal efficiency of malic acid, acetic acid and lactic acid was calculated based on reported equation:

$$E(\%) = \frac{C_{in} - C_{fin}}{C_{in}} \times 100$$

where E is the substrate removal efficiency (%), C_{in} is the initial VFA concentration in the cultivation medium, and C_{fin} is the final VFA concentration.

3.8.2. Ammonium concentration

Ammonium concentration was monitored due to its key regulatory role in photofermentative hydrogen production. Ammonium ions are readily assimilable nitrogen sources for PNSB; however, they strongly inhibit nitrogenase activity, leading to a marked reduction in hydrogen production rates. Tracking ammonium levels is therefore essential to interpret hydrogen yields correctly and to assess potential nitrogen-repression effects. For quantification, samples (2 mL) were first filtered (0.2 µm) to remove cells and particulates and then diluted.

Ammonium was then measured using a cationic ion chromatography system (Metrohm 761 compact IC) equipped with a Metrosep C3 250/4.0 cation separation column.

A calibration curve was prepared using NH_4^+ standards (25, 50, and 100 mg L⁻¹). The calibration showed a linear response within the working range, and the resulting regression was used to convert peak areas (µS cm⁻¹ s) into ammonium concentrations (mg L⁻¹) for all samples.

3.9. Immobilization on alginate matrix

To immobilize bacterial biomass in sodium alginate beads were prepared by ionic gelation in calcium chloride solution (CaCl_2).

Different alginate concentrations (2%, 4%, and 6% w/v) were initially tested to determine the most suitable formulation that could combine an efficient H_2 production and good mechanical resistance of the beads. In addition, different initial optical densities of the inoculum, $\text{OD}_{660} = 0.1$, 0.2, 0.4, and 1.2 were tested to monitor bacterial growth within the immobilization matrix.

For hydrogen production tests, higher initial biomass concentration was used (see Section 3.8.3).

3.9.1. Immobilization procedure

The immobilization protocol includes two main steps:

1. Preparation of the bacterial inoculum
2. Preparation of alginate–bacteria beads

Both procedures are described in detail below.

3.9.1.1. Preparation of the Bacterial Inoculum

The bacterial inoculum used for bead preparation was obtained from an actively growing *Rhodospseudomonas palustris* culture in RPN medium. Cells were collected during the exponential phase to ensure high metabolic activity and viability.

An aliquot of culture was centrifuged at 3900 rpm for 15 minutes to remove the growth medium. The resulting pellet was gently resuspended in a known volume of autoclaved deionized water, thus obtaining a sterile and nitrogen-free cell suspension suitable for immobilization.

The concentrated suspension was then used to inoculate the sterile sodium alginate solution. For bead production aimed at monitoring biomass growth, the alginate mixture was adjusted to an initial OD_{660} of 0.1. In contrast, for hydrogen production experiments, the inoculum concentration was increased to reach an initial OD_{660} of 3.0.

The final volume used to inoculate alginate solutions corresponded to 10 μL of concentrated cell suspension per mL of alginate solution.

3.9.1.2. Preparation of Alginate–Bacteria Beads

The immobilization of *R. palustris* in alginate was performed testing the following combinations of sodium alginate and calcium chloride concentrations (Table 8).

Table 8 Alginate and CaCl₂ concentrations tested for *R. palustris* immobilization (w/v).

Formulations tested for alginate bead preparation	
Sodium alginate (% w/v)	Calcium chloride (% w/v)
2	2
4	4

Although 6% (w/v) alginate was initially evaluated, only 2% and 4% formulations were carried forward for bead production and batch tests due to the extremely high viscosity of 6% alginate solution that made impossible beads formation.

Sodium alginate (sodium alginate salt) was dissolved in distilled water and sterilized by autoclaving.

After adding the bacterial inoculum, the mixture was refrigerated at 4 °C for approximately 2 hours to allow air bubbles formed due to the high viscosity of the solution to dissipate.

Bead formation was achieved by dripping the alginate–bacteria mixture into a sterile calcium chloride solution using a peristaltic pump (flow rate = 48 mL min⁻¹) as shown in Figure 10.



Figure 10 immobilization procedure; Dripping of the alginate solution containing *R. palustris* using a peristaltic pump into a CaCl₂ solution for the formation of immobilized microspheres.

The beads were left in the calcium chloride solution overnight to allow complete gelation and were then rinsed with autoclaved deionized water. All steps were carried out under aseptic conditions.

3.9.2. Growth monitoring of immobilized biomass

To monitor biomass growth inside the alginate beads, the beads were first dissolved, and the released cells were then analyzed by spectrophotometry. Samples were collected daily for growth-curve construction. Each sample of beads was dissolved in 0.5 M sodium citrate using a bead-to-citrate ratio of 1:4 (v/v).

After dissolution, the optical density of the released biomass was measured at 660 nm using a spectrophotometer, subtracting the blank.

In this experimental configuration, dry weight could not be determined because the high viscosity of the alginate matrix made filtration not feasible.

3.9.3. H₂ production with immobilized *R. palustris*

For hydrogen production tests with immobilized biomass, alginate beads were prepared using a higher initial inoculum corresponding to OD₆₆₀ = 3.0.

The photobioreactor was operated under the same illumination and environmental conditions described in Paragraph 3.7

Since immobilized beads require homogeneous exposure to light, adequate mixing was ensured throughout the experiment. The reactor was loaded with 150 mL of alginate beads and 400 mL of culture medium, and mixing was maintained by magnetic stirring to promote uniform light distribution and nutrient diffusion. This operational choice is consistent with literature on alginate-immobilized purple bacteria, where stirring is commonly used and insufficient mixing can lead to bead aggregation and reduced light penetration, with a negative impact on H₂ productivity (Moia *et al.*, 2024).

The biogas generated during photofermentation was collected using volumetric water-displacement traps connected to glass cylinders and subsequently analyzed by micro-GC to determine its composition.

3.10. Biomass characterization

At the end of each test, the biomass was collected by centrifugation at 9000 rpm for 15 minutes. After removing the supernatant, the pellet was washed with distilled water, resuspended and centrifuged three times to ensure the removal of culture medium residues. The pellet was freeze-dried and used for the analyses described below to quantify the intracellular lipids, proteins, and carbohydrates accumulated during growth.

3.10.1. Lipid analysis

The quantification of the lipid content present in the bacterial biomass is achieved through spectrophotometric analysis based on the sulfo-phospho-vanillin technique (Mishra *et al.*, 2014). Freeze-dried biomass (2 mg) was suspended in 1 mL of Milli-Q water and homogenized.

Then, 100 μ L of the suspension was mixed with 2 mL of concentrated H₂SO₄ and heated at 100°C for 10 min, followed by cooling on ice for 5 min.

Subsequently, 5 mL of phospho-vanillin reagent was added and allowed to react for 15 min at 40°C, with gentle mixing. After 45 min of cooling in the dark, absorbance was read at 530 nm. The blank was prepared by replacing the sample with Milli-Q water.

Calibration was performed using rapeseed oil (0.2–20 mg mL⁻¹) processed in the same way.

3.10.2. Protein analysis

Protein content was determined using the Bradford spectrophotometric assay (Andreeva, Budenkova, Babich, Sukhikh, Ulrikh, *et al.*, 2021)

Freeze-dried biomass (1–2 mg) was solubilized in an equal volume (1–2 mL) of 0.5 M NaOH and heated at 80°C for 10 min, followed by centrifugation at 3900 rpm for 20 min. In a 3-mL cuvette, 2 mL of Bradford reagent, 40 μ L of supernatant, and 1.96 mL of distilled water were mixed. After 10 min of incubation, absorbance was measured at 595 nm. The blank was prepared following the same procedure with Milli-Q water instead of the sample.

Calibration was performed with BSA (Bovine Serum Albumin) standard solutions at different concentrations (0.2, 0.4, 0.6, 0.8 e 1.0 mg mL⁻¹).

Bradford reagent was prepared by adding 100 mg di Coomassie Brilliant Blue G-250 in 50 mL ethanol 95%. Then, adding 100 mL phosphoric acid 85% and 850 mL distilled water; the solution can be stock in the dark in a brown bottle.

3.10.3. Carbohydrate analysis

Carbohydrate quantification was conducted using the phenol-sulfuric acid method (Andreeva, Budenkova, Babich, Sukhikh, Dolganyuk, et al., 2021).

Freeze-dried biomass (2 mg) was dissolved in 2 mL of distilled water. An aliquot of 1 mL was mixed with 3 mL of concentrated H₂SO₄ and 1 mL of 5% phenol.

The mixture was heated at 90°C for 5 min and cooled to room temperature before measuring absorbance at 490 nm.

A blank was prepared using Milli-Q water instead of the sample.

Calibration was established using glucose standards (0–100 µL, final volume 2 mL).

4. Results and discussion

This chapter presents and discusses the results of the tests with *Rhodopseudomonas palustris*, with particular attention to how the carbon source and the operating conditions influence growth performance and hydrogen production.

The first section focuses on batch tests with suspended biomass and compares results obtained with different substrates (malic, acetic, lactic acid and fermented media) in terms of growth kinetics and ammonia concentration. The second section explores the H₂ production profiles in relation to growth and VFA consumption.

Then discuss the performance of biomass immobilized in alginate matrices.

The final section focuses on the biochemical characterization of biomass by analyzing the lipid, protein, and carbohydrate composition as a function of the growth conditions.

4.1. Reactivation of *Rhodopseudomonas palustris* biomass

The first weeks of the experimental activity were dedicated to the reactivation of the *Rhodopseudomonas palustris* biomass, this step was necessary to obtain an active and metabolically stable culture for the subsequent growth and hydrogen production tests.

The initial biomass had been stored in sealed bottles, kept at room temperature and exposed to natural laboratory light, as shown in (Figure 11a). Since these conditions lead to a gradual decrease in metabolic activity, a reactivation phase was required.

Under sterile conditions, an aliquot of culture (approximately 10–20 mL) was taken from the storage bottle and inoculated into 200 mL of fresh RPN synthetic medium (Figure 11b). The bottle was then placed in the illuminated thermostated chamber (30 °C, white-LED lamp with intensity of approximately 80 μmol photons m⁻² s⁻¹).

During the week-long reactivation phase, the culture was monitored daily by visual assessment of the colour shift towards the characteristic red-violet pigmentation typical of active PNSB, and optical density measurements at 660 nm.

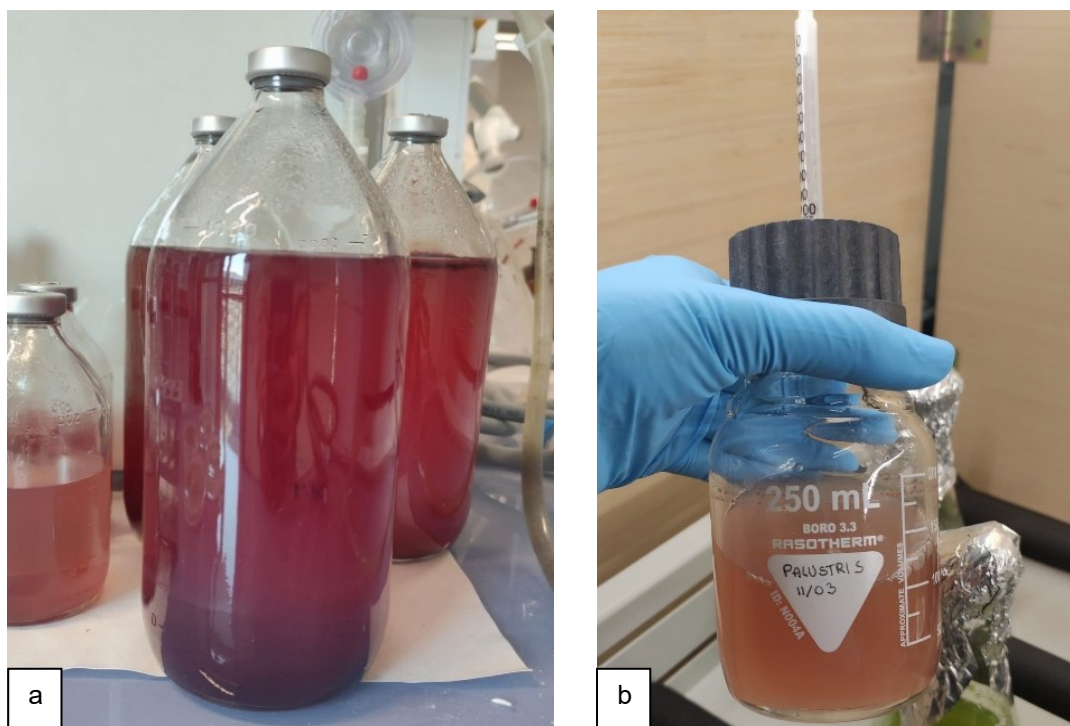


Figure 11 *R. palustris* biomass starter biomass (a) and reactivation of *R. palustris* in RPN media (b)

Once the exponential phase was reached, the culture was transferred into fresh RPN medium which was subsequently used as inoculum for the growth and hydrogen production experiments. However, prolonged storage of the culture can decrease metabolic activity and productivity, and longer retention time in media specifically formulated for growth can shift bacterial metabolism to alternative pathways such as the production of PHB (Koku *et al.*, 2003).

4.2. Batch tests with suspended biomass for growth

Batch experiments with suspended biomass were performed to study the growth and metabolic adaptation of *R. palustris* under different nutritional conditions.

The aim was to evaluate the influence of culture medium composition and carbon source on biomass development, maintaining constant environmental conditions in all experiments to have comparable results.

The growth performance of *R. palustris* was evaluated in two synthetic media with distinct physiological purposes: RPN medium, formulated to promote biomass growth, and RPP medium, designed to favour photofermentative hydrogen production.

Then, *R. palustris* growth was also evaluated on an VFA-rich effluent from fermentation.

Optical density at 660 nm (OD_{660}) was used to describe growth trends over time (Bosman, Pott and Bradshaw, 2023).

4.2.1. Effects of media composition on growth kinetics

This section describes the growth trends and kinetics of *R. palustris* cultivated in two different synthetic media, named RPN and RPP, under the same environmental conditions.

Results are plotted in Figure 12 Comparison of *R. palustris* biomass growth in standard RPN and RPP media

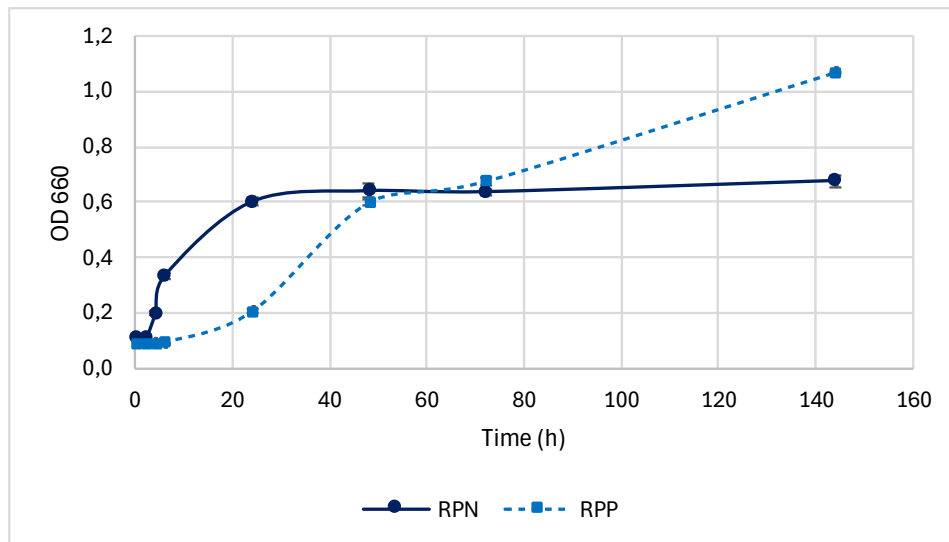


Figure 12 Comparison of *R. palustris* biomass growth in standard RPN and RPP media

In RPN medium, the culture rapidly entered the exponential phase, reaching an OD₆₆₀ of approximately 0.6 ± 0.01 in the first 24 hours resulting in a specific growth rate of 0.2 h^{-1} . After 24 hours entry into the stationary phase occurs, the OD remains almost constant until the end of monitoring period (144 hours) with the final value OD=0,677 and a final dry weight of 0.185 g L^{-1} . This behaviour is consistent with the formulation of RPN media, which provides readily assimilable carbon and nitrogen sources that support fast biomass accumulation (Bianchi *et al.*, 2010; Muzziotti *et al.*, 2016).

The growth trends observed are coherent with studies reporting that more oxidized organic acids such as malate supports an efficient carbon flux through the TCA cycle thus promoting biomass formation (Koku *et al.*, 2002; Bianchi *et al.*, 2010; McKinlay and Harwood, 2011).

In RPP, biomass increase was slower compared to RPN and with a prolonged lag phase. This phenomenon can be attributed to the lower nitrogen availability and its specific formulation which is oriented towards the metabolic pathways for hydrogen production or PHA accumulation rather than the maximization of biomass production.

The culture continued to grow steadily and after approximately 144 hours, OD₆₆₀ values exceeded 1.0 and the final dry weight equal to $0,229 \text{ g L}^{-1}$.

The resulting specific growth rate was 0.0438 h^{-1} , this value is consistent with specific growth rate reported by Koku et al., (2003), in photofermentative tests with *R. sphaeroides* O.U. 001 in synthetic media supplemented with malic acid in which reported specific growth rate in the exponential phase of $0.035 - 0.073 \text{ h}^{-1}$.

In nitrogen-limited or nitrogen-depleted photofermentative conditions the specific growth rate is reduced and carbon source and reducing equivalents are directed toward the activation nitrogenase for H_2 production (Hallenbeck and Benemann, 2002; McKinlay et al., 2014).

Kim and Lee (2000), studied *R. palustris* in batch cultivation for biomass production using a nutrient rich medium with the same malic acid concentration (2 g L^{-1}) and substantially higher level of yeast extract (3 g L^{-1} compared to 0.4 g L^{-1} in RPN). They obtained $\mu_{\text{max}} = 0.12 \text{ h}^{-1}$ lower compared to μ value obtained in this study with RPN (0.2 h^{-1}) and a higher biomass productivity of $55 \text{ mg L}^{-1} \text{ h}^{-1}$ ($\approx 1.32 \text{ g L}^{-1} \text{ d}^{-1}$), and cell dry weight (2.65 g L^{-1}) respect to the value obtained in this experimental thesis. The higher cell DW and productivity compared to the present RPN tests are consistent with differences in medium formulation and process configuration.

4.2.2. Effect of carbon source on growth kinetics

This section describes the growth behaviour of *R. palustris* cultivated in synthetic RPN and RPP media supplemented with different carbon sources, growth curves and kinetics parameters are used to describe differences among substrates.

4.2.2.1. Growth kinetics in RPN medium with different carbon sources

The growth curves of *Rhodopseudomonas palustris* cultivated in RPN medium respectively with malic acid (2 g L^{-1}), acetic acid (2 g L^{-1}), and in a fermented substrate are reported in Figure 13a. to better visualize the growth trend in RPN medium with lactic acid (2 g L^{-1}) is reported separately in Figure 13b.

The results obtained indicate that the carbon source strongly influences growth kinetics, including the duration of the lag phase and the specific growth rate.

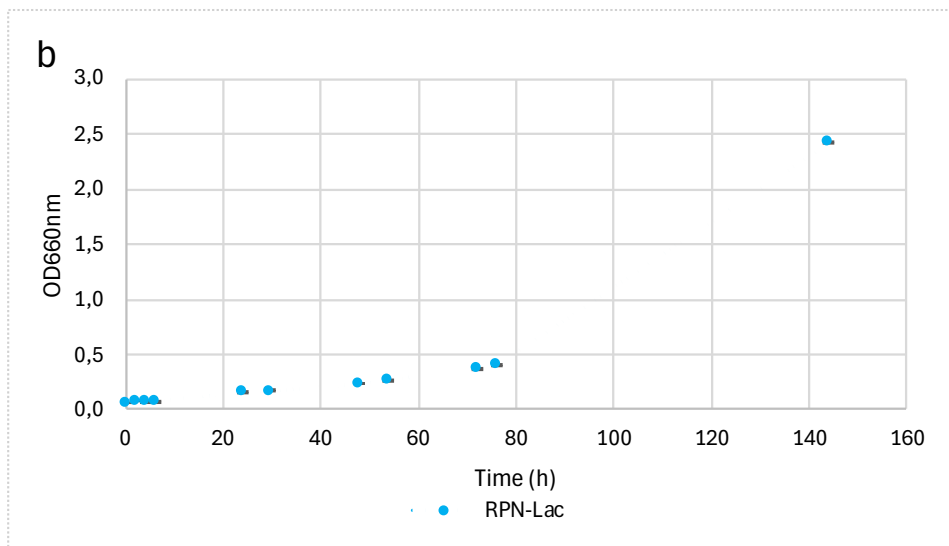
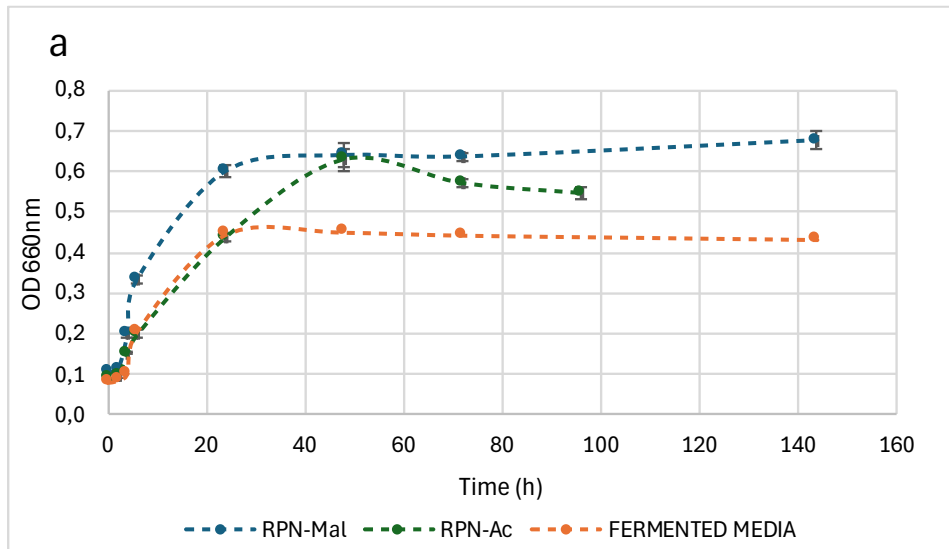


Figure 13- a. Growth kinetics of *R. palustris* in RPN media with different carbon sources (malic and acetic acid) and in fermented substrate.

b. Growth kinetics of *R. palustris* in RPN+ lactic acid

To visualize the differences in the early adaptation phase, Figure 14 provides a magnified view of the first 24 h of cultivation, focusing on the lag phase to better highlight the growth dynamics.

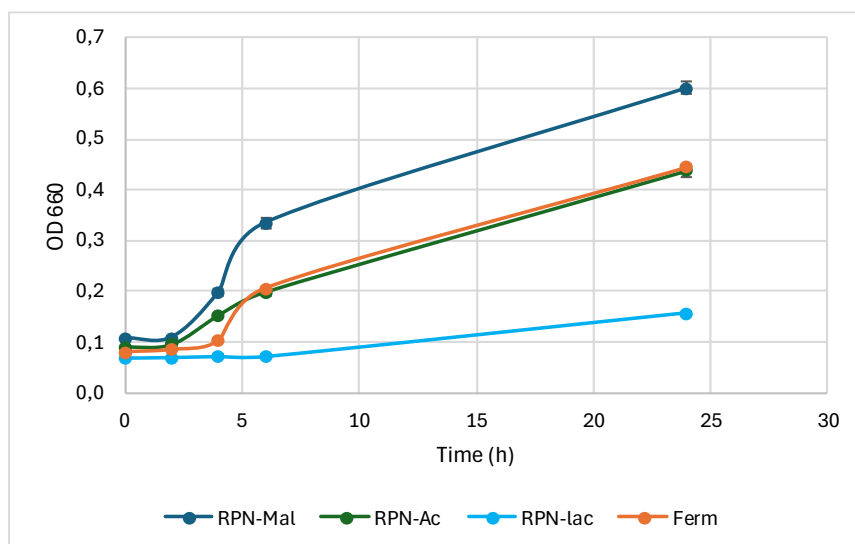


Figure 14 Detail of the initial growth phase (0–24 h): OD_{660} trends highlighting lag-phase behavior under the different tested conditions.

Acetic acid

As shown in Figure 13a, in RPN medium with acetic acid (2 g L^{-1}) as the sole carbon source, growth was slower compared with the other tested conditions ($\mu = 0.0635 \text{ h}^{-1}$) and the exponential phase appeared less pronounced but longer, reaching a final $OD_{660} = 0.547 \pm 0.02$ after 96 h.

The measured μ is consistent with literature values for *R. palustris* grown with acetic acid under photofermentative conditions. In particular, Lo et al.,(2011) modelled growth kinetics of *R. palustris* WP3-5 on acetate in a synthetic medium supplemented with 0.2 g L^{-1} yeast extract, with a Monod model ($\mu_{\max} = 0.06 \text{ h}^{-1}$ and $K_s = 1.42 \text{ g L}^{-1}$) corresponding to a μ value of 0.035 h^{-1} with an initial acetic acid concentration of 2 g L^{-1} , which is lower than the value measured here, the difference is likely due to differences in cultivation conditions.

According to McKinlay and Harwood (2011), reduced substrates such as acetate can limit biomass accumulation compared to less reduced organic acids.

Growth on acetate requires the activation of acetyl-CoA and the use of the glyoxylate shunt and additional anaplerotic routes, such as PFOR-associated carboxylation, to replenish TCA intermediates, which can limit biomass formation compared to more oxidized substrates resulting in prolonged adaptation phases (Figure 14) (Bayon-Vicente *et al.*, 2025).

Acetic acid consumption was monitored through HPLC analysis.

Figure 15 shows the increase in biomass growth and acetic acid consumption over time.

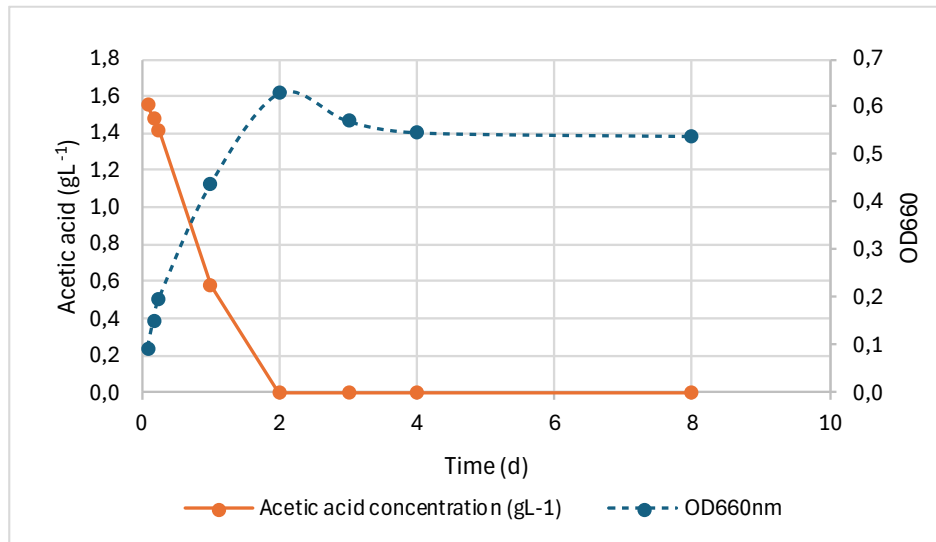


Figure 15 Acetate concentration (g L^{-1}) and biomass growth (OD_{660}) over time during batch cultivation in RPN medium with acetate (2 g L^{-1}).

Acetate decreased progressively during the first hours, reaching 1.42 g L^{-1} after 6 h, then decreased more markedly to 0.58 g L^{-1} after 24 h, until it was completely depleted after 48 h. This rapid consumption phase coincided with the main increase in biomass (OD_{660}), indicating that acetate uptake sustained cell growth during early cultivation phase. After acetate depletion, OD_{660} remained nearly constant until the end of the experiment, consistent with a transition to carbon-limited stationary phase in the absence of alternative carbon sources.

Lactic acid

Biohydrogen production by photosynthetic bacteria has been widely studied using lactate as carbon source (Barbosa *et al.*, 2001) especially because, together with acetate, are common products of dark fermentation processes performed by anaerobic chemotrophs and thus representative of waste-derived feedstocks (Bianchi *et al.*, 2010).

Figure 13b shows that when RPN medium was supplemented with lactic acid (2 g L^{-1}) as carbon source OD_{660} increased slowly during the first part of the experiment with a prolonged lag phase (Figure 14) and then rose sharply at the latest time point ($\text{OD}_{660} = 2.43$ at 144 h), reaching a final $\text{DW} = 0.75 \text{ g L}^{-1}$ with a specific growth rate equal to 0.0545.

Measurements were not collected between 72 and 144 h, so the exact timing of the shift to rapid growth cannot be reconstructed.

This longer adaptation phase is consistent with literature, showing that *R. palustris* does not readily grow on lactate as a sole carbon source under anaerobic phototrophic conditions. Govindaraju, McKinlay and La Sarre, (2019) reported that using only lactate (10mM) *R. palustris* growth was detected only after 150–200 h, whereas lactate consumption was stimulated when

using a co-substrate such as acetate or succinate. The growth behavior observed here with the final “growth burst” may reflect a slow physiological adjustment to lactate assimilation.

This delayed adaptation is also supported by genomic analysis on *R. palustris* CGA009, indicating that lactate transport mechanisms and oxidation are associated to a tightly regulated lactate permease and D-lactate dehydrogenase genes expression, which can lead to an initial prolonged acclimation time (Larimer *et al.*, 2004).

Lo *et al.*, (2011a) demonstrated that *R. palustris* WP3-5 can grow on lactate as a sole carbon source (with 0.2 g L⁻¹ yeast extract) and described the influence of lactate concentration on specific growth rate by a Monod model ($\mu_{\max} = 0.08 \text{ h}^{-1}$; $K_s = 0.13 \text{ g L}^{-1}$). Using these parameters the expected μ values at lactate concentrations of 3–4 g L⁻¹ was around 0.0767 h⁻¹. They reported a complete lactate utilization at low concentration (1-2 g L⁻¹), indicating that once cells are adapted can use lactate as carbon source.

Fermented substrate

The fermented effluent represents a chemically complex matrix containing a mixture of VFAs and other components derived from anaerobic fermentation, which can lead to a less predictable growth behavior due to substrate preference and potentially sequential assimilation (Ghosh *et al.*, 2017).

The fermented substrate showed in Figure 13a has a specific growth rate of $\mu = 0,0715 \text{ h}^{-1}$. OD₆₆₀ reached a maximum of approximately 0.45 after 24 h, followed by a slight decrease. At the end of the test dry weight was 0.33 g L⁻¹.

Literature often reports longer lag phases on complex effluents such as fermented media (Ghosh *et al.*, 2017), due to substrate heterogeneity and the possibility to have inhibitory compounds, but also the reduced light availability due to the colored media.

The fermented media used in this study was mainly composed of acetic acid, several studies have shown that mixtures of VFAs can support higher growth rates than individual VFAs and acetate often plays a key role as a co-substrate by supporting acetyl-CoA availability and improving the uptake of other VFAs (Alloul *et al.*, 2019).

In addition, the short adaptation phase observed in this test (Figure 14) may have been facilitated because the inoculum was precultured in RPN with acetic acid and was therefore likely partially adapted to acetate-rich conditions; as shown in Figure 13a the growth behavior of these two conditions are similar.

4.2.2.2. Growth kinetics in RPP medium with different carbon sources

Growth performance in RPP medium was also evaluated in batch tests performed in 250 mL bottles under the same environmental conditions used for the RPN growth experiments and reported in Figure 16a-b.

RPP medium is designed to promote hydrogen production rather than maximize biomass accumulation. Batch tests in RPP for growth were performed to better understand *R. palustris* behavior and adaptation to nitrogen limited conditions.

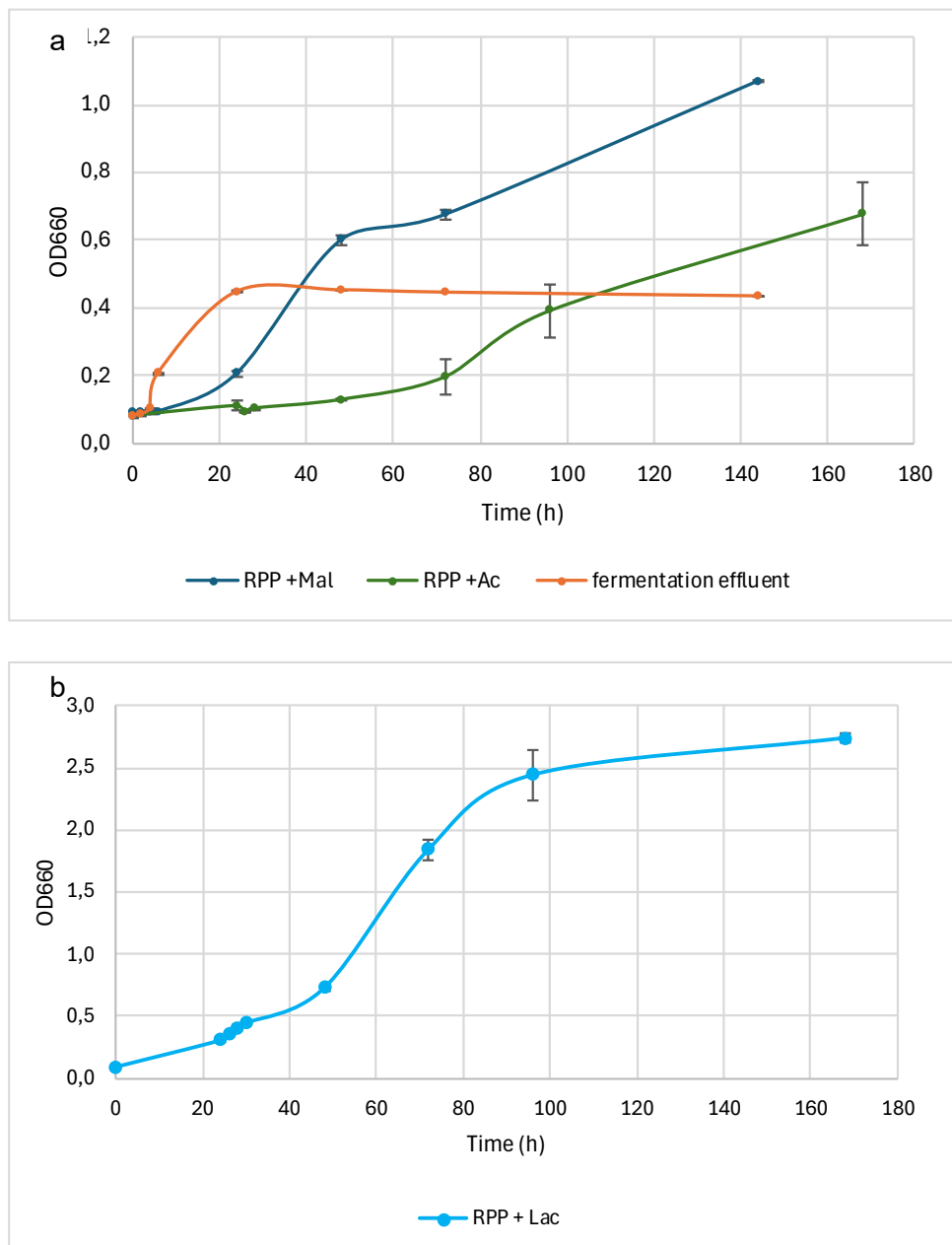


Figure 16 a. Growth curves of *Rhodospseudomonas palustris* cultivated in RPP medium with different carbon sources (malic acid, acetic acid) and in the fermented effluent.
b. Growth curve of *R. palustris* cultivated in RPP with lactic acid.

In RPP with acetic acid (Figure 16a), initial adaptation phase was longer compared to the other tested conditions, ($OD_{660} = 0.128 \pm 0.004$ at 48h) and then increased progressively, reaching $OD = 0.68 \pm 0.092$ at 168 h. This condition showed the lowest growth rate among the RPP tests ($\mu = 0.0144 \text{ h}^{-1}$). The final DW was 0.155 g L^{-1} .

In RPP with lactic acid (Figure 16b) growth was fast and reached the highest OD values among the tested conditions. OD_{660} increased to 0.73 ± 0.02 at 48 h and exceeded 2.7 ± 0.04 at 168 h. The corresponding growth rate ($\mu = 0.0455 \text{ h}^{-1}$) was similar to, or slightly higher than, that observed on malate in RPP, supporting the idea that lactate even if requires a longer adaptation time can be efficiently used by *R. palustris* under anaerobic light conditions, once adapted (Lo *et al.*, 2011; Hu, Choy and Giannis, 2018).

A detailed discussion is reported in Section 4.3, where grow profiles were monitored in photobioreactors operated under photofermentative conditions with different RPP media, and growth behavior and kinetics are analyzed in relation to substrate consumption and hydrogen production kinetics.

McKinlay and Harwood (2011) demonstrated that substrate oxidation state, nitrogen availability, and Calvin cycle flux influences how carbon and electrons are distributed between biomass synthesis and redox balancing pathways, including hydrogen evolution.

The highest growth rate was observed in RPN medium, where readily assimilable nitrogen supported rapid biomass formation. Lower μ values were obtained in RPP-based media, consistent with nitrogen limitation, and a shift toward a hydrogen-producing metabolic state.

Based on DW values, specific growth rate (μ) and biomass productivity (P_x) were calculated for each experimental condition and shown in Table 9

*Table 9 Final DW, specific growth rates (μ) and exponential-phase biomass productivity (P_x) of *R. palustris* cultivated under different batch conditions.*

TEST	DW _{final} (g L ⁻¹)	μ (h ⁻¹)	P _x (g L ⁻¹ d ⁻¹)
RPN	0.185	0.201	0.250
RPP	0.228	0.044	0.060
RPN Acetic acid	0.31	0.063	0.197
RPP Acetic acid	0.155	0.014	0.052
RPN Lactic acid	0.75	0.055	0.104
RPP Lactic acid	0.81	0.046	0.094
Fermented media	0.32	0.072	0.271

The calculated biomass productivity values reveal substantial differences among the tested conditions (Table 9). The highest productivity was observed for cultures grown on the fermented substrate ($P_x = 0.271 \text{ g L}^{-1} \text{ d}^{-1}$), followed by cultures in RPN medium supplemented with malic acid and acetic acid ($P_x = 0.250 \text{ g L}^{-1} \text{ d}^{-1}$ and $P_x = 0.197 \text{ g L}^{-1} \text{ d}^{-1}$, respectively).

In contrast, as expected, lower biomass productivity values were obtained in synthetic RPP media formulated for hydrogen production, reflecting the trade-off between biomass accumulation and the metabolic state associated with nitrogen limitation.

4.2.3. Ammonium consumption in batch test

The ammonium (NH_4^+) concentration was monitored during batch experiments performed in RPN with malic acid and in RPN with acetic batch tests for growth and in the photofermentative H_2 production test with fermented substrate, to evaluate nitrogen availability and its relationship with the growth of *R. palustris*.

Ammonium is a readily assimilable nitrogen source for PNSB and the determination of ammonium consumption is fundamental, since its presence inhibits nitrogenase synthesis and activity. NH_4^+ depletion is a prerequisite for sustained photofermentative H_2 evolution (Koku *et al.*, 2002; Bianchi *et al.*, 2010).

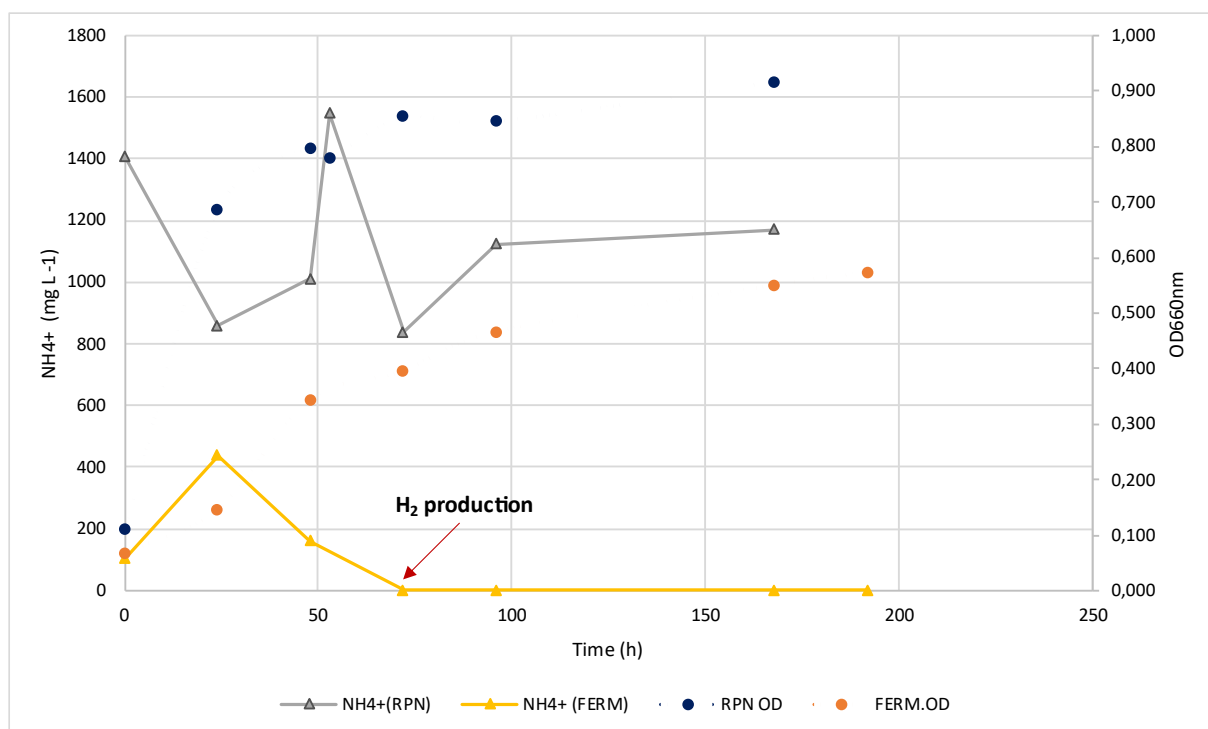


Figure 17 Ammonium (NH_4^+) consumption and biomass growth during batch cultivation of *Rhodospseudomonas palustris* in RPN medium supplemented with malic acid and in fermented substrate operated in a photobioreactor.

In Figure 17 ammonium analysis was focused on two representative experimental configurations; the RPN medium supplemented with malic acid (oriented to growth), and the fermented substrate operated in a photobioreactor for H₂ production. These tests were selected to compare the bacterial performance under a chemically defined condition and a real and chemically complex matrix, characterized by variable nutrient composition and potential inhibitory compounds.

As reported in Figure 17, the two conditions showed a different NH₄⁺ concentration and different temporal trends.

In RPN medium, ammonium is not a limiting factor because the media is formulated specifically to support biomass growth; RPN contains inorganic nitrogen, yeast extract, a complex nutrient source commonly included in culture media to increase the availability of essential growth factors. In this test ammonium showed relatively high initial concentrations, it started at approximately 1409 mg L⁻¹ and was initially consumed, reaching a value below 858 mg L⁻¹ after 24 h and then started to increase reaching the higher peak at 53 h, reaching a value of 1548 mg L⁻¹.

Transient increases in NH₄⁺ in the RPN medium can be explained by the presence of yeast extract, which supplies organic nitrogen in the form of amino acids and peptides. During cultivation, proteolysis and subsequent mineralization of these compounds can release ammonium into the broth, temporarily counterbalancing cellular uptake and causing net NH₄⁺ accumulation (Park and Lee, 1998).

After that, it drops again and finally stabilize after 96 h at values around 1100 mg L⁻¹. Fluctuations observed at intermediate time points may be related to sampling variability or transient release of nitrogen compounds from cellular turnover.

Overall, nitrogen availability was not a limiting factor under RPN conditions and supports the rapid growth phase observed in OD measurements.

The fermented substrate shows a different ammonium profile. The initial NH₄⁺ concentration, after the dilution, was lower compared to RPN media. At T₀ value corresponds to 104 mg L⁻¹

During the first 24 h it shows an increase from 104 mg L⁻¹ to 437 mg L⁻¹.

The transient increase in NH₄⁺-N during the first 24 h likely reflects a net release of ammonium from the complex fermented matrix; dark-fermentation effluents are often rich in fixed nitrogen and dissolved organic nitrogenous compounds that can be broken down into ammonium and for this reason increase in NH₄⁺ can be detected in the liquid phase during early incubation steps (Wu *et al.*, 2016).

The presence of ammonium in fermentation effluents is well recognized as a key bottleneck in photofermentative H₂ production because NH₄⁺ represses nitrogenase-dependent H₂ production, and dilution is commonly applied to mitigate its inhibitory impact (Adessi, McKinlay, *et al.*, 2012; Androga *et al.*, 2012).

After the transient increase, ammonium was progressively consumed and decreased again to 159 mg L^{-1} (48 h) before to approach values below the detection limit. This condition is a prerequisite for photofermentative hydrogen production since ammonium is known to repress nitrogenase activity in purple non-sulfur bacteria (McKinlay and Harwood, 2010). The beginning of H_2 production occurred after NH_4^+ had been depleted; this temporal coupling between NH_4^+ depletion and H_2 onset is discussed in detail in 4.3.1 together with substrate consumption and hydrogen production kinetics.

This behavior is consistent with reports on sequential dark–photofermentation systems, where low residual ammonium result in an efficient photohydrogen production, for example Lo et al., (2011a) reported that residual $\text{NH}_4^+-\text{N} = 46.9 \pm 3.6 \text{ mg L}^{-1}$ present in the diluted substrate from dark fermentation were efficiently consumed by *R.palustris* WP3-5 (95-96% of consumption) during the photofermentative process.

Androga et al.(2012) in their study also highlighted that the dilution of fermentation effluent is a strategy commonly applied to reduce ammonium concentration in the media; but dilution can also affect the concentration of other essential components potentially leading to a decrease in H_2 production. In addition, dilution can increase the cost of the processes and is difficult to apply to scaled up systems. For this reason, in their study they investigated the potential use of biological and physicochemical methods to remove ammonium from waste stream for example using natural zeolite.

4.3. Hydrogen production by *Rhodopseudomonas palustris*

Batch experiments were carried out to study the photofermentative hydrogen production by *R. palustris* cultivated in RPP medium supplemented with different organic acids and on a VFA-rich fermentation effluent.

Hydrogen production was monitored over time by biogas analysis to calculate the cumulative hydrogen production ($V_{H_2,cum}$) and maximum hydrogen production rate (HPR_{max}); in parallel, organic acids consumption was measured over time.

In the first section cumulative hydrogen production is discussed in relation to bacterial growth, comparing $V_{H_2,cum}$ and HPR_{max} across substrates and against representative literature data. Then temporal substrate-consumption profiles are analyzed to clarify whether hydrogen production was driven by carbon availability, and in the last section hydrogen yields and substrate-to-hydrogen conversion efficiencies are calculated and discussed.

When comparing the present results to literature data, it is important to consider that hydrogen yields and production rates can vary widely across studies due to differences in experimental setups and operating conditions as also discussed by Lazaro et al. (2012).

In this work two factors were particularly relevant: the strain used was a non-engineered wild-type culture maintained in the laboratory for a long time, and the light conditions were not optimized for maximum hydrogen production. Both parameters are reported to have a strong influence on photofermentative performances (Hu, Choy and Giannis, 2018).

In aged inocula prolonged retention times within media specifically formulated for growth can shift bacterial metabolism away from H_2 production toward pathway like the production of PHB (Koku *et al.*, 2003).

The present work mainly focused on comparing substrates under same environmental conditions. Each condition was evaluated in a single batch run.

4.3.1. Cumulative hydrogen production

H_2 production was detected in all tested conditions but with different kinetics and final amounts depending on the substrate. Acetate showed the highest $V_{H_2,cum}$ and HPR_{max} , followed by lactate and fermentation effluents. Malate on the other hand showed an early onset of H_2 production but only for a short period, resulting in a low final yield. In all tests, H_2 production generally appeared after an initial lag phase, consistent with nitrogenase regulation in PNSB, which requires oxygen depleted and nitrogen limited conditions (Lo *et al.*, 2011).

An overview of the results obtained is represented in Figure 18.

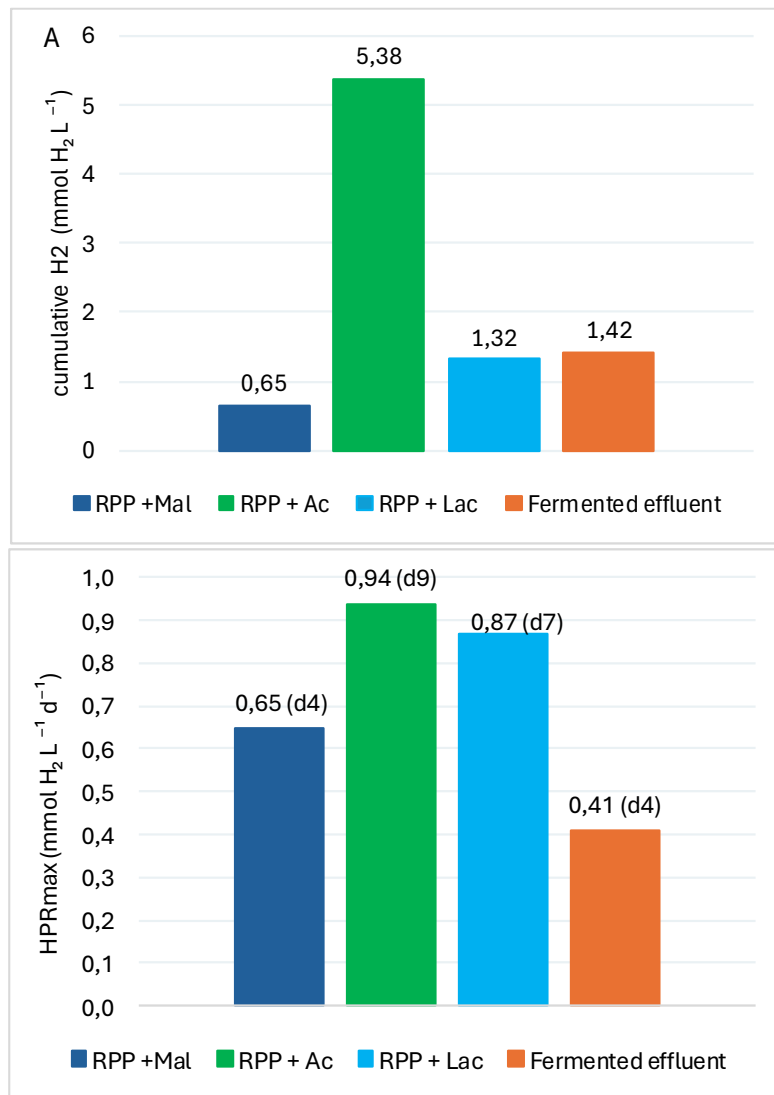


Figure 18 Overview of hydrogen production performance under the different substrate conditions.
 (A) Final cumulative hydrogen production, expressed as mmol H₂ L⁻¹ of culture.
 (B) Maximum hydrogen production rate (HPR_{max}, mmol H₂ L⁻¹ d⁻¹); the onset time of detectable hydrogen production is reported in parentheses. Values were normalized to the working volume

The experimental setup was designed to resemble the approach of Bianchi et al. (2010); key methodological differences between the two studies include light condition and strain age. Bianchi et al. (2010) used incandescent lamps (150–200 μmol photons m⁻² s⁻¹), which provide a broad spectrum with a significant NIR component that matches bacteriochlorophyll absorption (dominant in the 800–900 nm region), whereas 4000 K white LEDs mainly deliver in the visible. Spectral quality together with intensity can markedly affect photofermentative H₂ kinetics (Tiang et al., 2020).

In addition, Bianchi et al. (2010) tested fresh isolates, including the high-performing strain AV33, while the present work relied on a long-maintained wild-type culture, which may show reduced photofermentative activity.

In this section for each tested condition $V_{H_2,cum}$ is presented together with the corresponding biomass growth profiles (OD_{660}) to describe the temporal relationship between them.

Malic acid

In RPP medium with malic acid, OD increased was slow but steadily until day 10 when it reaches its maximum value and approached a plateau (Figure 19).

Based on the OD–DW calibration, the final dry weight corresponds to 0.282 g L^{-1} .

Malate is often considered as a favourable substrate for photofermentative hydrogen production by PNSB since it can directly enter the TCA cycle and readily provide reducing equivalents for nitrogenase activity (Barbosa *et al.*, 2001; Koku *et al.*, 2002).

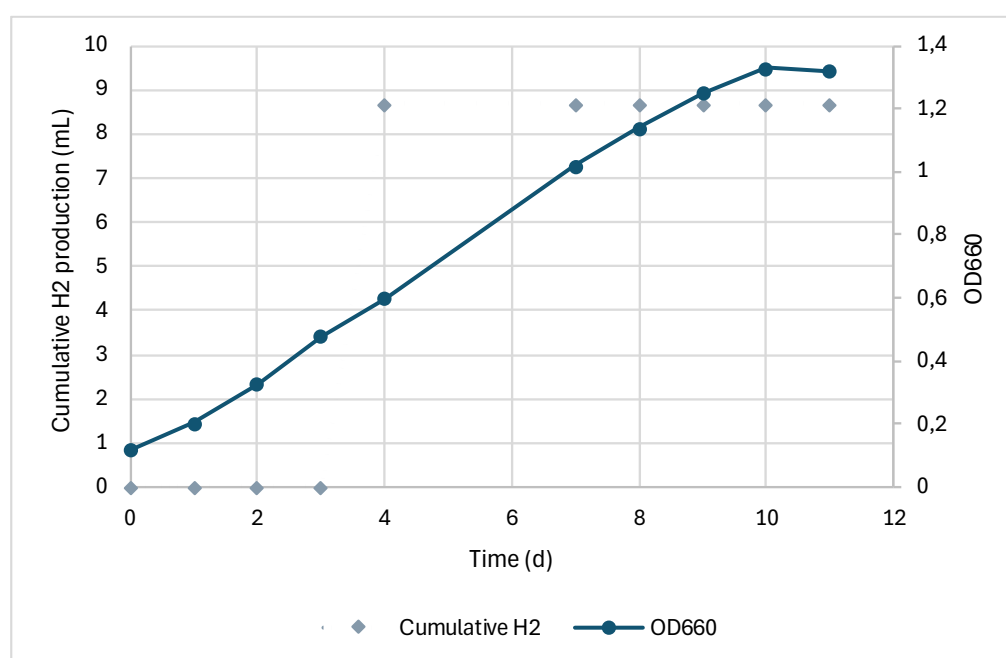


Figure 19 Cumulative hydrogen production and biomass growth (OD_{660}) of *Rhodospseudomonas palustris* cultivated in RPP medium with malic acid as carbon source

Hydrogen was detected only after a short lag phase between day 3 and 4, when it produced 8.70 mL ($16.11 \text{ mL H}_2 \text{ L}^{-1}$). Then H_2 did not increased further while biomass continued rise.

This trend is in contrasts with typical late-exponential phase onset reported by Koku *et al.* (2003) indicating that hydrogen production on malate was not limited nutrient depletion, but another limitation was dominant and reducing equivalents were likely directed toward growth and maintenance of biomass rather than to nitrogenase activity.

Based this single measured value, HPR_{max} calculated was $0.647 \text{ mmol H}_2 \text{ L}^{-1} \text{ d}^{-1}$ (about $0.6\text{--}0.7 \text{ mL H}_2 \text{ L}^{-1} \text{ h}^{-1}$).

Studies found in literature often report higher rates than those observed in the present study.

For example, Uyar et al. (2009) tested individual VFAs with *Rhodobacter sphaeroides* O.U.001 and reported an HPR of 24 mL H₂ L⁻¹ h⁻¹ on malate (15mM). The difference is likely due to the experimental setup; they operated in small 55 mL bottles with a short optical path to have higher light availability inside the photobioreactor, and under tungsten illumination providing a spectrum enriched in near-IR wavelengths. In the present study the larger working volume (0.540 L) and the use of 4000 K LEDs at lower irradiance likely reduced the photon availability inside the culture. In a previous study Uyar et al. (2007) also investigate the impact of light composition showing that infrared wavelengths play an important role in photofermentative performance, since removing the infrared fraction decreased H₂ production of about 39%. In the present study light conditions were not optimal and this might to explain why hydrogen production rates were substantially lower.

Acetic acid

In RPP medium with acetic acid (\approx 63 mM), biomass growth showed a longer adaptation phase. OD₆₆₀ remained below 0.2 for the first 72 h and then increased steadily, approaching a plateau around day 10 with OD approximately around 2.0 (Figure 20).

Based on the OD–DW calibration, the final biomass concentration reached 0.465 g L⁻¹

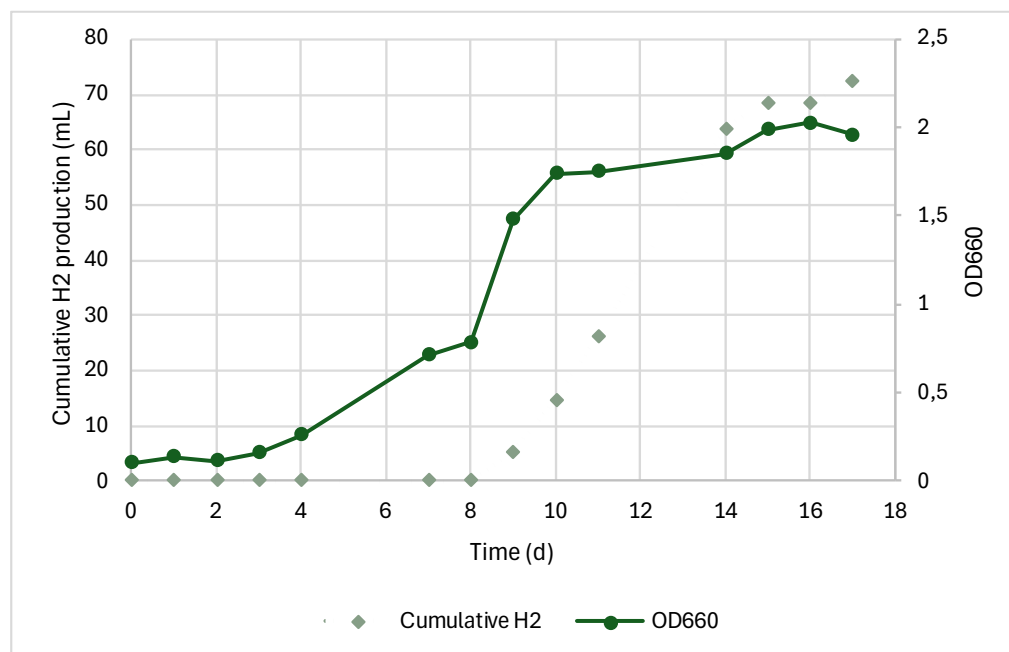


Figure 20 Cumulative hydrogen production and biomass growth (OD₆₆₀) of *Rhodospseudomonas palustris* cultivated in RPP medium with acetic acid as carbon source

Hydrogen production started only after an adaptation phase, H₂ was first detected at day 9 and then increased steadily to a final volume of 72.21 mL H₂, corresponding to 5.38 mmol H₂ L⁻¹, (normalized to the working volume). The maximum HPR was 0.938 mmol H₂ L⁻¹ d⁻¹ (\approx 0.876 mL H₂ L⁻¹ h⁻¹).

The longer adaptation phase observed on acetate is consistent with the literature observations; in *R. palustris*, acetate assimilation by the TCA cycle requires additional pathways such as the glyoxylate shunt and pyruvate:ferredoxin oxidoreductase (PFOR), and their activation can contribute to a prolonged lag phase (McKinlay and Harwood 2011).

In general, acetate is often reported as an efficient substrate for H₂ production by PNSB, and particularly by *R. palustris*, sometimes performing better than other VFAs under comparable conditions (Lo *et al.*, 2011; McKinlay and Harwood, 2011). However, reported performances can vary substantially with strain physiology, light availability and reactor design.

As already mentioned, in the present study, the larger working volume, the lower irradiance and a different light spectrum likely reduced the effective photon availability within the culture (Uyar *et al.*, 2009). In addition, in this test acetate supported the highest biomass accumulation, which might interfere with hydrogen production processes because substrate and reducing equivalents are directed toward biomass accumulation rather than nitrogenase activity and it can also increase the self-shading effect, further reducing light availability (Uyar *et al.*, 2009).

Strain physiology is another important source of variability; Bianchi *et al.* (2010) tested different freshly isolated *R. palustris* strains and reported very low H₂ activity on acetate for their best-performing strain AV33, which produced 8–10 mL H₂ after 250 h. In that condition cells accumulated PHB up to 21.4 \pm 3.4% (w/w) of cell dry weight. Under conditions that favour PHB storage reducing equivalents can be directed away from nitrogenase, resulting in a lower H₂ production (Koku *et al.*, 2002; Bianchi *et al.*, 2010; Cardeña, Valdez-Vazquez and Buitrón, 2017). In this study, PHB was not measured, so this aspect cannot be confirmed, but could be a possible contributing factor to the comparatively low H₂ rates observed on acetate.

Differences in light availability also should be considered; for example, Barbosa *et al.* (2001) achieved 56 mL H₂ per vessel and HPR_{max} of 2.2 mL H₂ L⁻¹ h⁻¹, with *R. palustris* in acetate (22 mM) and sodium glutamate (0.8 mM) using smaller vessels (150-mL working volume), under high-intensity tungsten/halogen lamps.

The cumulative hydrogen production obtained in this study (5.38 mmol H₂ L⁻¹) matches values reported by Lazaro *et al.* (2012) (7.8 mmol H₂ L⁻¹); in their study they are working with a phototrophic microbial consortium, grown on acetate (30 mM), using fluorescent lamps.

However, their maximum rates were estimated by fitting the cumulative H₂ curves with a modified Gompertz model, which is not directly comparable with point-to-point rates calculated from consecutive measurements.

Lactic acid

The long lag phase observed cultivating *R. palustris* in RPP medium with lactic acid is consistent with literature observation reporting that when lactate is provided as the sole carbon source, *R. palustris* do not readily grow on it requiring longer incubation times (Govindaraju, McKinlay and LaSarre, 2019). In additions studies performed at genomic level on *R. palustris* CGA009 demonstrated that lactate uptake and oxidation are genetically linked to the presence of D-lactate dehydrogenase and a lactate permease gene which are subjected to physiological regulation, consistently resulting in a prolonged adaptation phase (Larimer et al., 2004; Li et al., 2022a). In this test biomass increased during the first days and reached a final dry weight of 0.130 g L⁻¹ (vs. 0.465 g L⁻¹ on acetate).

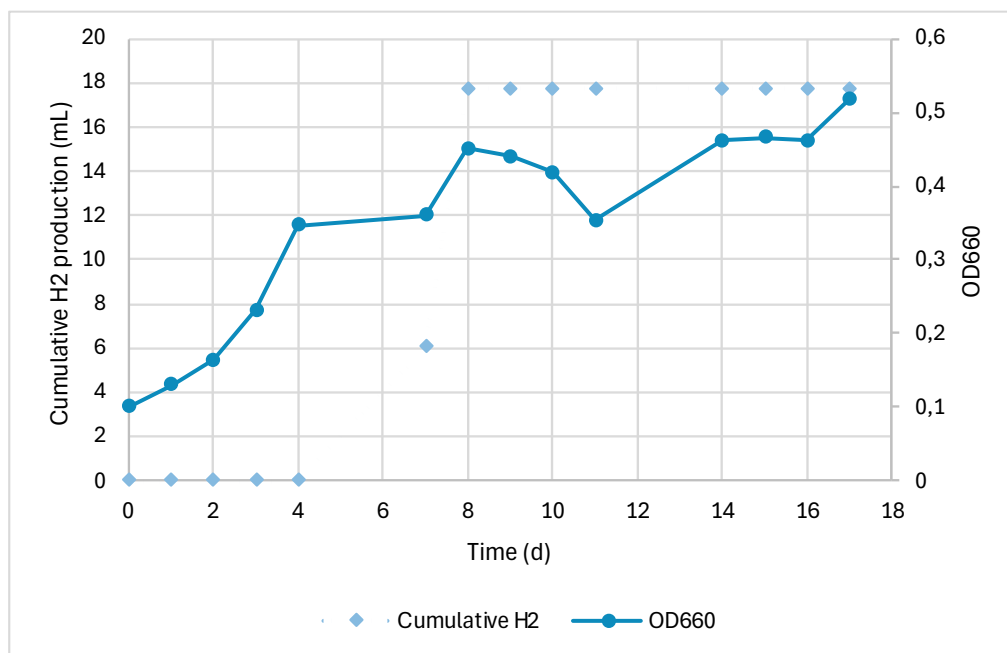


Figure 21 Cumulative hydrogen production and biomass growth (OD₆₆₀) of *Rhodospseudomonas palustris* cultivated in RPP medium with lactic acid as carbon source

As shown in Figure 21, hydrogen production in RPP medium with lactic acid occurs in a short period of time and ended earlier than on acetate. Hydrogen production became detectable at day

7, and increase at day 8, reaching a final volume of 17.73 mL H₂ (0.713 mmol H₂) corresponding to 1.32 mmol H₂ L⁻¹, normalized to reactor working volume.

The HPR_{max} measured was 0.869 mmol H₂ L⁻¹ d⁻¹ (≈0.8 mL H₂ L⁻¹ h⁻¹).

After day 8 no further H₂ production was recorded, even though biomass continued to grow.

To check whether the early stop in H₂ production was mainly due to carbon availability, at day 10 a lactate pulse was applied adding 0.980 mL of lactic acid to restore the lactate concentration to 2 g L⁻¹, but H₂ production did not restart.

This result suggests that, under the tested conditions, hydrogen production on lactate was limited by factors other than lactate availability, likely a limited photon availability due to non-optimized light conditions or possible metabolic redirection of reducing equivalents toward competing electron sinks such as PHB formation.

Bianchi et al. (2010) testing the freshly isolated *R. palustris* strains AV33 and reported that cells cultivated in lactate accumulated PHB up to 10.9 ± 3.3% (w/w) of cell dry weight, showing however a total production for their best performing strain of approximately 721 mL of H₂ and a HPR_{max} equal to 50.7 ± 2.6 mL H₂ L⁻¹ h⁻¹ (at 75 h) in 250-mL vessels illuminated by an incandescent lamp.

When compared with literature, lactate-supported photofermentation frequently shows higher rates under more favorable light and reactor configurations.

Barbosa et al. (2001) report a maximum H₂ production rate of 9.1 mL H₂ L⁻¹ h⁻¹ for *R. palustris* cultivated on lactate (50 mM), however these rates were obtained in small batch cultures (150 mL culture volume) and illuminated by at high energy intensity halogen/tungsten lamps.

Lo et al., (2011a) investigated *R. palustris* WP3-5 using different lactate concentrations (1.0–5.0 g L⁻¹), they demonstrated that *R. palustris* produced hydrogen at all tested concentrations with maximum volumetric HPR at the higher concentration reaching a value of 17.0 mL H₂ L⁻¹ h⁻¹. On the other hand, values close to those reported in this study were reported by Lazaro et al. (2012) with the mixed phototrophic consortium on lactate (23 mM) reporting a $V_{H_2,cum}$ of 5.6 mmol H₂ L⁻¹, with an estimated HPR_{max} of 0.3 mL H₂ L⁻¹ h⁻¹ (based on modified Gompertz equation); in this case batch test were performed in closed 0.5 L photobioreactors (0.35-L working volume) illuminated by three fluorescent lamps (81 μmol m⁻² s⁻¹).

Overall, lower production and HPR_{max} observed in this experimental test reflects the combined effect of lower effective photon availability, larger working volume and inoculum history, those patterns are consistent across the tested substrates (Koku et al., 2003).

Fermented substrate

Hydrogen production was also observed when *R. palustris* was cultivated on VFA-rich fermentation effluent (Figure 22). Differently from the defined media containing a single carbon

source, the effluent was a complex matrix containing a mixture of organic acids, residual nutrients and other soluble compounds originating from dark fermentation process; this compositional complexity, together with resistance to light penetration, are reported to be the major bottlenecks limiting H₂ production from waste derived substrates (Ghosh *et al.*, 2017).

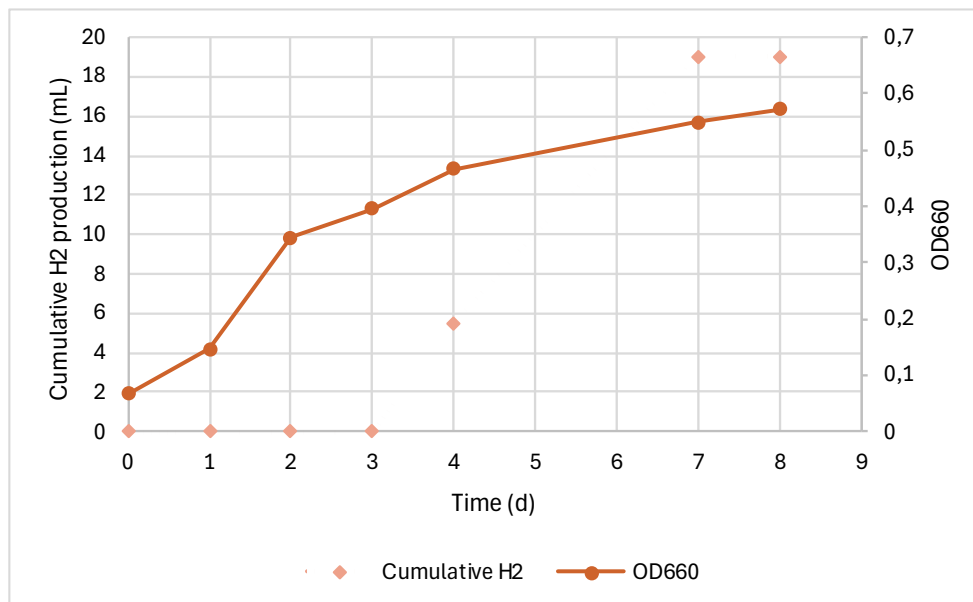


Figure 22 Cumulative hydrogen production and biomass growth (OD₆₆₀) of *Rhodospseudomonas palustris* cultivated on VFA-rich fermentation effluent under photofermentative conditions.

In this test, biomass increased steadily during the experiment. OD₆₆₀ rose from 0.068 to 0.573 by the end of the test, with a rapid entrance into the active growth phase.

Dry increased from 0.050 g L⁻¹ at day 0 to 0.407 g L⁻¹ at day 7.

The inoculum used in this test was previously cultured in RPP media with acetic acid; this acclimation step likely contributed to the rapid increase in biomass growth and relatively short adaptation phase.

Despite the early biomass increase, H₂ became detectable after 4 days and increased at the next sampling point on day 7. The lag phase observed before active H₂ production is often observed in photofermentative H₂ production and reflects the time required for the activation of nitrogenase activity and could be likely due to non-optimal carbon to nitrogen ratio or reduced light penetration (Ghosh *et al.*, 2017).

Micro-GC confirmed that the net produced gas was H₂-rich; H₂ accounted for 69% at day 4 and 85% at day 7, while CO₂ remained very low (0–2%).

Final cumulative hydrogen production reaches a value to 19.03 mL H₂, corresponding to 0.765 mmol H₂ (1.42 mmol H₂ L⁻¹, normalized to the reactor working volume).

The HPR_{max} measured was 0.409 mmol H₂ L⁻¹ d⁻¹ (corresponding to approximately 0.4 mL H₂ L⁻¹ h⁻¹).

It should be noted that no measurements were performed between day 4 and day 7, and the exact production profile during this interval cannot be reconstructed and the actual onset and peak rate may be partially underestimated.

Compared to the RPP with acetate (Figure 20), the fermented effluent resulted in a lower final cumulative H_2 and a lower HPR_{max} . This difference can be explained by the compositional complexity of the effluent such as the presence of fixed nitrogen, which promotes biomass synthesis and represses nitrogenase expression. This is also supported by studies by Lee, Hung and Yang (2011) which cultivated *R. palustris* WP 3-5 in lab-scale serial photobioreactor configuration in continuous on ammonia-containing wastewaters, in which the initial stage was developed to consume ammonia for cell synthesis, then in the next steps obtained a stable H_2 production.

A second relevant key limitation is light availability, which can be substantially reduced by coloured effluents and together with biomass increase can further reduce light penetration by self-shading. The review by Ghosh et al. (2017) also reports that photofermentation on real food-processing wastewaters even if properly diluted and pretreated, still yields moderate rates, around $\sim 9\text{--}10 \text{ mL } H_2 \text{ L}^{-1} \text{ h}^{-1}$, highlighting light penetration and matrix complexity as primary limitations.

In terms of volumetric productivity, the HPR values obtained in this study are lower to the one commonly reported for waste derived substrates under optimized configurations.

For example, Bianchi et al. (2010) studied freshly isolated *R. palustris* AV33 cultivated on a fermentation broth derived from vegetable residues, reporting that the fermentation broth supported substantially higher biomass formation 2.2 times higher than in synthetic medium, suggesting that carbon and reducing power were preferentially channeled toward cell synthesis rather than H_2 evolution. In their test they reported a maximum HPR of $9.7 \pm 0.7 \text{ mL } H_2 \text{ L}^{-1} \text{ h}^{-1}$, which increased to $16.4 \pm 2.3 \text{ mL } H_2 \text{ L}^{-1} \text{ h}^{-1}$ using fermented broth supplemented with Fe(III). Iron is an essential a co-factor stimulating nitrogenase function and limited iron availability can constrain H_2 production.

Given the complexity of the fermented effluent and the higher analytical uncertainty (due to dilution effects and values close to the detection limit), substrate consumption is discussed in the following sections using acetate as a reference compound, consistently with literature describing acetate as a dominant soluble metabolite in dark fermentation effluents and a relevant substrate for photo- H_2 production (Cardeña, Valdez-Vazquez and Buitrón, 2017).

4.3.2. Relationship between substrate consumption and hydrogen evolution

Monitoring substrate consumption gives direct information about how *R. palustris* metabolizes carbon sources and how these are converted into biomass, H₂ and other metabolic products.

In this section progressive VFA concentration is reported together with $V_{H_2,cum}$, to describe substrate depletion patterns and relate them to hydrogen production profiles.

Malic acid

Figure 23 shows the temporal evolution of malic acid concentration in relation to cumulative hydrogen production during the test in RPP medium with malic acid.

Nominal malic acid concentration in the media was 4 g L⁻¹.

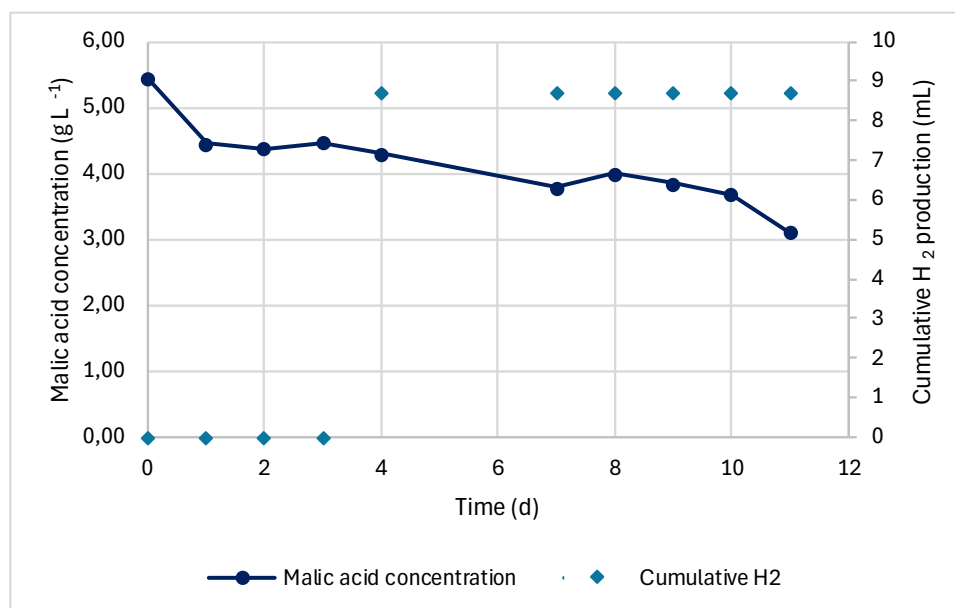


Figure 23 Malic acid concentration (g L⁻¹, left axis) and cumulative hydrogen volume (mL, right axis) over time during the RPP + malic acid test

However, the measured value at day 0 was 5.45 g L⁻¹, suggesting a possible error in systematic preparation of the media. For this reason, the measured value was used as the baseline, and small fluctuations in intermediate samples were considered within the expected uncertainty.

During the test malic acid decreased to 3.11 g L⁻¹, corresponding to a net consumption of 2.34 g L⁻¹ (43% malic acid consumed).

Hydrogen production was detected only at day 4 (16.11 mL H₂ L⁻¹) and did not increase further at later sampling points, despite continued biomass growth and the presence of residual malic acid in the medium. This indicates that, under the tested conditions, H₂ production was not limited by substrate depletion, but another limitation was dominant before carbon exhaustion.

Lazaro et al. (2012) reported complete malate consumption within 9 days and a higher final H₂ accumulation (13.9 mmol H₂ L⁻¹) when feeding malate at ~14.5 mM using a phototrophic microbial consortium. In their case, H₂ production continued even after malate depletion, likely supported by by-products such as acetate generated by the microbial consortium, where non-phototrophic members can convert malate into fermentation products. The different behaviour observed here suggests that further tests, especially with improved light availability and a fresh bacterial inoculum, would be useful to clarify whether, in these experimental conditions, the early stop is mainly related to the experimental setup or to a limitation associated with malate-based metabolism.

Adessi et al.(2012) reported that in outdoor 50 L tubular photobioreactor, malate (initially 4 g L⁻¹) decreased to 1.46 g L⁻¹ by day 4 at that point they restored the initial malate concentration; H₂ production started around day 5 and continued for the following five days. At day 10 malate dropped to 0.65 g L⁻¹, re-feeding was followed by a 2-day lag phase before H₂ production restarted; later, at day 15 (0.55 g L⁻¹), a partial replacement of the medium was required to reactivate H₂ production, while a further malate addition at day 19 did not restore H₂ evolution, indicating that, at that point, sustained production can be constrained by factors other than carbon availability.

Acetic acid

Acetate concentration was quantified by HPLC analysis and compared with the cumulative H₂ profile. Based on the medium recipe, the nominal initial acetate concentration was 3.8 g L⁻¹ (≈ 63 mM).

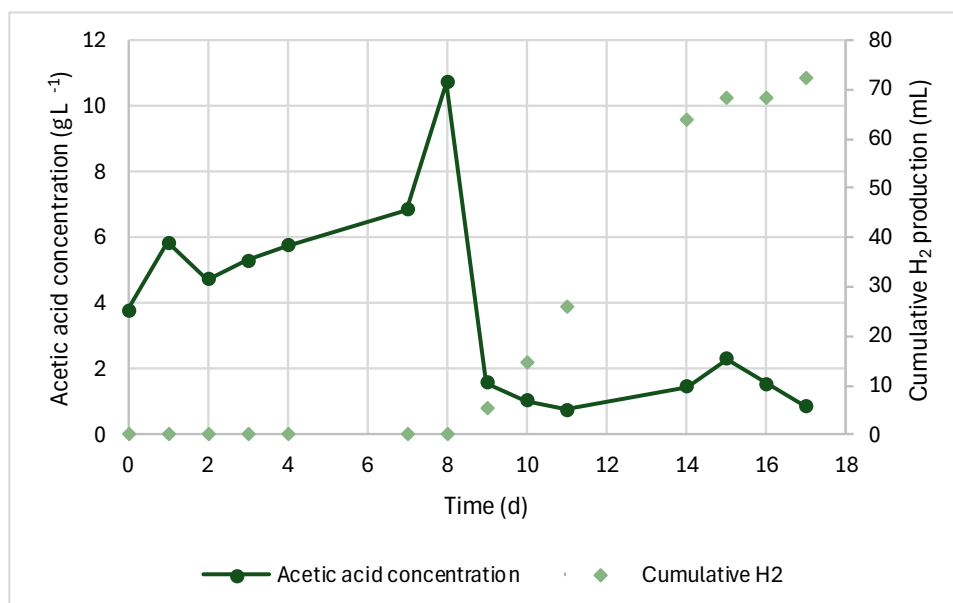


Figure 24 Acetate concentration (g L⁻¹, left axis) and cumulative hydrogen volume (mL, right axis) over time during the RPP + acetate test

During the first week, measured acetate values fluctuated between 4.73 and 6.83 g L⁻¹, and an isolated higher value was recorded at day 8 (10.73 g L⁻¹) (Figure 24). Since acetate is not expected to increase in a chemically defined medium, this behavior is likely to reflect preparation or analytical variability. Therefore, the acetate consumption is discussed in terms of the overall depletion pattern, rather than point-to-point changes during the early stages.

Over the first 8 days cumulative H₂ remained zero, a delay consistent with the adaptation phase observed in the growth profile discussed in section 4.2.2. Acetate concentration decreased markedly from day 9 until day 17, reaching a final value of 0,84 g L⁻¹ with a net consumption of 2.96 g L⁻¹ (approximately 78% of the initial nominal concentration).

Acetate uptake coincided with H₂ production phase, indicating active substrate utilization during the hydrogen-producing phase.

This result is consistent with values reported by Lo et al. (2011a), which tested different acetate concentrations and showed that substrate utilization was nearly 100% with acetate concentration of 1-2 g L⁻¹ and it decreased to 76-77% with increased acetate concentrations around 3 or 4 g L⁻¹, even though in their study they did not report exact cumulative H₂ production volume, the hydrogen production rate obtained at 4 g L⁻¹ was 19.8 mL h⁻¹ L⁻¹, higher than the values reported in the present experiment.

A different behavior is reported by Lazaro et al. (2012) which shows that a phototrophic hydrogen-producing bacterial consortium fed with acetate (30 mM) produced 7.8 mmol H₂ L⁻¹ and consumed only 43% of the acetate, highlighting that mixed communities may display different balances between substrate utilization and H₂ evolution.

In the present work, acetate removal was higher (~78% based on the nominal concentration) but the final H₂ accumulation was slightly lower (5.38 mmol H₂ L⁻¹), suggesting that a fraction of acetate-derived carbon and reducing equivalents were directed to biomass synthesis and maintenance and possibly to storage polymers, rather than to nitrogenase-driven H₂ evolution (Bianchi *et al.*, 2010; Chen, Wu and Lee, 2012).

This interpretation is supported by Uyar et al. (2007), reporting that acetate can sustain the highest biomass growth which is likely to limit H₂ production because substrates are diverted away from H₂ formation and can increase the self-shading which further limiting light availability.

In addition, Bianchi et al.(2010) reported that under photofermentative conditions optimized for H₂ production *R. palustris* strains AV33 and reported very low H₂ activity, but cells accumulated PHB up to 21.4 ±3.4% (w/w) of cell dry weight. In this study, PHB was not measured, so this aspect cannot be confirmed.

Lactic acid

Lactic acid consumption during the photofermentative test was monitored using an enzymatic assay, allowing direct quantification of total D/L-lactic acid. Lactate concentration was not measured daily; instead, selected samples taken at representative time intervals, describe the overall consumption pattern and its relation to H₂ evolution.

As shown in Figure 25, lactate decreased markedly during the first part of the experiment.

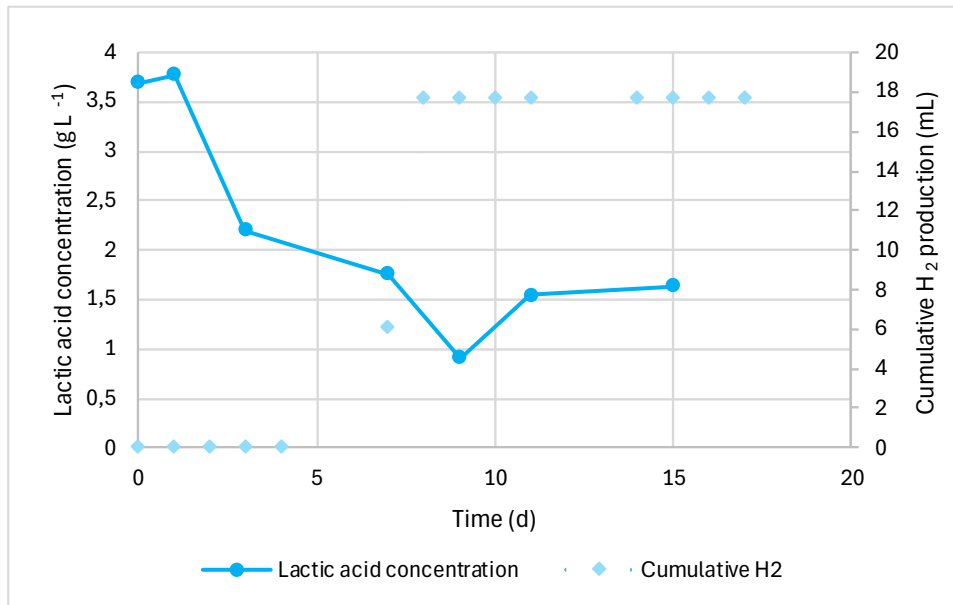


Figure 25 D/L-Lactic acid concentration (g L⁻¹, left axis) and cumulative hydrogen volume (mL, right axis) over time during the RPP + lactic test

The concentration dropped from 3.78 g L⁻¹ (day 1) to approximately 1.7–1.8 g L⁻¹ (day 7) and reaching its minimum at day 9 (0.91 g L⁻¹), resulting in consumption of 2.87 g L⁻¹ (≈75%, relative to nominal concentration), while biomass increased (final dry weight: 0.130 g L⁻¹), indicating active substrate utilization during growth.

Hydrogen production was negligible during the initial phase, and it was first observed at day 7 and day 8, reaching a final cumulative volume of 17.73 mL. At day 10, a lactate pulse was applied to restore the lactic acid concentration to 2 g L⁻¹; the addition is visible in the lactate profile which increased again to approximately 1.5–1.6 g L⁻¹ at later sampling points.

Despite that, no further increase in cumulative H₂ production was detected after the pulse.

Following the lactate addition OD₆₆₀ increased from 0.42 to 0.52 by the end of the experiment, suggesting that the added lactate mainly supported further biomass growth and maintenance, rather than resuming nitrogenase-driven H₂ evolution under the tested conditions.

These results indicate that hydrogen was produced only in a short time window during the phase of lactate utilization and was not resumed by restoring lactate availability suggesting that possible

metabolic shift, such as PHB accumulation, or physiological constraints affected hydrogen evolution (Govindaraju, McKinlay and LaSarre, 2019; Bernabò *et al.*, 2025).

PHB production was not measured during the course of the experiment, so the proposed metabolic shift cannot be confirmed, however biomass samples were collected and stored at -4°C for possible future PHB analysis.

When compared with literature, lactate conversion and H₂ production on lactate can vary strongly across studies.

Lo *et al.* (2011a) investigated photofermentative hydrogen production with *Rhodospseudomonas palustris* WP3-5 cultivated with different lactate concentrations (1–5 g L⁻¹). Although the experimental conditions are different in terms of strain, medium composition, light intensity, and initial biomass concentration, they reported that with higher lactate concentration (≥3 g L⁻¹) its conversion was often incomplete, indicating that substrate utilization strongly depend on lactate concentration and operating conditions. Similarly, Lazaro *et al.* (2012) observed only partial lactate consumption (49%) using a phototrophic microbial consortium in closed 0.5 L photobioreactors (0.35 L working volume) illuminated by three fluorescent lamps (81 μmol m⁻² s⁻¹), further supporting that lactate conversion can vary depending on the microbial system and operating conditions.

Acetic acid consumption in fermented media

Volatile fatty acids consumption in the fermented effluent was monitored by HPLC to relate substrate utilization to biomass growth and hydrogen evolution.

Acetic acid was the dominant organic acid quantified in all samples, propionate was detected only at lower concentrations; since minor acids were quantified with higher uncertainty due to the dilution factor and values close to the detection limit, the next sections focus on acetate as the reference VFA. This choice is supported by literature on dark-fermentation effluents, which frequently identifies acetate as a dominant and readily assimilated substrate for photofermentative H₂ production by *R. palustris* (Ghosh *et al.*, 2017).

Figure 26 shows the acetic acid concentration and cumulative hydrogen production measured over time.

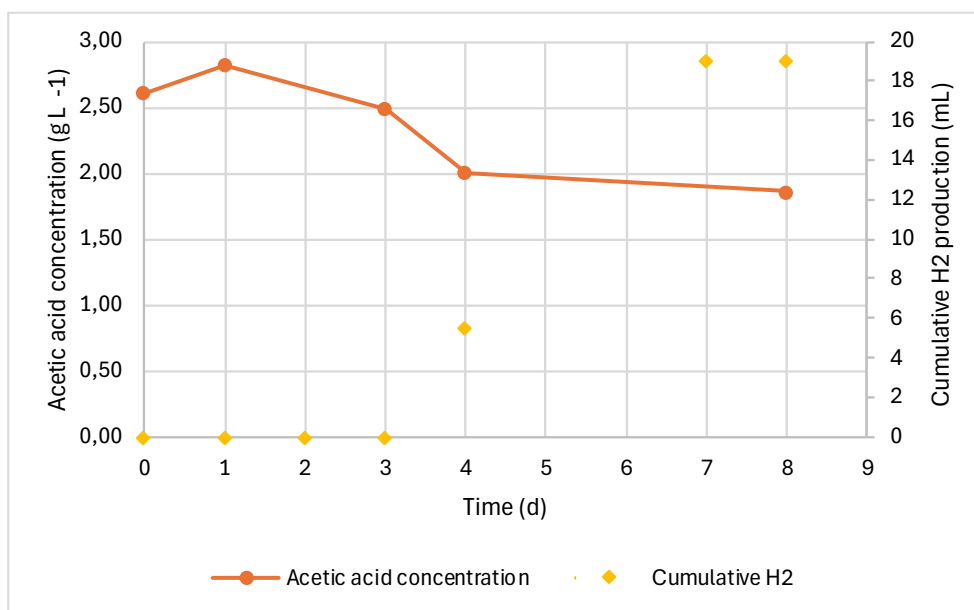


Figure 26 Acetic acid consumption and cumulative H₂ production in fermented effluent

At the beginning of the experiment, the acetic acid concentration was 2.61 g L⁻¹, acetate decreased to 1.86 g L⁻¹ resulting in a net consumption of 0.742 g L⁻¹ (corresponding to 6.68 mmol in the reactor working volume) and to an overall consumption of 28.5%. A small increase was observed at day 1, reaching 2.83 g L⁻¹; which can be interpreted as analytical or sampling variability rather than true acetate formation.

Compared to RPP media with acetic acid acetate depletion in fermented substrate was slower and the amount of acetic acid consumed was lower. This is likely a direct consequence of matrix composition and complexity, in which the presence of other substrates can lead to simultaneous or sequential uptake of the organic acids available.

In addition, also medium dark colour can reduce the light penetration inside the photobioreactor lowering the energy available for photoheterotrophic substrate assimilation and hydrogen formation (Ghosh *et al.*, 2017).

Cumulative hydrogen production remained undetectable in the first days and became measurable at day 4, reaching 5.49 mL, followed by a further increase to 19.03 mL at day 7. This lag phase observed before H₂ production is consistent with the adaptation required for the establishment of nitrogen limited conditions required for nitrogenase activity (Koku *et al.*, 2002).

Over the same interval, acetate showed a decrease, indicating that acetate consumption occurred during the period of H₂ accumulation.

To better interpret the delayed onset, Figure 27 also reports ammonium (NH₄⁺) together with the shaded H₂ detection window. The increase in NH₄⁺-N observed during the first 24 h is consistent with a net release of fixed nitrogen from the complex fermented matrix already discussed in

paragraph 4.2.3, fermentation effluents can contain dissolved ammonium but also organic nitrogenous compounds that are progressively converted into NH_4^+ (Androga *et al.*, 2012).

In purple non-sulfur bacteria, ammonium is a well-known repressor/inhibitor of nitrogenase (Koku *et al.*, 2002); even low concentrations can rapidly suppress nitrogenase activity until ammonium is depleted, delaying H_2 onset and lowering the overall conversion of substrate into hydrogen.

Compared with defined media, a fermented effluent contains higher amount of fixed nitrogen (e.g., ammonia and other nitrogen sources), which supports biomass growth and can reduce the fraction of electrons channelled to nitrogenase-driven H_2 production.

The figure shows the NH_4^+ -N values obtained in this experimental test decreased markedly during the early phase, while H_2 became detectable only after day 4, supporting the idea that residual fixed nitrogen initially favoured biomass formation and delayed nitrogenase-driven H_2 evolution.

During the H_2 -detection window (day 4–7), acetate concentration continued to slowly decrease, indicating that carbon uptake was ongoing while net H_2 accumulated.

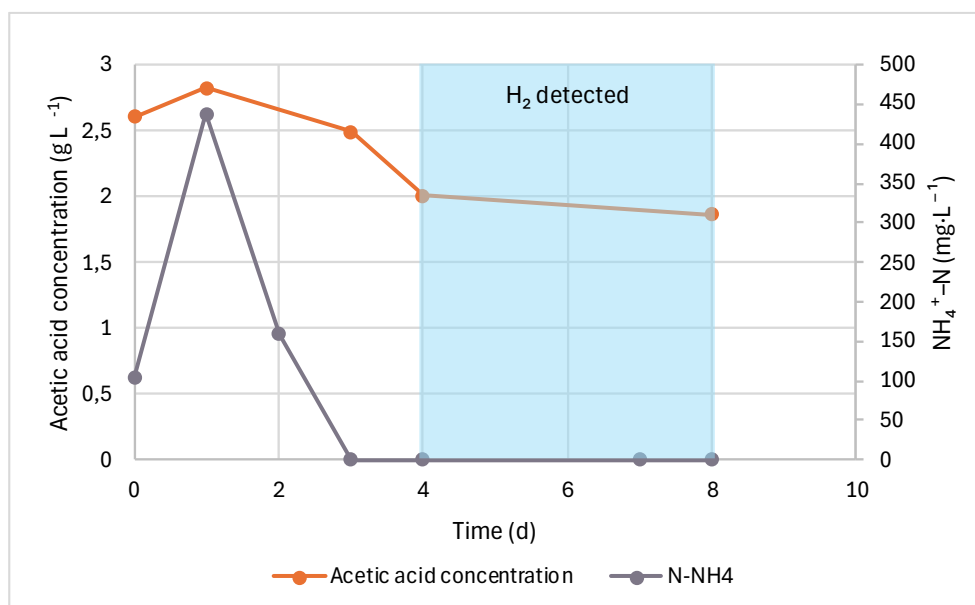


Figure 27 temporal profiles of acetate concentration and ammonium (NH_4^+) during photofermentation of the VFA-rich effluent by *Rhodospseudomonas palustris*, together with the time window in which H_2 was detected (shaded area).

Bianchi *et al.* (2010) reported that when *R. palustris* AV33 was cultivated on a vegetable-residue fermentation broth observed a higher biomass development and low H_2 conversion, compared to the corresponding synthetic medium, likely attributed it to ammonia and other nitrogen sources that diverted substrate utilization toward biomass rather than H_2 production. In addition, VFA consumption in mixed substrates does not necessarily translate stoichiometrically into H_2 because reducing equivalents generated during VFA catabolism can be dissipated through alternative electron sinks, notably intracellular polyhydroxybutyrate storage (Bianchi *et al.*, 2010).

Finally, micronutrient availability may further affect conversion efficiency when using real fermentation broth: Bianchi et al. (2010) also showed that Fe(III) supplementation (as ferric citrate) which acts as a biocatalyst to facilitate electron transfer, increased H₂ production rates and substrate conversion yield in the fermentation broth.

The end of H₂ production despite residual acetate was still available indicates that acetate was not the sole limiting factor. In complex effluents, nitrogenase activity was strongly inhibited by nitrogen, reduced effective light availability further limited by medium colour and self-shading and micronutrient limitations (e.g., Fe/Mo), and possible competition for reducing equivalents with biomass synthesis and maintenance and PHB synthesis. Those factors likely contributed to continued substrate uptake without further H₂ accumulation.

Overall, the relationship between substrate consumption and hydrogen evolution differed markedly among the tested conditions. Acetate supported the highest cumulative hydrogen production, while malate and lactate showed shorter hydrogen-producing phases and lower final hydrogen amounts. These differences are analyzed in more detail in the following section through hydrogen yields and substrate conversion efficiency calculations.

4.3.3. Hydrogen yields and substrate conversion efficiency

Cumulative hydrogen production and HPR_{max} describe the amount of hydrogen produced and the production kinetics. However, these parameters do not indicate how efficiently the consumed substrate was converted into hydrogen and for this reason, the hydrogen yield and the substrate conversion efficiency (SCE) were calculated for all tested conditions.

The experimental hydrogen yield was expressed as the amount of hydrogen produced per unit of substrate consumed reported as mmol H₂ mmol substrate⁻¹, the yield was also expressed as a percentage of the theoretical maximum hydrogen yield, reported as substrate conversion efficiency. This parameter was used to evaluate the hydrogen production performance of each specific carbon source in relation to the theoretical maximum hydrogen that can be obtained from complete substrate conversion, based on stoichiometric reactions (Uyar *et al.*, 2009).

In this way, SCE describes how close the process approached the theoretical hydrogen potential of the substrate.

For the defined substrates the theoretical hydrogen yields are defined by their respective stoichiometric reactions, corresponding to a maximum of 6 mol H₂ mol⁻¹ for malate, 4 mol H₂ mol⁻¹ for acetate, and 6 mol H₂ mol⁻¹ for lactate (Barbosa *et al.*, 2001).

In the literature, substrate-to-hydrogen conversion efficiencies in photofermentative processes are highly variable and depend on different parameters such as the microorganism, the substrate, and the operating conditions (Uyar *et al.*, 2009).

Table 10 shows hydrogen yields and substrate conversion efficiency. Values refer to the working volume. For lactate calculations refer to the phase before the lactate pulse.

Table 10 Hydrogen yields and substrate conversion efficiency.

Substrate	Substrate consumed (mmol)	H ₂ produced (mmol)	Yield (mmol H ₂ mmol substrate ⁻¹)	Theoretical yield (mmol H ₂ mmol substrate ⁻¹)	SCE (%)
Malic acid	9.39	0.35	0.04	6	0.62
Acetic acid	26.64	2.90	0.11	4	2.72
Lactic acid	17.17	0.71	0.04	6	0.69

Overall, acetate showed the highest yield and SCE among the tested defined substrates, while malate and lactate resulted in lower conversion efficiencies. In general, conversion efficiencies are often far below the theoretical maximum, with SCE reported between 14 and 50% for various VFAs (Uyar *et al.*, 2009) and values around ~44% reported for *R. palustris* on fermentation broth (Bianchi *et al.*, 2010), since part of the carbon is required for biomass formation and maintenance and therefore not fully available for nitrogenase-driven H₂ formation. In addition, PNSB may divert reducing power to intracellular storage polymers, especially PHB, which competes with H₂ formation (Bianchi *et al.*, 2010).

Finally, inoculum history may contribute to lower conversion; since the strain used in this study was a long-maintained laboratory culture, an “aged” inoculum may require a longer physiological adaptation before activating high nitrogenase activity, and a larger fraction of substrate may be directed to growth and maintenance rather than to H₂.

Malic acid

During the test malate decreased from 40.61 to 23.21 mmol L⁻¹, corresponding to 17.39 mmol L⁻¹ consumed (9.39 mmol in the reactor), while final cumulative hydrogen production was 8.70 mL (0.350 mmol H₂). Based on these values, the experimental hydrogen yield was 0.037 mmol H₂ mmol malate⁻¹. Considering the theoretical maximum of 6 mol H₂ per mol of malate, the theoretical hydrogen that can be obtained from the consumed malic acid was 56.34 mmol. This results in a SCE of 0.62%.

In this test, hydrogen production stopped while residual malate was still present, indicating that H₂ production was not primarily limited by carbon depletion but another limitation occurred before

malate exhaustion. When comparing with the literature, substantially higher malate conversion is reported when illumination and reactor optics are more favourable.

For example, Uyar et al. (2009) reported 50% SCE on malate (15 mM) and a maximum rate of 24 mL H₂ L⁻¹ h⁻¹ using *Rhodobacter sphaeroides* in 55 mL bottles under tungsten illumination. Similarly, Carlozzi, (2012) cultivated *Rhodopseudomonas palustris* (42OL) in a small cylindrical photobioreactor under high irradiance and reported a maximum hydrogen yield of 3.03 mol H₂ per mol malate, which corresponds to approximately 50% of the theoretical maximum.

In contrast, Lazaro et al. (2012) reported an intermediate performance using a phototrophic microbial consortium with malate (14.5 mM), in their study they report a complete substrate consumption and a higher cumulative production (13.9 mmol L⁻¹) resulting in a yield 0.9 mmol H₂ mmol⁻¹ malate and a SCE 15.6%. They also reported that H₂ production continued even after malate depletion, likely due to acetate formation and secondary substrate utilization, a behaviour enhanced by the use of mixed cultures.

Acetic acid

Acetate net consumption was 49.33 mmol L⁻¹, considering the 0.54 L working volume, the total amount of acetate consumed was 26.64 mmol. Final cumulative hydrogen production was 72.21 mL (2.903 mmol H₂). Based on these values, the experimental hydrogen yield was 0.109 mmol H₂ mmol acetate⁻¹ while the theoretical hydrogen obtainable from the consumed acetate was 106.56 mmol H₂, resulting in substrate conversion efficiency of 2.72%. Even if this was the highest SCE among the tested substrates, it remained far from the theoretical maximum, indicating that only a small fraction of the substrate-derived reducing equivalents was converted into H₂.

A useful comparison is provided by Lo et al. (2011a) who tested *R. palustris* WP3-5 on acetate (1–5 g L⁻¹) and demonstrated that at acetate concentrations of 3–4 g L⁻¹, acetate utilization was around 77% and the H₂ yield was much higher, reaching 3.46 mol H₂/mol acetate at 3 g L⁻¹ (approximately 68% of the theoretical yield). Since in the present test acetate consumption percentage was in the same order of magnitude, the main difference is not the extent of acetate uptake, but how the consumed acetate was metabolically spent.

One important competing sink is the accumulation of storage polymers. Bianchi et al.(2010) showed that when *R. palustris* AV33 was grown on acetate, hydrogen production was very low (only 8–10 mL accumulated after 250 h), while PHB reached approximately 21% of cell dry weight. This supports the idea that acetate can be preferentially diverted to PHB synthesis, which competes with H₂ production for reducing power. In this study PHB was not measured, so this mechanism cannot be confirmed directly, but it remains a plausible explanation for the low conversion despite high acetate consumption.

Lactic acid

Considering only the phase before the lactate pulse, the total amount of lactate consumed was 17.17 mmol (considered the reactor working volume) and the final cumulative hydrogen production was 17.73 mL corresponding to 0.713 mmol H₂.

The experimental hydrogen yield was 0.04 mmol H₂ mmol lactate⁻¹. and the theoretical hydrogen was 103 mmol H₂, corresponding to the SCE of 0.69%; the lowest among the tested substrates. In literature, much higher conversions on lactate have been reported under more favorable configurations. In the conditions studied by Lo et al. (2011), lactate performance was markedly higher, reporting SCE values of 52–53 %, with substrate utilization of 84.7% at 3 g L⁻¹ lactate and 66.3% at 4 g L⁻¹ of lactate, which in yield correspond to approximately 3.1–3.2 mol H₂ per mol lactate.

The large gap with SCE values reported in the present test suggests that only a small fraction of the electrons was channelled to nitrogenase and converted into H₂.

This interpretation is consistent with what was observed after the lactate pulse, where OD increased while H₂ production did not resume, indicating that the added carbon mainly supported biomass growth and maintenance rather than hydrogen evolution.

The possibility of competing sinks is also supported by Bianchi et al. (2010), who reported PHB accumulation also under lactate-fed condition.

Among the tested defined substrates, acetate gave the highest hydrogen recovery, while malate and lactate showed much lower conversion efficiencies. In the malate test, H₂ production stopped despite residual substrate, indicating that limitations other than carbon depletion became dominant before exhaustion. For lactate, the lack of H₂ recovery after the pulse together with continued biomass increase suggests that the added carbon mainly supported biomass growth and maintenance rather than resuming hydrogen evolution.

Overall, the low SCE values obtained here are consistent with the expected gap between theoretical stoichiometry and experimental photofermentation, and they should be interpreted as a comparative assessment under the same non-optimized setup, since literature shows that higher conversions can be achieved under intensified light supply, favourable reactor optics, and optimized physiological conditions.

Fermented substrate

Since the fermented effluent is a mixture and minor VFAs were close to the detection limit after dilution, yield and SCE are reported as apparent acetate-based values, using acetate as a reference compound.

Table 11 comparison between the results obtained with defined RPP media with acetic acid and the results obtained in the test with the fermented substrate

Substrate	Substrate consumed (mmol)	H ₂ produced (mmol)	Yield (mmol H ₂ mmol substrate ⁻¹)	Theoretical H ₂ (mmol)	SCE (%)
Fermented substrate	6.68	0.765	0.115	26.7	2.9
Acetic acid	26.64	2.90	0.11	106.55	2.72

For the fermented effluent, 6.68 mmol acetate were consumed and 0.765 mmol H₂ were produced, giving a yield of 0.115 mmol H₂ mmol⁻¹ acetate and an SCE of 2.9% (theoretical H₂ = 26.7 mmol).

When directly compared to the acetate-defined test, the two conditions exhibited very similar conversion efficiencies (2.72% vs 2.9%) and essentially the same apparent yield per mmol of acetate consumed (0.11–0.115 mmol H₂·mmol⁻¹). This indicates that, under the tested setup, the fraction of acetate-derived reducing equivalents recovered as H₂ was similarly limited in both media. The main difference between the two tests was instead the extent of acetate consumption, which was substantially higher in the defined acetate medium (26.64 mmol) than in the fermented effluent (6.68 mmol) resulting in a higher final H₂ amount mainly because more substrate was converted overall.

These SCE values obtained in this study are much lower than values typically reported under optimized or semi-optimized photofermentative conditions. For example, Uyar et al. (2009) investigated synthetic VFA mixtures mimicking dark-fermentation effluents using *Rhodobacter sphaeroides* O.U.001 and obtained, for an acetate-rich mixture (composed by 40 mM acetate, 10 mM butyrate and 5 mM propionate), a substrate conversion efficiency of 47%.

4.4. Immobilization of *R. palustris* on alginate matrix

Cell immobilization of purple non sulfur bacteria in polymeric matrices has been widely proposed as a strategy to improve biomass stability, to enable higher cell densities and facilitate biomass handling and reuse in photofermentative hydrogen production processes (Ross and Pott, 2021; Sagir and Alipour, 2021; Moia *et al.*, 2024).

However, immobilized systems used in photofermentation also introduce specific bottlenecks due to limitations in light transfer, mass transfer limitation and possible problems related to beads integrity over time (Moia *et al.*, 2024).

In this study, sodium alginate was selected as immobilization matrix since it is widely used for PNSB because it is low-cost, easy to prepare and allows mild immobilization conditions generally compatible with the physiology of photosynthetic microorganisms such as *R. palustris*.

The gel structure affects both diffusional properties and light penetration; as reported by Sagir and Alipour (2021), and the mechanical stability and diffusional properties of alginate matrices are strongly dependent on alginate concentration and immobilized biomass concentration.

At the same time, alginate beads are known to be chemically sensitive (e.g., to phosphates/chelators) and can progressively lose mechanical integrity, especially under mixing (Moia *et al.*, 2024).

For these reasons, immobilization was tested stepwise to identify an immobilization configuration suitable for the experimental setup, with particular attention to cost reduction and operational simplicity.

First, *R. palustris* was grown within a 2% (w/v) alginate beads to verify the biological compatibility and the growth inside the matrix. Then, a higher alginate concentration was tested to improve mechanical stability and evaluate their impact on bacterial growth and hydrogen production performance.

4.4.1. Effect of alginate concentration on biomass growth

Preliminary immobilization tests were carried out using calcium alginate beads at 2% (w/v) to evaluate the compatibility of the alginate matrix with the growth of *R. palustris*. Different initial inoculum concentrations were tested ($OD_{660} = 0.1, 0.2, 0.4$ and 1.0), as shown in Figure 28.

Growth was first evaluated qualitatively, based on the appearance and progressive intensification of the typical red color of the biomass and by changes in medium turbidity.

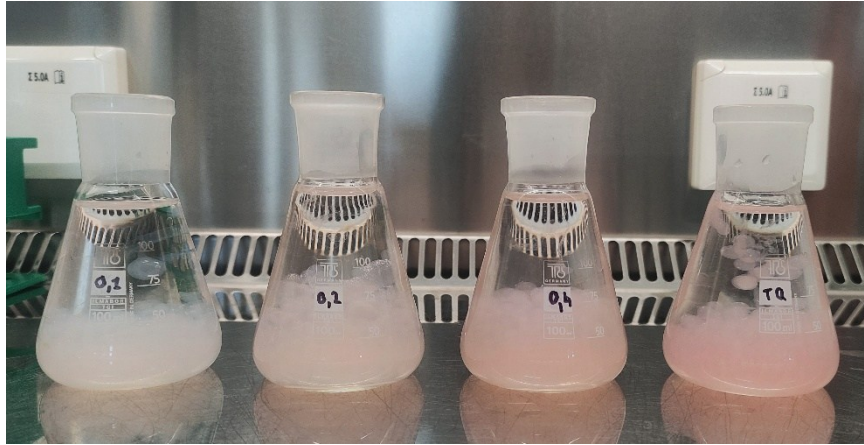


Figure 28 Different *R. palustris* inoculum concentrations ($OD_{660} = 0.1, 0.2, 0.4$ and 1) used for preliminary immobilization tests

After about one week, beads showed a clear intensification of red color, suggesting active microbial growth within the alginate matrix (Figure 29).

These observations indicated that alginate at 2% (w/v) did not inhibit *R. palustris* viability and metabolic activity.

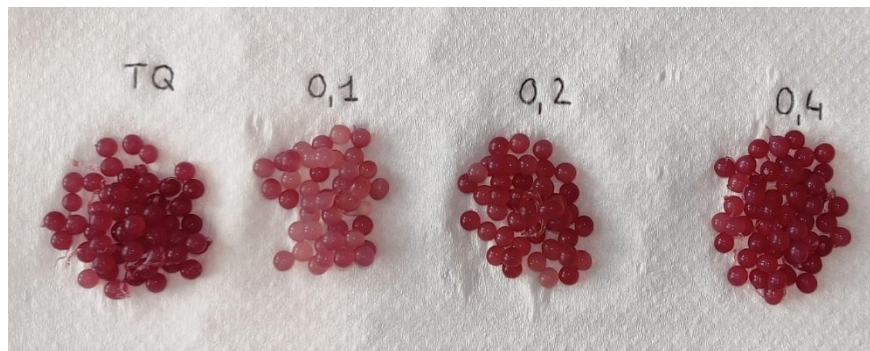


Figure 29 Immobilized *R. palustris* on alginate beads grown for 1 week

Growth was then monitored quantitatively over 192 h. Each day, a constant number of beads (13 beads) was dissolved in 4 mL sodium citrate solution ($\approx 4:1$ citrate-to-bead ratio) and OD_{660} was measured on the released cells.

OD values were blank-corrected (blank = 0.07). The resulting growth curve is shown in Figure 30

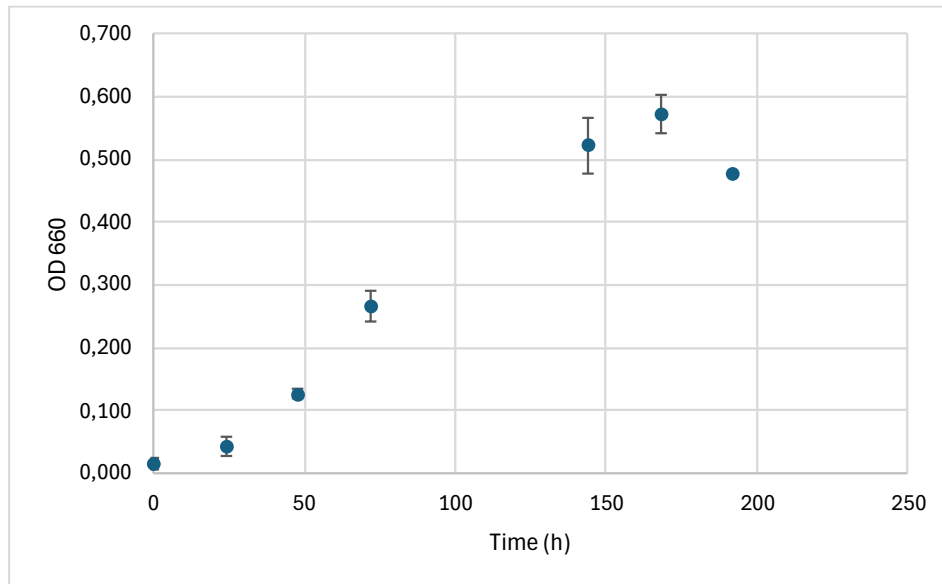


Figure 30 Growth curve of *Rhodospseudomonas palustris* immobilized in 2% (w/v) sodium alginate beads, with an initial inoculum concentration of $OD_{660} = 0.1$, cultivated in RPN medium

As shown in Figure 30, immobilized cells exhibited a relatively short adaptation phase, with limited OD increase during the first 24 h. OD then increased between 24 and 48 h, indicating the start of exponential growth.

Biomass accumulation continued up to $OD_{660} = 0.52 \pm 0.02$ at 144 and $OD_{660} = 0.57 \pm 0.04$ at 168 h, followed by a slight decrease at later time points.

In parallel, the medium became visibly more turbid, suggesting that part of the biomass was released from the beads (Figure 31).

A possible explanation is a combination of nutrient limitation over time, and partial loss of bead integrity which leads to cell leakage.



Figure 31 *Rhodospseudomonas palustris* immobilized in 2% (w/v) sodium alginate beads after 160h showing an evident media turbidity.

This interpretation is consistent with literature indicating that alginate beads can lose mechanical strength over time, especially when the medium composition promotes Ca^{2+} displacement from the gel network such in the presence of phosphates, and under mechanical stress; this behavior has been discussed by Moia et al. (2024) which try to assess the reusability of the spheres by refreshing the growth medium, however the new phosphate input, made the calcium alginate beads became more fragile and more susceptible to mechanical stress.

The growth pattern demonstrates that *R. palustris* can effectively adapt to immobilization within a 2% alginate matrix and to sustain active growth, but beads stability was limited over long incubation times.

To improve bead stability, a higher alginate concentration (4% w/v) was subsequently tested. When 4% (w/v) alginate beads were inoculated at an initial OD_{660} of 0.1, biomass growth was markedly limited. A prolonged lag phase was observed, and even after approximately 168 h the OD remained low ($\text{OD}_{660}=0.177$), suggesting that increasing alginate concentration improved gel compactness but likely introduced biological constraints, such as reduced pore size and increased diffusion resistance for nutrients and metabolites.

In addition, the extended incubation times required to approach the exponential phase were associated with increased turbidity of the medium. This type of trade-off is also discussed in literature: despite enhanced stability, denser matrices can be limiting factors for growth and photofermentative activity (Sagir and Alipour, 2021).

Based on these observations, it is possible to conclude that immobilized systems typically require a balance between matrix density, particle size and biomass loading.

Zhang et al. (2017) tested alginate granules under photofermentative conditions (30 °C, pH 7, 8000 lux) report that they obtained the best results when cells were immobilized at their exponential phase, with a biomass loading of approximately 2.5 g L^{-1} and granule size of 1–1.5 mm.

These findings supports that, in this experiment the high matrix density and low initial inoculum and the need of longer incubation time increased the probability of bead weakening and cell leakage; for this reason, subsequent experiments were performed using a higher initial inoculum concentration to promote a faster metabolic activity.

4.4.2. Hydrogen production tests with immobilized biomass.

After the immobilizations tests discussed in the previous section, hydrogen production experiments were carried out using *R. palustris* immobilized in alginate beads, with the aim of evaluating whether the immobilized system could produce H₂ under photofermentative conditions (Figure 32).

Bead preparation and reactor set-up are described in section 3.8

The operational conditions, including light intensity, temperature, pH, mixing, and reactor configuration, were maintained identical to those used in the experiments with suspended cultures to allow a direct comparison between free and immobilized systems.



Figure 32 Column photobioreactor containing immobilized *R. palustris* encapsulated in alginate beads. The system was operated under anaerobic and nitrogen-limited conditions to evaluate photofermentative hydrogen production.

Considering the limitations observed during the growth phase in alginate (4% w/v), particularly the prolonged lag phase and the progressive loss of beads mechanical stability, the test was designed to reduce the need for cell growth inside the beads.

To promote immediate activity, beads were prepared with a higher initial biomass concentration (OD₆₆₀ = 3.0). This approach was chosen to ensure a sufficiently high active biomass within the matrix from the beginning of the experiment, minimizing the need for cell proliferation inside the beads and reducing the stress associated with prolonged incubation times. However, despite the increased inoculum density, no measurable hydrogen production was observed. Comparison with

literature suggests that immobilized systems often require additional operational precautions to reach a physiological state compatible with nitrogenase-driven H₂ evolution. In particular, medium composition and operational strategy can strongly influence whether immobilized cells enter an effective H₂-producing state.

Moia et al., (2024) achieved sustained H₂ production with alginate-immobilized *Rhodospseudomonas sp.* using a modified Van Niel medium containing 4.0 g L⁻¹ acetate, 1.0 g L⁻¹ glutamate as N source, and a reduced phosphate concentration, with pH controlled at 7.2. They operated in cylindrical photobioreactor (200 mL working volume) in 3 sequential steps each separated by washing phases and medium renewal; in the first production step that lasted 149 h, they reported a total of 198.6 mL H₂, with a maximum HPR of 1.3 mL h⁻¹.

In the present study the modified RPP medium in which sodium glutamate was removed, phosphate salts were reduced, and NaCl was omitted, while malic acid, Mg²⁺, Ca²⁺, ferric citrate, trace elements, and vitamins were kept unchanged, to directly promote nitrogenase activity, intentionally bypassing biomass growth.

This choice simplified the set-up, but it may also have reduced the physiological adaptation of *R. palustris* to nitrogen-limited conditions, especially in the immobilized state, thereby contributing to the lack of detectable hydrogen production.

A second key aspect is the maintenance of anaerobic conditions; this step can be important because nitrogenase is highly sensitive to oxygen and requires reduced conditions to become active (Dhar, Venkateswarlu and Megharaj, 2023).

In the experimental tests, anaerobiosis was promoted by argon flushing, which should have rapidly displaced oxygen from the headspace and reduced dissolved O₂ in the liquid phase. This approach differs from the protocol adopted in the study Moia et al. (2024) immobilized cells were incubated overnight in the dark prior to illumination to allow the consumption of dissolved oxygen, monitored through ORP measurements, and the establishment of reduced conditions suitable for nitrogenase activation.

In their experiment H₂ production began only after anaerobic conditions were achieved, with an onset reported at approximately 55 h.

Further methodological differences concern beads preparation; several immobilization protocols use saline buffers to reduce osmotic shock and stabilize gel properties (Zhang *et al.*, 2017; Moia *et al.*, 2024). In this study, beads (4% w/v) were prepared resuspending the cells using deionized distilled water to minimize the entrainment of pre-culture medium components within the alginate beads. At the same time, preparing alginate and CaCl₂ solutions in distilled water represents a trade-off, because it may have exposed cells to transient osmotic stress during gelation and early operation.

In Moia et al.(2024) protocol, cells were washed with 0.9% NaCl, mixed with alginate in saline, and gelled in CaCl₂ in saline; beads were also washed with saline after formation.

Finally, light availability represents a major bottleneck in immobilized photofermentation systems in which light attenuation within alginate beads and shading effects caused by high biomass density can significantly limit nitrogenase-driven hydrogen evolution (Zhang *et al.*, 2017; Sagir and Alipour, 2021).

Moia et al. (2024) reported better performance on their cylindrical PBR than on flat panel photobioreactor, due to more uniform mixing and better light utilization.

They reported to use 1200 beads (51.5 mL total bead volume) in a 200 mL working volume, and the system was magnetically stirred. In the present test, the reactor had the same conformation, it was loaded with 150 mL beads in approximately 530 - 540 mL working volume, to have a similar beads-to medium fraction.

After the test performed with modified RPP with malic acid, additional experiments were carried out under the same operational conditions and procedures described above, using the modified synthetic RPP medium supplemented with acetic acid (4 g L⁻¹) and the fermented effluent as carbon source.

In both cases, results were consistent with those obtained with malate, and no measurable H₂ production was detected. This result suggests that, under the tested configuration, the lack of hydrogen production was not due to carbon source used but was likely related to limitations associated with the immobilization set-up itself, as discussed above.

4.5. Biomass characterization

Biomass composition is a key aspect for the evaluation of photofermentative processes with purple non-sulfur bacteria as it reflects how cells allocate assimilated carbon and nitrogen.

In this study, biomass composition was analyzed for *R. palustris* cultivated under different nutritional and operational conditions, in order to support the interpretation of growth and hydrogen production results.

The literature, photofermentative processes with PNSB are frequently discussed mainly in terms of H₂ production, OD and dry weight, and a complete biochemical characterization of the residual biomass is often not reported.

However, PNSB biomass is recognized as a valuable product itself, potentially rich in proteins and other high-value compounds, and its composition can be strongly affected by substrate type and cultivation regime (Policastro, Cesaro and Fabbricino, 2024; Bayon-Vicente *et al.*, 2025).

In this study, biomass composition was quantified in terms of total lipid, protein, and carbohydrate content using established spectrophotometric methods.

Lipid content was determined by the sulfo-phospho-vanillin method, proteins by the Bradford assay, and carbohydrates by the phenol–sulfuric acid method. Results were expressed on a dry-weight basis (%).

4.5.1. Biomass composition under different cultivation conditions

The biochemical composition of *Rhodospirillum rubrum* varied across cultivation conditions, as shown in Table 12, biomass cultivated in RPN and RPP media highlights the strong influence of nitrogen availability in the definition of macromolecular allocation.

Under growth oriented RPN conditions, proteins represented the dominant macromolecular fraction of biomass (30 to 34% of dry weight) while lipids and carbohydrates remained comparatively lower (around 17-19% DW and 4-5% DW respectively).

In RPP medium, designed to favor photofermentative hydrogen production through nitrogen limitation, exhibited a different allocation pattern. Lipids were in a comparable range (20.4–22.4 %DW) and carbohydrates showed a pronounced increase, especially in acetate-grown cultures reaching 23.3% DW, compared to 9.28–11.34 %DW in malate and lactate.

Protein content was around 24-35% DW depending on the carbon source.

Table 12 Biochemical composition of *Rhodopseudomonas palustris* biomass cultivated under different growth conditions, expressed as percentage of dry weight (% DW).

Values marked with an asterisk correspond to single measurements ($n = 1$); therefore, no standard deviation is reported.

Cultivation condition	Carbon source/medium	DW (g L ⁻¹)	Lipids (%DW)	Proteins (%DW)	Carbohydrates (%DW)
RPN	Malic	0.185	17.5 *	30.59 *	3.83 *
	Acetic	0.31	19.3 ± 2.56	34.13 ± 3.25	4.89 ± 0.65
	Lactic	0.75	not determined	not determined	not determined
RPP (for H ₂ production)	Malic	0.28	21.0 *	23.83 *	9.28 *
	Acetic	0.46	22.4 *	27.79 *	23.35 *
	Lactic	0.13	20.4 *	34.98 *	11.34 *
Fermented substrate	VFA-rich effluent	0.42	26.6 *	30.62 *	3.11 *
Immobilized biomass			20.7 ± 1.299	45.16 ± 1.49	17.14 ± 4.12

RPN medium provides readily available nitrogen to support rapid biosynthesis and biomass accumulation. RPP medium, on the other hand, has reduced fixed nitrogen to promote nitrogenase synthesis and activity to support photofermentative H₂ production.

A key observation is that comparing the biomass characterization is that RPP showed lower protein fraction and higher carbohydrate fraction compared to the growth oriented RPN medium, in particular in acetate. When growth is limited, and carbon source still available, carbon sources and reducing power can be redirected away from protein synthesis to intracellular storage compounds rather than channeling electrons exclusively to hydrogen production (Koku et al., 2002; Ghosh et al., 2017).

In agreement, Wada, Pasha, et al. (2025) reported that when substrate is still available, but growth is limited for example by nitrogen limitation, PNSB may shift metabolism toward PHA accumulation instead of synthesizing protein.

The lipid fraction observed in this study (approximately between 17- 27% DW) falls within the range observed in photofermentative tests by Carlozzi et al., (2010) with *Rhodopseudomonas palustris* (strain 42OL) where total lipid content was between 22 ± 1% and 39 ± 2% DW, with the higher lipid content obtained at lower irradiance.

Another example is reported for *Rhodobacter* sp. KKU-PS1 which under photofermentative conditions optimized for hydrogen production reached an higher HPR while lipid content remained low (3.2% DW) but increasing the C/N ratio (132 -147) lipid contents increased in the range of 21.5–35% DW, despite a lower H₂ production rate (Assawamongkholsiri, Plangklang and Reungsang, 2016).

Regarding protein amount, the results obtained in RPP with malic acid and acetic acid are lower compared to the corresponding RPN cultures.

In line with this, Policastro, Cesaro and Fabbricino, (2024) showed that under photofermentative conditions using a mixed PNSB culture lower H₂ production volume (190± 24 mL H₂ L⁻¹) was associated with higher proteins (29% DW) and PHB (27% DW) detection.

This interpretation is consistent with hydrogen production results discussed in chapter 4.3.

In RPP, the experimental yields obtained and SCE values were low (SCE%: 0.62 for malic acid, 2.72 for acetic acid, 0.69 in lactic acid and 2,86 for fermentation effluent) indicating that most substrate-derived electrons were not used for H₂ production.

Therefore, the increased carbohydrate and lipid fraction observed in RPP could be likely associated with a shift in carbon and electron flux toward other products which were not quantified in this work.

It should be noted that the phenol–sulfuric acid assay quantifies total carbohydrates (such glycogen and extracellular polysaccharides), but it does not capture PHA/PHB.

For the VFA-rich fermented substrate, the biomass showed the highest lipid fraction among all tested conditions 26.6% DW, with proteins around 30.6% DW comparable to RPN media and a low fraction of carbohydrates 3.1% DW, which remain comparable to values observed under RPN conditions.

In general, PNSB can convert diverse organics, including VFAs, into biomass rich in valuable components, but the process is influenced by waste-stream characteristics and operational conditions (Bayon-Vicente *et al.*, 2025).

Fermentation effluent is a complex and heterogeneous matrix, in which cells find heterogeneous substrates mix and variable nitrogen availability as previously discussed in Section 4.2.2 and supported by Ghosh *et al.*, (2017).

In this tested condition the relatively high protein content comparable RPN conditions is explained by the nitrogen availability in the media.

In addition, acetate removal was incomplete (acetate consumed = 28,74%) and SCE = 2,86%, supporting the idea that carbon and electron flux was partially diverted away from photofermentative H₂ production.

A comparable lipid composition has been reported for *Rhodobacter sp. KKU-PS1* grown on VFA rich wastewater in which the detected lipid content was 21% DW (Assawamongkholisiri, Reungsang and Sittijunda, 2019).

A useful comparison can be made with Wada, Alherbawi, et al. (2025) studies in which PNSB are applied on wastewaters with high organic content, where recovered PNSB biomass typically contained 25-39% DW lipids, highlighting that lipid concentration is strongly affected by feedstock type and culture conditions, and also reported that *R. palustris* lipid content decreased from 39% to 22% when the light intensity was strongly decreased.

4.5.2. Biomass characterization of immobilized biomass

Immobilized biomass composition was analysed as a key technological parameter, as immobilized cells are known to exhibit different metabolic and physiological behaviours from suspended cultures. Growth in a solid matrix modifies cellular microenvironment affecting nutrient and metabolites diffusion resulting in different growth behaviour compared to the suspension culture (Sagir and Alipour, 2021). This compositional comparison allows to evaluate how cultivation technology affects not only the performance of the product but also the quality of the final biomass.

Biomass immobilization in calcium–alginate beads resulted in a distinct biomass compositional profile compared to suspended cultures (Figure 33, Table 12).

Biomass compositional analysis was possible only for the 2% (w/v) alginate since in 4% (w/v) alginate test, the high viscosity of the matrix prevented efficient biomass recovery despite repeated centrifugation cycles. Before biochemical assays, alginate beads were dissolved and the recovered biomass was washed and centrifuged repeatedly to minimise residual medium and matrix-derived interference.

For comparison across cultivation strategies, RPN and RPP with malic, were selected as representative conditions. The three selected conditions exhibit markedly different growth kinetics.

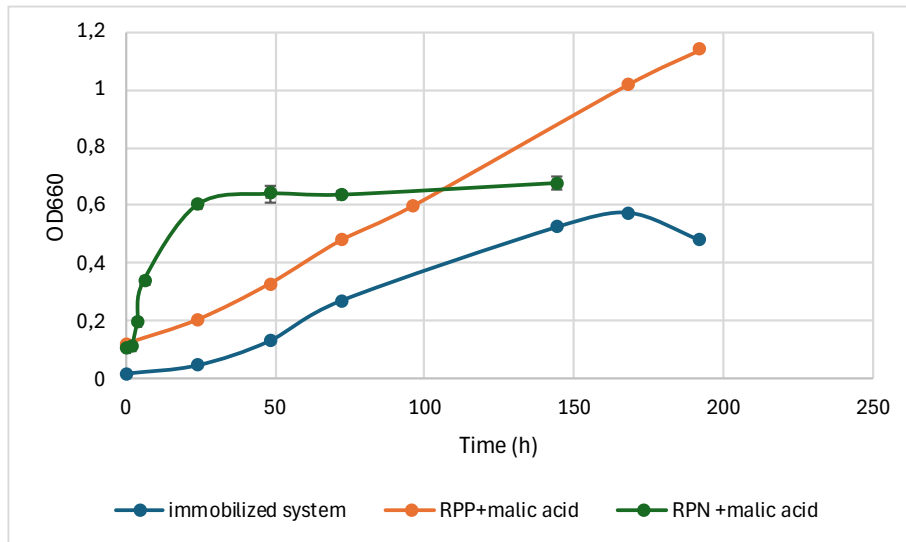


Figure 33 Growth kinetics of *R. palustris* cultivated in RPN-Mal , RPP-Mal and in immobilized system.

RPN+malate reached a rapid plateau within ~24 h while RPP+malate showed slower but sustained growth up to ~1.1–1.2 OD₆₆₀. In the immobilized configuration, growth was slower and reached a lower maximum value (OD₆₆₀=0.6) the slower and limited growth observed in immobilized system has already been explained in section 4.4.1, and it is due to possible restriction in substrate and nutrient diffusion inside the beads and reduced light availability. These kinetic differences provide a mechanistic basis to interpret the observed macromolecular allocation patterns in the corresponding biomass samples.

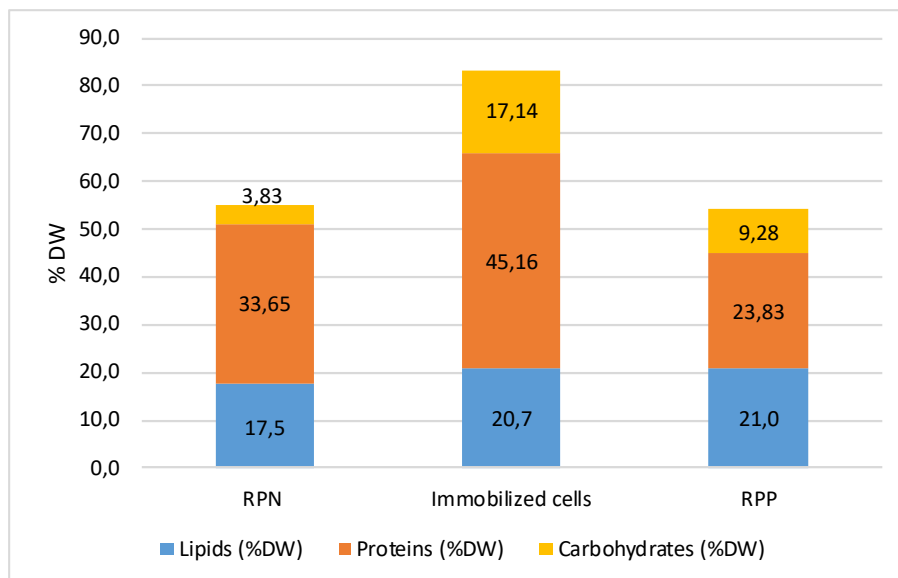


Figure 34 Macromolecular composition of *R. palustris* biomass cultivated under different experimental conditions. Lipids, proteins, and carbohydrates are expressed as percentage of dry weight (% DW). Values represent mean values.

As reported in Figure 34, immobilized cells displayed a shift toward protein-rich biomass ($45.16 \pm 1.49\%$ DW) compared to the suspended cultures. Lipids remained in the same order of magnitude as the suspended cultures ($20.7 \pm 1.30\%$ DW), and the carbohydrate fraction increased substantially ($17.14 \pm 4.12\%$ DW), markedly higher than that observed in suspended cultures grown RPN and RPP.

Immobilization technique has been widely investigated as a strategy to improve photofermentation performance and stability but the complete biochemical composition of immobilized biomass is rarely reported in literature.

A comparison study between suspended and immobilized cultures was made by Shaikh et al. (2023) reported a cellular protein content of $\sim 40\text{--}44\%$ in biofilm growth conditions, and highlighted a high fraction of EPS polysaccharides and EPS proteins in biofilm cultures respect to suspended cultures. This result shows that changing cultivation technology from suspended to immobilized growth can shift macromolecular allocation toward a more protein-rich biomass while increasing the carbohydrate-associated fraction, linked to the attached growth physiology.

5. Conclusions

The present work investigated photofermentative hydrogen production by PNSB *Rhodospseudomonas palustris* cultivated under anaerobic conditions on defined synthetic media containing malic acid, acetic acid and lactic acid and on a VFA-rich fermentation effluent. This research inserts in the framework of organic waste valorization, in a circular bioeconomy approach, investigating the feasibility of coupling treatments of fermentation effluents with the production of a green energy source with the purpose of simultaneously reducing the environmental impact of a waste stream difficult to valorise and decrease the dependence of fossil fuels.

The obtained results will contribute to the understanding of photofermentative metabolism of PNSB, highlighting the main factors that influenced the process and at the same time the critical issues associated.

Even though hydrogen production was limited, it was observed under all tests performed with suspended cultures and highlights that media composition and environmental conditions strongly affects photoheterotrophic metabolism in particular nitrogen regulation that reflected in both final yield H₂ production volume and kinetics.

The VFA-rich fermentation effluent used in this experimental thesis originates from a real semisolid fermentation process designed to resemble potentially a waste stream produced in space stations and, even if not optimized for photofermentative processes, allowed a limited hydrogen production.

Overall, the obtained results allowed the comparison among the different condition tested during this study and helps to recognize the major bottlenecks of the process, results reported in this study are lower to results commonly found in literature due to not fully optimized conditions.

Tests carried out with immobilized biomass have highlighted interesting potential but also practical limitations; the main issue was to find the proper alginate concentration to allow biomass retention and avoid limitations in the transport of nutrients, gas and light penetration. Immobilization is therefore a promising strategy but requires further studies to establish optimized process conditions.

A key limiting parameter was light availability. In the present work white-LED light were used at 4000K and a low light intensity 80 $\mu\text{mol m}^{-2} \text{s}^{-1}$, their main advantage is the low thermal emission and the possibility to selectively control light intensity. However, LED light used in the present experiments were missing the IR /near IR component, which has been demonstrated to be the essential to promote PNSB photosynthetic activity.

In particular, some recent studies demonstrated that optimized red LED light (~660 nm) + NIR (730–850 nm) resulted in optimal growth and improved photosynthetic activity (Uyar *et al.*, 2007; Tiang *et al.*, 2020).

Compared to the most frequently used light source for PNSB cultivation, such as tungsten and halogen lamps, LED light has an economic advantage, requires less energy and ensured reproducible conditions over the course of the experimentation. In the present study cylindrical PBR were used, since are reported to have best performances compared to other reactor configurations used in laboratory scale batch studies (Chen *et al.*, 2011). However, lights set up could be implemented in order to ensure a short light path and uniform light distribution on the reactor surface.

Finally, a relevant factor concerns the age and physiological state of the inoculum, which likely affected photofermentative yields. PNSBs are known for their ability to produce PHB, a process that competes with hydrogen production (Chen, Wu and Lee, 2012).

During this experimental period such measurements were not performed but future analysis are in plan. These would provide a better understanding of the mechanisms of electron distribution between growth, accumulation of intracellular reserves, and hydrogen production, and enable the design of strategies aimed at optimizing hydrogen production.

6. References

Adessi, A., McKinlay, J.B., *et al.* (2012) "A *Rhodospseudomonas palustris* nifA* mutant produces H₂ from NH₄⁺-containing vegetable wastes," *International Journal of Hydrogen Energy*, 37(21), pp. 15893–15900. Available at: <https://doi.org/10.1016/j.ijhydene.2012.08.009>.

Adessi, A., Torzillo, G., *et al.* (2012) "Sustained outdoor H₂ production with *Rhodospseudomonas palustris* cultures in a 50 L tubular photobioreactor," *International Journal of Hydrogen Energy*, 37(10), pp. 8840–8849. Available at: <https://doi.org/10.1016/j.ijhydene.2012.01.081>.

Adessi, A. and De Philippis, R. (2013) "Purple Bacteria: Electron Acceptors and Donors," *Encyclopedia of Biological Chemistry: Second Edition*, pp. 693–699. Available at: <https://doi.org/10.1016/B978-0-12-378630-2.00371-6>.

Adessi, A. and De Philippis, R. (2014) "Photobioreactor design and illumination systems for H₂ production with anoxygenic photosynthetic bacteria: A review," *International Journal of Hydrogen Energy*. Elsevier Ltd, pp. 3127–3141. Available at: <https://doi.org/10.1016/j.ijhydene.2013.12.084>.

Akram, F. *et al.* (2024) "Biohydrogen: Production, promising progressions and challenges of a green carbon-free energy," *Sustainable Energy Technologies and Assessments*, 69, p. 103893. Available at: <https://doi.org/10.1016/J.SETA.2024.103893>.

Alloul, A. *et al.* (2019) "Volatile fatty acids impacting phototrophic growth kinetics of purple bacteria: Paving the way for protein production on fermented wastewater," *Water Research*, 152, pp. 138–147. Available at: <https://doi.org/10.1016/j.watres.2018.12.025>.

Amini, A. *et al.* (2025) "The promising role of purple phototrophic bacteria in achieving the United Nations Sustainable Development Goals," *Journal of Hazardous Materials Advances*, p. 100884. Available at: <https://doi.org/10.1016/J.HAZADV.2025.100884>.

Andreeva, A., Budenkova, E., Babich, O., Sukhikh, S., Dolganyuk, V., *et al.* (2021) "Influence of Carbohydrate Additives on the Growth Rate of Microalgae Biomass with an Increased

Carbohydrate Content,” *Marine Drugs*, 19(7), p. 381. Available at: <https://doi.org/10.3390/md19070381>.

Andreeva, A., Budenkova, E., Babich, O., Sukhikh, S., Ulrikh, E., *et al.* (2021) “Production, Purification, and Study of the Amino Acid Composition of Microalgae Proteins,” *Molecules*, 26(9), p. 2767. Available at: <https://doi.org/10.3390/molecules26092767>.

Androga, D.D. *et al.* (2012) “Amelioration of photofermentative hydrogen production from molasses dark fermenter effluent by zeolite-based removal of ammonium ion,” *International Journal of Hydrogen Energy*, pp. 16421–16429. Available at: <https://doi.org/10.1016/j.ijhydene.2012.02.177>.

Assawamongkholisiri, T., Plangklang, P. and Reungsang, A. (2016) “Photofermentation and lipid accumulation by *Rhodobacter* sp. KKU-PS1 using malic acid as a substrate,” *International Journal of Hydrogen Energy*, 41(15), pp. 6259–6270. Available at: <https://doi.org/10.1016/j.ijhydene.2016.02.118>.

Assawamongkholisiri, T., Reungsang, A. and Sittijunda, S. (2019) “Photo-hydrogen and lipid production from lactate, acetate, butyrate, and sugar manufacturing wastewater with an alternative nitrogen source by *rhodobacter* sp. kku-ps1,” *PeerJ*, 2019(4). Available at: <https://doi.org/10.7717/peerj.6653>.

Baeyens, J. *et al.* (2020) “Reviewing the potential of bio-hydrogen production by fermentation,” *Renewable and Sustainable Energy Reviews*, 131, p. 110023. Available at: <https://doi.org/10.1016/j.rser.2020.110023>.

Barbosa, M.J. *et al.* (2001) *Acetate as a carbon source for hydrogen production by photosynthetic bacteria*, *Journal of Biotechnology*. Available at: www.elsevier.com/locate/jbiotec.

Basak, N. and Das, D. (2007) “The prospect of purple non-sulfur (PNS) photosynthetic bacteria for hydrogen production: The present state of the art,” *World Journal of Microbiology and Biotechnology*, 23(1), pp. 31–42. Available at: <https://doi.org/10.1007/s11274-006-9190-9>.

Bayon-Vicente, G. *et al.* (2025) "Metabolic pathways to sustainability: review of purple non-sulfur bacteria potential in agri-food waste valorization," *Frontiers in Bioengineering and Biotechnology*. Frontiers Media SA. Available at: <https://doi.org/10.3389/fbioe.2025.1529032>.

Bernabò, L. *et al.* (2025) "Selected-Wavelength Illumination for Enhanced Hydrogen and Poly- β -hydroxybutyrate Production from Second Cheese Whey by *Rhodopseudomonas palustris*," *Microorganisms*, 14(1), p. 32. Available at: <https://doi.org/10.3390/microorganisms14010032>.

Bianchi, L. *et al.* (2010) "Hydrogen-producing purple non-sulfur bacteria isolated from the trophic lake Averno (Naples, Italy)," *International Journal of Hydrogen Energy*, 35(22), pp. 12216–12223. Available at: <https://doi.org/10.1016/j.ijhydene.2010.08.038>.

Bosman, C.E., Pott, R.W.M.C. and Bradshaw, S.M. (2023) "The effect of light emission spectrum on biohydrogen production by *Rhodopseudomonas palustris*," *Bioprocess and Biosystems Engineering*, 46(6), pp. 913–919. Available at: <https://doi.org/10.1007/s00449-023-02863-8>.

Brown, B., Wilkins, M. and Saha, R. (2022) "Rhodopseudomonas palustris: A biotechnology chassis," *Biotechnology Advances*. Elsevier Inc. Available at: <https://doi.org/10.1016/j.biotechadv.2022.108001>.

Budiman, P.M. and Wu, T.Y. (2018) "Role of chemicals addition in affecting biohydrogen production through photofermentation," *Energy Conversion and Management*, 165, pp. 509–527. Available at: <https://doi.org/10.1016/J.ENCONMAN.2018.01.058>.

Cardeña, R., Valdez-Vazquez, I. and Buitrón, G. (2017) "Effect of volatile fatty acids mixtures on the simultaneous photofermentative production of hydrogen and polyhydroxybutyrate," *Bioprocess and Biosystems Engineering*, 40(2), pp. 231–239. Available at: <https://doi.org/10.1007/s00449-016-1691-9>.

Carlozzi, P. *et al.* (2010) "Production of bio-fuels (hydrogen and lipids) through a photofermentation process," *Bioresource Technology*, 101(9), pp. 3115–3120. Available at: <https://doi.org/10.1016/j.biortech.2009.12.049>.

Carlozzi, P. (2012) "Hydrogen photoproduction by rhodospseudomonas palustris 420l cultured at high irradiance under a semicontinuous regime," *Journal of Biomedicine and Biotechnology*, 2012. Available at: <https://doi.org/10.1155/2012/590693>.

Chen, C.Y. *et al.* (2011) "Perspectives on cultivation strategies and photobioreactor designs for photo-fermentative hydrogen production," *Bioresource Technology*, 102(18), pp. 8484–8492. Available at: <https://doi.org/10.1016/j.biortech.2011.05.082>.

Chen, Y.T., Wu, S.C. and Lee, C.M. (2012) "Relationship between cell growth, hydrogen production and poly- β -hydroxybutyrate (PHB) accumulation by *Rhodospseudomonas palustris* WP3-5," *International Journal of Hydrogen Energy*, pp. 13887–13894. Available at: <https://doi.org/10.1016/j.ijhydene.2012.06.024>.

Cheng, J. *et al.* (2011) "Hydrogen production by mixed bacteria through dark and photo fermentation," *International Journal of Hydrogen Energy*, 36(1), pp. 450–457. Available at: <https://doi.org/10.1016/j.ijhydene.2010.10.007>.

Chiarini, L. *et al.* (2025) "Selection and characterization of bacterial consortia for the degradation of space organic waste," *Life Sciences in Space Research*, 46, pp. 191–200. Available at: <https://doi.org/10.1016/j.lssr.2025.05.007>.

Dhar, K., Venkateswarlu, K. and Megharaj, M. (2023) "Anoxygenic phototrophic purple non-sulfur bacteria: tool for bioremediation of hazardous environmental pollutants," *World Journal of Microbiology and Biotechnology*. Springer Science and Business Media B.V. Available at: <https://doi.org/10.1007/s11274-023-03729-7>.

Draget, K.I. and Taylor, C. (2011) "Chemical, physical and biological properties of alginates and their biomedical implications," *Food Hydrocolloids*, 25(2), pp. 251–256. Available at: <https://doi.org/10.1016/j.foodhyd.2009.10.007>.

George, D.M., Vincent, A.S. and Mackey, H.R. (2020) "An overview of anoxygenic phototrophic bacteria and their applications in environmental biotechnology for sustainable Resource

recovery,” *Biotechnology Reports*. Elsevier B.V. Available at: <https://doi.org/10.1016/j.btre.2020.e00563>.

Ghimire, A. *et al.* (2015) “A review on dark fermentative biohydrogen production from organic biomass: Process parameters and use of by-products,” *Applied Energy*, 144, pp. 73–95. Available at: <https://doi.org/10.1016/J.APENERGY.2015.01.045>.

Ghimire, A. *et al.* (2016) “Concomitant biohydrogen and poly- β -hydroxybutyrate production from dark fermentation effluents by adapted *Rhodobacter sphaeroides* and mixed photofermentative cultures,” *Bioresource Technology*, 217, pp. 157–164. Available at: <https://doi.org/10.1016/j.biortech.2016.03.017>.

Ghosh, S. *et al.* (2017) “Hydrogen from food processing wastes via photofermentation using Purple Non-sulfur Bacteria (PNSB) – A review,” *Energy Conversion and Management*. Elsevier Ltd, pp. 299–314. Available at: <https://doi.org/10.1016/j.enconman.2016.09.001>.

Govindaraju, A., McKinlay, J.B. and LaSarre, B. (2019) “Phototrophic lactate utilization by *Rhodospseudomonas palustris* is stimulated by cocultivation with additional substrates,” *Applied and Environmental Microbiology*, 85(11). Available at: <https://doi.org/10.1128/AEM.00048-19>.

Guevara-López, E. and Buitrón, G. (2015) “Evaluation of different support materials used with a photo-fermentative consortium for hydrogen production,” *International Journal of Hydrogen Energy*. Elsevier Ltd, pp. 17231–17238. Available at: <https://doi.org/10.1016/j.ijhydene.2015.08.057>.

Hallenbeck, P.C., Abo-Hashesh, M. and Ghosh, D. (2012) “Strategies for improving biological hydrogen production,” *Bioresource Technology*, pp. 1–9. Available at: <https://doi.org/10.1016/j.biortech.2012.01.103>.

Hallenbeck, P.C. and Benemann, J.R. (2002) *Biological hydrogen production; fundamentals and limiting processes*, *International Journal of Hydrogen Energy*. Available at: www.elsevier.com/locate/ijhydene.

Haq, I.U., Christensen, A. and Fixen, K.R. (2024) "Evolution of *Rhodopseudomonas palustris* to degrade halogenated aromatic compounds involves changes in pathway regulation and enzyme specificity," *Applied and Environmental Microbiology*, 90(2). Available at: <https://doi.org/10.1128/aem.02104-23>.

Hendrickx, L. *et al.* (2006) "Microbial ecology of the closed artificial ecosystem MELiSSA (Micro-Ecological Life Support System Alternative): Reinventing and compartmentalizing the Earth's food and oxygen regeneration system for long-haul space exploration missions," *Research in Microbiology*, pp. 77–86. Available at: <https://doi.org/10.1016/j.resmic.2005.06.014>.

Hossain Bhuiyan, M.M. and Siddique, Z. (2025) "Hydrogen as an alternative fuel: A comprehensive review of challenges and opportunities in production, storage, and transportation," *International Journal of Hydrogen Energy*. Elsevier Ltd, pp. 1026–1044. Available at: <https://doi.org/10.1016/j.ijhydene.2025.01.033>.

Hu, C., Choy, S.Y. and Giannis, A. (2018) "Evaluation of Lighting Systems, Carbon Sources, and Bacteria Cultures on Photofermentative Hydrogen Production," *Applied Biochemistry and Biotechnology*, 185(1), pp. 257–269. Available at: <https://doi.org/10.1007/s12010-017-2655-5>.

Jeong, T.Y. *et al.* (2008) "Comparison of hydrogen production by four representative hydrogen-producing bacteria," *Journal of Industrial and Engineering Chemistry*, 14(3), pp. 333–337. Available at: <https://doi.org/10.1016/J.JIEC.2007.09.014>.

Kantachote, D. *et al.* (2016) "Biofertilizers from *Rhodopseudomonas palustris* strains to enhance rice yields and reduce methane emissions," *Applied Soil Ecology*, 100, pp. 154–161. Available at: <https://doi.org/10.1016/j.apsoil.2015.12.015>.

Kim, J.K. and Lee, B.-K. (2000) *Mass production of *Rhodopseudomonas palustris* as diet for aquaculture*, *Aquacultural Engineering*. Available at: www.elsevier.nl/locate/aqua-online.

Koku, H. *et al.* (2002) *Aspects of the metabolism of hydrogen production by Rhodobacter sphaeroides*, *International Journal of Hydrogen Energy*. Available at: www.elsevier.com/locate/ijhydene.

Koku, H. *et al.* (2003) *Kinetics of biological hydrogen production by the photosynthetic bacterium Rhodobacter sphaeroides O.U. 001*, *International Journal of Hydrogen Energy*. Available at: www.sciencedirect.comwww.elsevier.com/locate/ijhydene.

Larimer, F.W. *et al.* (2004) "Complete genome sequence of the metabolically versatile photosynthetic bacterium *Rhodospseudomonas palustris*," *Nature Biotechnology*, 22(1), pp. 55–61. Available at: <https://doi.org/10.1038/nbt923>.

Lazaro, C.Z. *et al.* (2012) "Hydrogen production and consumption of organic acids by a phototrophic microbial consortium," *International Journal of Hydrogen Energy*, 37(16), pp. 11691–11700. Available at: <https://doi.org/10.1016/j.ijhydene.2012.05.088>.

Lee, C.M., Hung, G.J. and Yang, C.F. (2011) "Hydrogen production by *Rhodospseudomonas palustris* WP 3-5 in a serial photobioreactor fed with hydrogen fermentation effluent," *Bioresource Technology*, 102(18), pp. 8350–8356. Available at: <https://doi.org/10.1016/j.biortech.2011.04.072>.

Lee, H.S., Vermaas, W.F.J. and Rittmann, B.E. (2010) "Biological hydrogen production: Prospects and challenges," *Trends in Biotechnology*, pp. 262–271. Available at: <https://doi.org/10.1016/j.tibtech.2010.01.007>.

Levin, D.B., Pitt, L. and Love, M. (2004) "Biohydrogen production: Prospects and limitations to practical application," *International Journal of Hydrogen Energy*, 29(2), pp. 173–185. Available at: [https://doi.org/10.1016/S0360-3199\(03\)00094-6](https://doi.org/10.1016/S0360-3199(03)00094-6).

Li, M. *et al.* (2022) "Characteristics and Application of *Rhodospseudomonas palustris* as a Microbial Cell Factory," *Frontiers in Bioengineering and Biotechnology*. Frontiers Media S.A. Available at: <https://doi.org/10.3389/fbioe.2022.897003>.

Liu, Y., Ghosh, D. and Hallenbeck, P.C. (2015) "Biological reformation of ethanol to hydrogen by *Rhodospseudomonas palustris* CGA009," *Bioresource Technology*, 176, pp. 189–195. Available at: <https://doi.org/10.1016/j.biortech.2014.11.047>.

Lo, Y.C. *et al.* (2011) "Photo fermentative hydrogen production using dominant components (acetate, lactate, and butyrate) in dark fermentation effluents," *International Journal of Hydrogen Energy*, pp. 14059–14068. Available at: <https://doi.org/10.1016/j.ijhydene.2011.04.148>.

Lopez-Romero, J. *et al.* (2020) "Enhanced carotenoid production by *Rhodospseudomonas palustris* ATCC 17001 under low light conditions," *Journal of Biotechnology*, 323, pp. 159–165. Available at: <https://doi.org/10.1016/j.jbiotec.2020.08.007>.

Luxem, K.E., Nguyen, A.J. and Zhang, X. (2022) "Biohydrogen production relationship to biomass composition, growth, temperature and nitrogenase isoform in the anaerobic photoheterotrophic diazotroph *Rhodospseudomonas palustris*," *International Journal of Hydrogen Energy*, 47(66), pp. 28399–28409. Available at: <https://doi.org/10.1016/j.ijhydene.2022.06.178>.

Madigan, M.T. and Jung, D.O. (2009) *Chapter 1 An Overview of Purple Bacteria: Systematics, Physiology, and Habitats*.

McKinlay, J.B. *et al.* (2014) "Non-growing *rhodospseudomonas palustris* increases the hydrogen gas yield from acetate by shifting from the glyoxylate shunt to the tricarboxylic acid cycle," *Journal of Biological Chemistry*, 289(4), pp. 1960–1970. Available at: <https://doi.org/10.1074/jbc.M113.527515>.

McKinlay, J.B. and Harwood, C.S. (2010) "Photobiological production of hydrogen gas as a biofuel," *Current Opinion in Biotechnology*, pp. 244–251. Available at: <https://doi.org/10.1016/j.copbio.2010.02.012>.

McKinlay, J.B. and Harwood, C.S. (2011) "Calvin cycle flux, pathway constraints, and substrate oxidation state together determine the H₂ biofuel yield in photoheterotrophic bacteria," *mBio*, 2(2). Available at: <https://doi.org/10.1128/mBio.00323-10>.

Mishra, S.K. *et al.* (2014) "Rapid quantification of microalgal lipids in aqueous medium by a simple colorimetric method," *Bioresource Technology*, 155, pp. 330–333. Available at: <https://doi.org/10.1016/j.biortech.2013.12.077>.

Moia, I.C. *et al.* (2024) "Photofermentative hydrogen production by immobilized *Rhodospseudomonas* sp. S16-VOGS3 cells in photobioreactors," *Energy Reviews*. Elsevier B.V. Available at: <https://doi.org/10.1016/j.enrev.2023.100055>.

Morrison, H.M. and Bose, A. (2025a) "Purple non-sulfur bacteria for biotechnological applications," *Journal of Industrial Microbiology and Biotechnology*. Oxford University Press. Available at: <https://doi.org/10.1093/jimb/kuae052>.

Morrison, H.M. and Bose, A. (2025b) "Purple non-sulfur bacteria for biotechnological applications," *Journal of Industrial Microbiology and Biotechnology*. Oxford University Press. Available at: <https://doi.org/10.1093/jimb/kuae052>.

Muzziotti, D. *et al.* (2016) "H₂ production in *Rhodospseudomonas palustris* as a way to cope with high light intensities," *Research in Microbiology*, 167(5), pp. 350–356. Available at: <https://doi.org/10.1016/j.resmic.2016.02.003>.

Padovani, G., Vaičiulyte, S. and Carlozzi, P. (2015) "BioH₂ photoproduction by means of *Rhodospseudomonas palustris* sp. cultured in a lab-scale photobioreactor operated in batch, fed-batch and semi-continuous modes," *Fuel*, 166, pp. 203–210. Available at: <https://doi.org/10.1016/j.fuel.2015.10.124>.

Pakpour, F. *et al.* (2014) "Biohydrogen production from CO-rich syngas via a locally isolated *Rhodospseudomonas palustris* PT," *Bioprocess and Biosystems Engineering*, 37(5), pp. 923–930. Available at: <https://doi.org/10.1007/s00449-013-1064-6>.

Park, C.B. and Lee, S.B. (1998) *Ammonia Production from Yeast Extract and Its Effect Growth of the Hyperthermophilic Archaeon Sulfolobus solfataricus on*, *Biotechnol. Bioprocess Eng.*

Policastro, G., Cesaro, A. and Fabbricino, M. (2024) "Valorization of Purple Phototrophic Bacteria Biomass Resulting from Photo Fermentation Aimed at Biohydrogen Production," *Molecules*, 29(7). Available at: <https://doi.org/10.3390/molecules29071679>.

Postels, S. *et al.* (2016) "Life cycle assessment of hydrogen production by thermal cracking of methane based on liquid-metal technology," *International Journal of Hydrogen Energy*, 41(48), pp. 23204–23212. Available at: <https://doi.org/10.1016/j.ijhydene.2016.09.167>.

Ross, B.S. and Pott, R.W.M. (2021) "Hydrogen production by immobilized *Rhodospseudomonas palustris* in packed or fluidized bed photobioreactor systems," *International Journal of Hydrogen Energy*, 46(2), pp. 1715–1727. Available at: <https://doi.org/10.1016/j.ijhydene.2020.10.061>.

Sagir, E. and Alipour, S. (2021) "Photofermentative hydrogen production by immobilized photosynthetic bacteria: Current perspectives and challenges," *Renewable and Sustainable Energy Reviews*. Elsevier Ltd. Available at: <https://doi.org/10.1016/j.rser.2021.110796>.

Shaikh, S. *et al.* (2023) "Nitrogen influence on suspended vs biofilm growth and resource recovery potential of purple non-sulfur bacteria treating fuel synthesis wastewater," *Biochemical Engineering Journal*, 190. Available at: <https://doi.org/10.1016/j.bej.2022.108754>.

Štumpf, S. *et al.* (2020) "Generation times of *e. Coli* prolong with increasing tannin concentration while the lag phase extends exponentially," *Plants*, 9(12), pp. 1–11. Available at: <https://doi.org/10.3390/plants9121680>.

Sun, Yujie, Sun, Yujiao and Li, X. (2023) "Removal of pollutants and accumulation of high-value cell inclusions in a batch reactor containing *Rhodospseudomonas* for treating real heavy oil refinery wastewater," *Journal of Environmental Management*, 345. Available at: <https://doi.org/10.1016/j.jenvman.2023.118834>.

Tao, Y. *et al.* (2008) "Characteristics of a new photosynthetic bacterial strain for hydrogen production and its application in wastewater treatment," *International Journal of Hydrogen Energy*, 33(3), pp. 963–973. Available at: <https://doi.org/10.1016/j.ijhydene.2007.11.021>.

Tiang, M.F. *et al.* (2020) "Recent advanced biotechnological strategies to enhance photo-fermentative biohydrogen production by purple non-sulphur bacteria: An overview," *International Journal of Hydrogen Energy*. Elsevier Ltd, pp. 13211–13230. Available at: <https://doi.org/10.1016/j.ijhydene.2020.03.033>.

Touloupakis, E., Faraloni, C. and Carlozzi, P. (2022) "An outline of photosynthetic microorganism growth inside closed photobioreactor designs," *Bioresource Technology Reports*. Elsevier Ltd. Available at: <https://doi.org/10.1016/j.biteb.2022.101066>.

Uyar, B. *et al.* (2007) "Effect of light intensity, wavelength and illumination protocol on hydrogen production in photobioreactors," *International Journal of Hydrogen Energy*, 32(18), pp. 4670–4677. Available at: <https://doi.org/10.1016/j.ijhydene.2007.07.002>.

Uyar, B. *et al.* (2009) "Photofermentative hydrogen production from volatile fatty acids present in dark fermentation effluents," *International Journal of Hydrogen Energy*, 34(10), pp. 4517–4523. Available at: <https://doi.org/10.1016/j.ijhydene.2008.07.057>.

Wada, O.Z., Pasha, M., *et al.* (2025) "Dim lights, bright prospects: Purple phototrophic bacteria-driven industrial wastewater treatment for biomass resource recovery at low light intensities," *Process Safety and Environmental Protection*, 194, pp. 1067–1080. Available at: <https://doi.org/10.1016/j.psep.2024.12.037>.

Wada, O.Z., Alherbawi, M., *et al.* (2025) "Purple nonsulfur bacteria biomass as a potential biofuel source: A study of lipid characterization methods using gas chromatography," *Biofuels, Bioproducts and Biorefining*, 19(3), pp. 819–834. Available at: <https://doi.org/10.1002/bbb.2743>.

Wu, X.M. *et al.* (2016) "Improved ammonium tolerance and hydrogen production in nifA mutant strains of *Rhodospseudomonas palustris*," *International Journal of Hydrogen Energy*, 41(48), pp. 22824–22830. Available at: <https://doi.org/10.1016/j.ijhydene.2016.10.093>.

Zhang, H. *et al.* (2017) "Photosynthetic hydrogen production by alginate immobilized bacterial consortium," *Bioresource Technology*, 236, pp. 44–48. Available at: <https://doi.org/10.1016/j.biortech.2017.03.171>.